공학석사 학위논문

Shear Retrofit of Single-layered RC Squat Wall with Section Enlargement

단면 증타 보강된 단근 배근 전단벽의

전단 보강 효과

2015 년 2 월

서울대학교 대학원

건축학과

이 유 선

Shear Retrofit of Single-layered RC Squat Wall with Section Enlargement

지도 교수 홍 성 걸

이 논문을 공학석사 학위논문으로 제출함
2015 년 2월

서울대학교 대학원
건축학과
이 유 선

이유선의 공학석사 학위논문을 인준함
2015 년 2 월

위 원 장 _____ (인)

부위원장 _____ (인)

위 원 _____ (인)

Abstract

Shear Retrofit of Single-layered RC Squat Wall with Section Enlargement

Yi, Yousun
Department of Architecture and Architectural Engineering
College of Engineering
Seoul National University

The single-layered squat wall has very poor performance in all aspects. Therefore, various retrofitting strategies have been researched can be applied to it to improve its seismic performance. The concrete section enlargement retrofitting method is one of the seismic retrofitting strategy generally used in working place due to its economic efficiency and practical reason. The insufficiency of flexural capacity of the single-layered squat wall can be retrofitted by providing column element at the both ends of the wall as giving boundary elements to single-layered squat wall. In addition, the insufficiency of shear capacity can be retrofitted by web section enlargement with reinforcements in that section.

However, in the case of the former one, consideration of shear strength of the retrofitted member is also needed. If the enlarged flexural capacity excesses the shear strength of it, unexpected brittle failure could be occurred. Therefore, this study proposed the analytical way to predict shear strength and initial stiffness of the retrofitted squat wall by revising existing shear strength model. The revised model considered not only reinforcement details of the column member, also compatibility condition between the column and the single-layered squat wall. Based on the test result of this study, the validity of the proposed analytical way is proved. Moreover, it was verified that the proposed method also could predict not only shear strength, also initial stiffness of the infilled RC squat

wall in RC frame by comparing the results of the test and that of the proposed method.

In the case of the latter one, there occurs space waste problem due to large area of the concrete section enlargement casted with normal strength concrete within reinforcements. Therefore, this study planned to use UHPFRC which has higher stiffness, tensile stress, and compressive stress than that of the normal strength concrete for the section enlargement retrofitting method. By using the UHPFRC for this method, it is supposed that it's possible to obtain required strength with much thinner section enlargement. However, since there exists few researches related to this topic, this study planned experimental and analytical approach to verify retrofitting effect of the single-layered squat wall retrofitted with the UHPFRC web section enlargement method. Therefore, this study proposed an algorithm for deriving shear stress-shear strain curve of the retrofitted squat wall. By this method, it is able to determine failure mode of the retrofitted squat wall, and find out that the ratio of thickness of the RC squat wall and that of the UHPFRC section can affect behavior and failure mode of the retrofitted member. In addition, the maximum stress occurred in the interface of the retrofitted squat wall can be determined based on the failure mode of it, and this study suggested design stress depending on the thickness ratio for preventing interface failure of retrofitted squat wall. Moreover, this study applied the method to the web retrofitted single – layered squat wall with the single - layered panel, and compared it with the double – layered squat wall. Therefore, the validity of the method also can be confirmed.

Therefore, it is able to verify shear retrofitting effect of the section enlargement retrofitting method by using the analytical and the experimental results of this study. Furthermore, the results of this study can be used for the guidelines of the section enlargement retrofitting method.

Keywords: Single-layered squat wall, Shear retrofitting effect, Section enlargement method, Strut action, UHPFRC
Student Number : 2013-20568

Contents

List of Tables

List of Figures

List of Symbols

A_c = area of retrofitting column section (mm^2)

A_{cv} = net area of concrete section bounded by web thickness and length of section in the direction of shear force considered (mm^2)

$A_{interface}$ = triangular area formed by diagonal crack in interface element (mm^2)

A_l = area of the longitudinal reinforcement in s_l (mm^2)

A_{str} = area of strut section $\left(= a_s \times t_w\right)$ (mm^2)

A_{th} = area of effective transverse reinforcement (mm^2)

A_{tv} = area of effective vertical reinforcement (mm^2)

A_{vh} = area of transverse reinforcement (mm^2)

a_s = width of strut (diagonal, flat, and steep strut) (mm)

a'_s = modified width of single diagonal strut (mm)

b_w = width of the web (mm)

D = strength of diagonal strut from diagonal strut mechanism (N)

D' = strength of modified diagonal strut for deriving initial stiffness (N)

d = effective length of wall section ($= 0.8l_w$, ACI 349-06) (mm)

$d-$ = direction of principal compressive stress of concrete after cracking

E_c^w = young's modulus of squat wall's concrete (MPa)

E_c = young's modulus of concrete (MPa)

EI_{eff} = effective flexural stiffness considering cracking concrete (MPa)

E_s = young's modulus of reinforcement (MPa)

E_{UHPC} = young's modulus of UHPFRC (MPa)

F_h = strength of horizontal tie from flat strut mechanism (N)

F_v = strength of vertical tie from steep strut mechanism (N)

f_{cd} = nominal compressive strength of K-UHPC (MPa)

f_{cr} = cracking stress of concrete (MPa)

f_c = compressive strength of normal strength concrete (MPa)

f_c^{UHPC} = compressive strength of UHPFRC (MPa)

f_{crk}^{UHPC} = cracking tensile stress of K-UHPC (MPa)

f_{ly} = yield strength of the longitudinal reinforcement (MPa)

f_{tk}^{UHPC} = nominal tensile stress of K-UHPC (MPa)

f_{ty} = yield strength of the transverse reinforcement (MPa)

f_s = stress of reinforcement (MPa)

f_{vd} = average tensile stress occurred in right angle of diagonal crack (MPa)

f_y = yield stress of reinforcement (MPa)

f'_y = smeared yield stress of reinforcement (MPa)

GA_{eff} = effective shear stiffness of retrofitting column (MPa)

h_w = height of wall section (mm)

$h-$ = direction horizontal reinforcement

I_c = moment of inertia of retrofitting column section (mm^4)

l_{ch} = characteristic length (1.01×10^4 mm)

l_w = length of wall section (mm)

$l-$ = direction of longitudinal reinforcement

N_u = factored axial force applied to wall section (N)

$\frac{R_h}{R_d}$ = relative stiffness ratio between horizontal and diagonal mechanism

$\frac{R_v}{R_d}$ = relative stiffness ratio between vertical and diagonal mechanism

$r-$ = direction of principal tensile stress of concrete after cracking

s_h, s_t = spacing of transverse reinforcement (mm)

s_l = spacing of longitudinal reinforcement (mm)

t_w = thickness of wall (mm)

$t-$ = direction of transverse reinforcement

t_{UHPC} = thickness of retrofitting UHPFRC panel (mm)

V_c = nominal shear strength provided by concrete (N)

V_{fd} = nominal shear strength provided by fiber (N)

V_n = nominal shear strength of squat wall from existing provisions (N)

$V_{n,c}$ = nominal shear strength of retrofitting column (N) (ACI318-11)

V_{rpcd} = nominal shear strength provided by matrix (N)

V_s = nominal shear strength provided by shear reinforcement (N)

$V_{u,W1}$ = ultimate strength of W1 from test result (N)

$V_{u,W2}$ = ultimate strength of W2 from test result (N)

$v-$ = direction of vertical reinforcement

$w_{\lim}$ = maximum crack width of UHPFRC (mm)

w_u = crack width when UHPFRC's ultimate tensile stress is occurred (mm)

z = distance from location of compressive resultant is applied and center of tensile reinforcement ($d/1.15$ is assumed, (mm))

α = angle of diagonal strut formed in squat wall (rad)

α_c = coefficient determined by aspect ratio of wall (rad)

α_1 = angle of applied principal compressive stress (2-axis) with respect to longitudinal steel reinforcements (*l*-axis) (rad)

β_u = formed angle between axial direction and diagonal crack (rad)

β_u = deviation angle between angle α_1 and angle α_r (rad)

Δ_s = concentrated shear deformation occurred in length h_s (mm)

$\Delta_{u,W1}$ = ultimate deformation of W1 from test result (mm)

$\Delta_{u,W2}$ = ultimate deformation of W2 from test result (mm)

ε_0 = strain at peak stress, f_c

ε_{cr} = cracking strain of concrete

ε_d = d – directional strain

ε'_d = d – directional strain computed from compatibility conditions

ε_l = biaxial strain in l – direction

ε_r = r – directional strain (r – d coordinate : principal coordinate)

ε_s = strain of reinforcement (arranged in h – v coordinate)

$\overline{\varepsilon_s}$ = uniaxial strain of longitudinal or transverse reinforcement

$\overline{\varepsilon_l}$ = l – directional uniaxial strain

ε_t = t – directional biaxial strain

$\overline{\varepsilon_t}$ = t – directional uniaxial strain

ε_1 = 1 – directional biaxial strain

$\overline{\varepsilon_1}$ = 1 – directional uniaxial strain

ε_2 = 2 – directional biaxial strain

$\overline{\varepsilon_2}$ = 2 – directional uniaxial strain

ϕ_b = reduction factor (0.77)

ϕ_c = material reduction factor (=0.8)

γ_h = fraction of horizontal shear transferred by the horizontal tie in absence of the vertical tie

γ_{hv} = h – v directional shear strain

γ_{lt} = l – t directional shear strain

γ_v = fraction of vertical shear transferred by the vertical tie in absence of the horizontal tie

γ_{12} = 1 – 2 directional shear strain

η = modification factor for deriving one wall panel's strength

κ = coefficient determined by shape of section (rectangular = 1.2)

$\sigma_{d,\max}$ = ultimate compressive stress applied in d - direction (MPa)

$\sigma_k(w)$ = tension softening curve of UHPFRC depending on crack width (MPa)

σ_l = l – directional stress of RC element (MPa)

σ_l^{UHPC} = l – directional stress of UHPFRC (MPa)

σ_t = t – directional stress of RC element (MPa)

σ_t^{UHPC} = t – directional stress of UHPFRC (MPa)

σ_1^c = 1 – directional stress of concrete (MPa)

σ_1^{UHPC} = 1 – directional stress of UHPFRC (MPa)

σ_2^c = 2 – directional stress of concrete (MPa)

σ_2^{UHPC} = 2 – directional stress of UHPFRC (MPa)

ρ_l = longitudinal reinforcement ratio of wall

ρ_s = ratio of longitudinal or transverse reinforcement

ρ_t = transverse reinforcement ratio of wall

$\tau_{\text{interface}}$ = shear stress occurred between squat wall and web retrofitting panel

τ_{lt} = $l - t$ directional shear stress carried by RC element

τ_{lt}^{UHPC} = $l - t$ directional shear stress carried by UHPFRC panel

τ_{12}^{UHPC} = 1 – 2 directional shear stress carried by UHPFRC

τ_{12}^{c} = 1 – 2 directional shear stress carried by concrete

ν = poisson's ratio of concrete (=0.2)

ν_{12} , ν_{21} = Hsu/Zhu ratios

ζ = softening coefficient considering cracking of concrete

ζ' = softening coefficient computed by strain

Chapter 1. Introduction

1.1 Backgrounds

The structural system of almost all low – rise buildings built in 1980's is squat wall structural system. However, they only have squat walls without not only boundary elements, also has only single-layered reinforcement as shown in **Fig. 1-1** due to absence of seismic detail provision at that time.

Since this type of wall is very poor against to seismic load, several retrofit strategies are needed to improve its seismic performance. There are lots of seismic retrofitting methods have been studied, and developed by lots of researchers. One of the most general method is section enlargement method, casting new RC section to retrofitting target[1)]. It's economical and practical advantages make it able to apply at the workplaces. However, it also has disadvantages related to noise, dust, and workability.

The section enlargement method can be applied to the single-layered squat wall in two ways; one is retrofitting at both ends of the squat wall to provide boundary elements (end retrofitting method), the other one is retrofitting at the web surface of the squat wall to enhance its shear strength (web retrofitting method). Therefore it is able to do selective retrofitting by using this method for the single-layered squat wall that has not only poor shear capacity, also poor flexural capacity.

Although the end retrofitting method can enhance the flexural strength of the single-layered squat wall by providing column elements at the both ends of the squat wall, the increased flexural moment capacity of it may cause unexpected shear failure of squat walls. The specification of the retrofitting column element is same as that of structural column; however, there does not

exist any provision considering it. Therefore, the shear strength of the retrofitted squat wall has to be considered.

The existing normal strength concrete section enlargement method is actually ineffective method in architectural view point, because vertical and transverse reinforcements have to be arranged in the enlarged section to improve squat wall's shear capacity. Therefore, the thickness of the enlarged section becomes too thick, and space waste problem can be occurred. To resolve this problem, a new material comes to the fore; the ultra-high performance fiber reinforced concrete (UHPFRC). Its high performance material properties can reduce the thickness of the retrofitting panel, and expected that the fibers mixed in the UHPFRC can play a role of the reinforcements. However, there exists almost no researches related to the retrofitting effect of UHPFRC web retrofitting method.

Period	Property	Detail
1980's	No boundary element	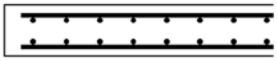
	Single-layered	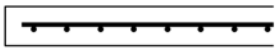
1995~2000	Confined with hoop	
	Concentrated reinforcements at boundary region	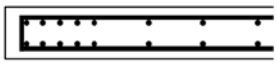
1995~	Confined with U-shaped reinforcement	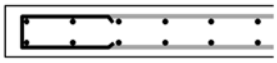

Fig. 1-1 Trend research of reinforcement detail of squat wall used in South Korea (1980's)

1.2 Objective and scopes

The section enlargement method has been researched less than the other retrofitting methods; using FRP, steel plate, and etc., though it is usually used in workplace to improve seismic performance of the squat wall. Therefore, this study planned to evaluate the retrofitting effect of the two applicable ways of the concrete section enlargement method; the end retrofitting method and the web retrofitting method in experimental and analytical way. Consequently, this study classified composition of theme into two sub-themes; retrofitting effect of end retrofitted single-layered squat wall, and retrofitting effect of UHPFRC web retrofitted single-layered squat wall. The objective and scopes of this study is illustrated in **Fig. 1-2**.

Retrofitting effect of end retrofitted single-layered squat wall

This study is going to propose analytical way for the shear strength of the end retrofitted squat wall considering not only details of the column member, also the shear strength of the RC squat wall. Moreover, this study considered compatibility condition between the squat wall and the column considering monolithic behavior of retrofitted member, and included this condition to the proposed model. The proposed model is also applicable to the case of infilled RC squat wall in RC frame inversed retrofitting method of end retrofitting method of this study, but widely used than it if the validity of the proposed model is verified.

Retrofitting effect of UHPFRC web retrofitted single-layered squat wall

Marini, A. and Meda, A. (2009)[2)] fulfilled a test evaluating retrofitting effect of squat wall strengthening with high performance RC jacket. They used UHPFRC jacket with wire mesh to retrofit slender RC wall, and just confirmed the flexural retrofitting effect of the jacket as shown in **Fig. 1-3.** However, there does not exist any research related to not only pure retrofitting effect of the UHPFRC without any tension member, also the shear retrofitting effect of

it. Moreover, web retrofitting of the squat wall is usually conducted at the only one-side web in common site. Therefore, the experimental and analytical study is needed to verify failure mode of the one-side UHPFRC web retrofitted squat wall, and this study planned experimental program and analytical study to confirm it. If the failure mode of the retrofitted wall is confirmed by this study, it is able to suggest proper retrofitting guidelines for the single-layered squat wall retrofitted with the UHPFRC.

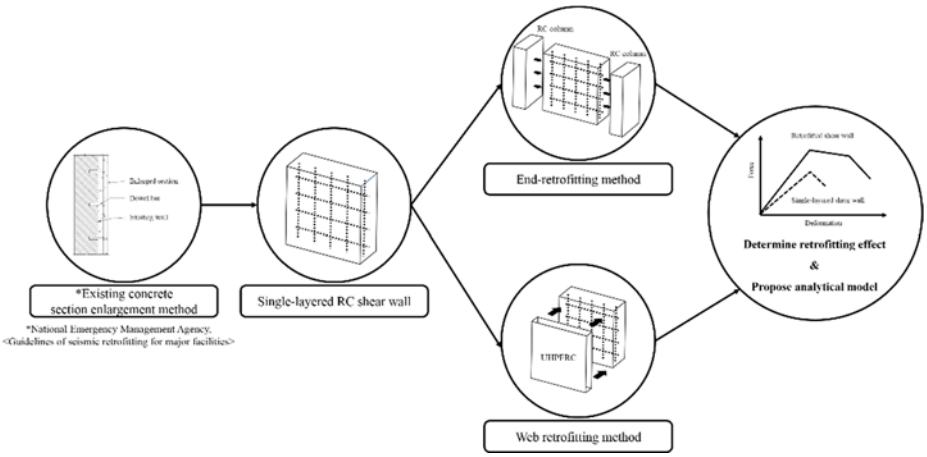

Fig. 1-2 Objective and scopes of this study

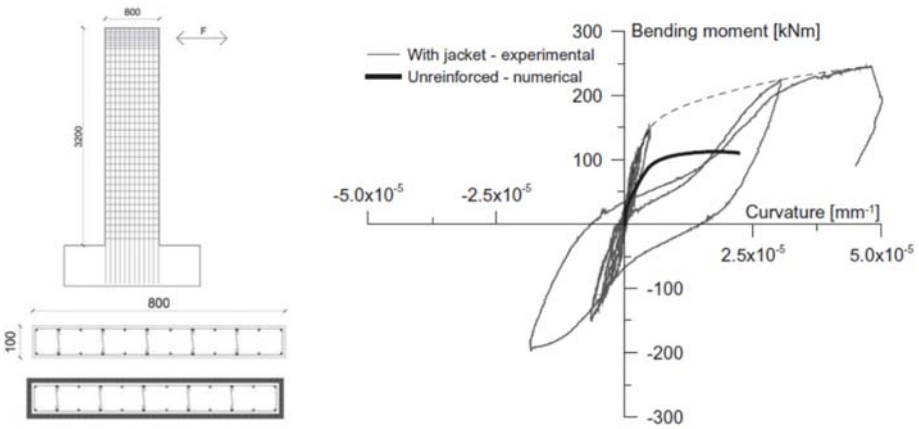

Fig. 1-3 Retrofitting effect of the UHPFRC jacket with wire mesh (A. Marini and A. Meda, 2009)

Chapter 2. End retrofitted single-layered squat wall

2.1 Experimental program

2.1.1 Material & reinforcement detail of retrofitting target

Since this study focused on the single-layered squat wall used for shear wall type low – rise building built in 1980's, material properties and reinforcement detail of the single-layered squat wall are based on structural drawing of existing shear wall type building built in 1980's. Compressive strength of concrete used in the single-layered squat wall is 21 MPa, and SS400 is used for reinforcement of the single-layered squat wall. Therefore, this study designed test specimens with concrete strength of 24 MPa and same type of reinforcement.

Moreover, vertical and horizontal reinforcement ratios of the specimens are also determined from structural drawing of the existing building. One of the single-layered squat walls in the structural drawing has 0.33 % vertical reinforcement ratio and 0.47 % transverse reinforcement ratio with HD10 reinforcement. Therefore, the same ratios are applied to the wall panels of the specimen. Similar to working level, all the vertical and transverse reinforcements in the wall panels are lap spliced with dowel bars from boundary element to observe essential retrofitting effect of the squat wall. Aspect ratio of the squat wall is one to induce shear failure of the wall panel.

Although specimens are planned to be 1 / 2 scaled at the first time, there exist some limitations. Since there's no deformed reinforcement has smaller diameter than HD10 and smaller thickness of the squat wall makes it hard to secure cover thickness of dowel bars placed between the squat wall and

retrofitting column component to behave monolithically, the specimens used geometric value of the original structural drawing only for diameter of vertical, horizontal reinforcements, and thickness of the squat wall. The detail of the wall panel used for retrofitting target is shown in **Fig. 2-1**.

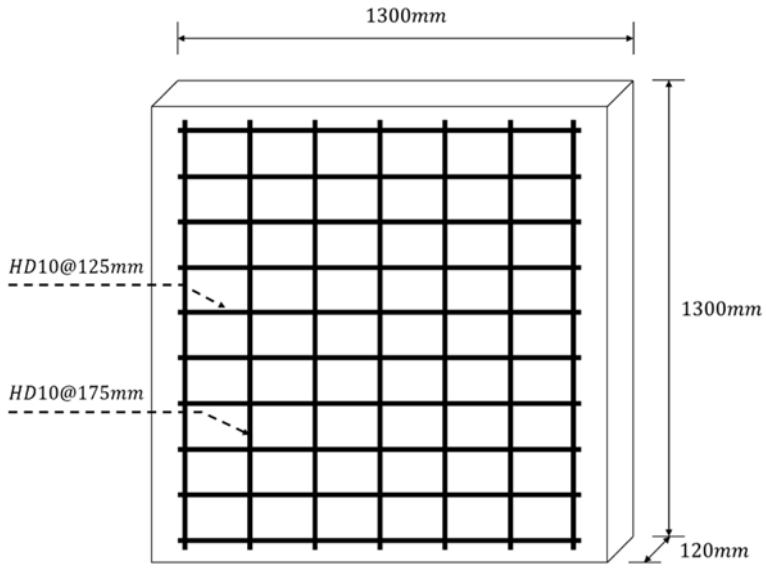

Fig. 2-1 Specification of retrofitting target (for end retrofitting)

2.1.2 Material & reinforcement detail of column component

The geometry of the column element is 250 mm square, and compressive strength of concrete used for providing boundary element to single-layered squat wall is 30 MPa, higher than that of retrofitting target. Since the column component is retrofitted to both ends of the retrofitting target, reinforcements of column are arranged by using dowel bars to behave monolithically. The dowel bars are classified to two types; one is placed at the end face of the single-layered squat wall, another one is placed between foundations and the column element. The former one used HD10 reinforcement, and the latter one used HD16 reinforcement, and both of them used SS400.

The amount of longitudinal reinforcement of the column element is 4-HD16, and that of hoop of it is 9-HD10 @ 150 mm. The arrangement of

longitudinal reinforcement and hoop of the column element are determined without violating any ACI318-11 provisions of reinforcement arrangement for RC column. Moreover, the amounts of dowel bars to prevent shear friction failure can be determined from the ACI318-11. Therefore, the arrangements of vertical and transverse dowel bar can be determined; the former one is 4-HD16, and the latter one is 8-HD10 @ 150 mm. The detail of the column component is shown in **Fig. 2-2.**

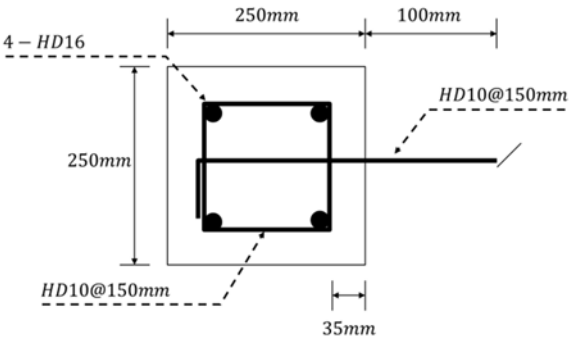

Fig. 2-2 Specification of retrofitting column

2.1.3 Specification of test specimens

To evaluate shear retrofit efficiency of the end retrofitting method, this study planned two types of specimens; one is non retrofitted single-layered squat wall(W1), another is end retrofitted single-layered squat wall(W2).

The test specimens consist of three boundary element, and two wall panel elements. Vladmir Cervenka and Kurt H. Gerstle (1972)[3)] had used this type of specimen to evaluate inelastic behavior of RC wall panel, and they showed that this type of specimen can be used for test of squat wall by concentrating all cracks in the wall panels. The boundary elements located at the both ends of the specimen are used to make fixed boundary condition, and the boundary element located at the center of the specimen used for loading point. Every boundary elements of the specimen has relatively large size to concentrate all cracks into the wall panel. The details of the specimens are shown in **Fig. 2-3** and **Table 1.**

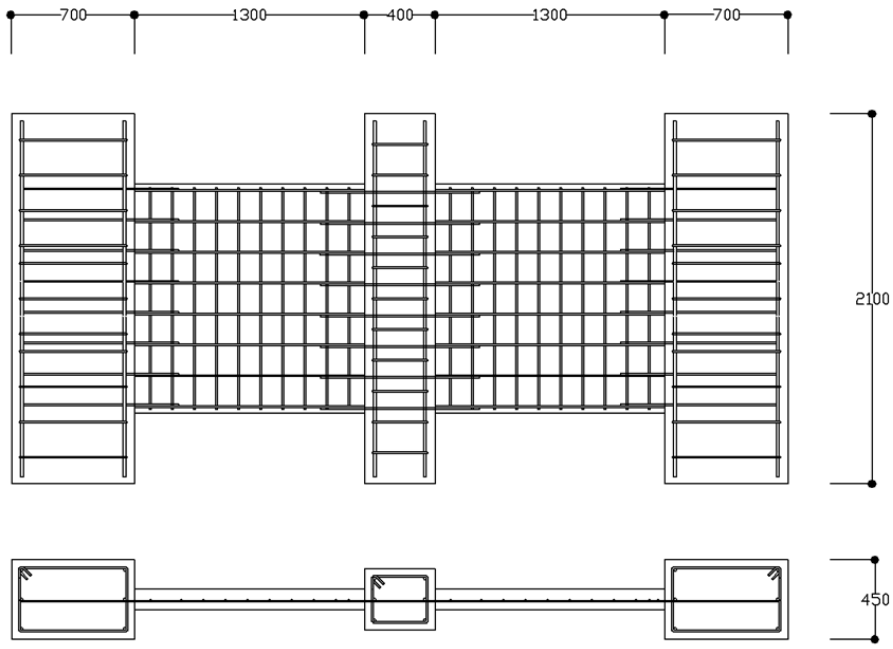

a) Specification of W1

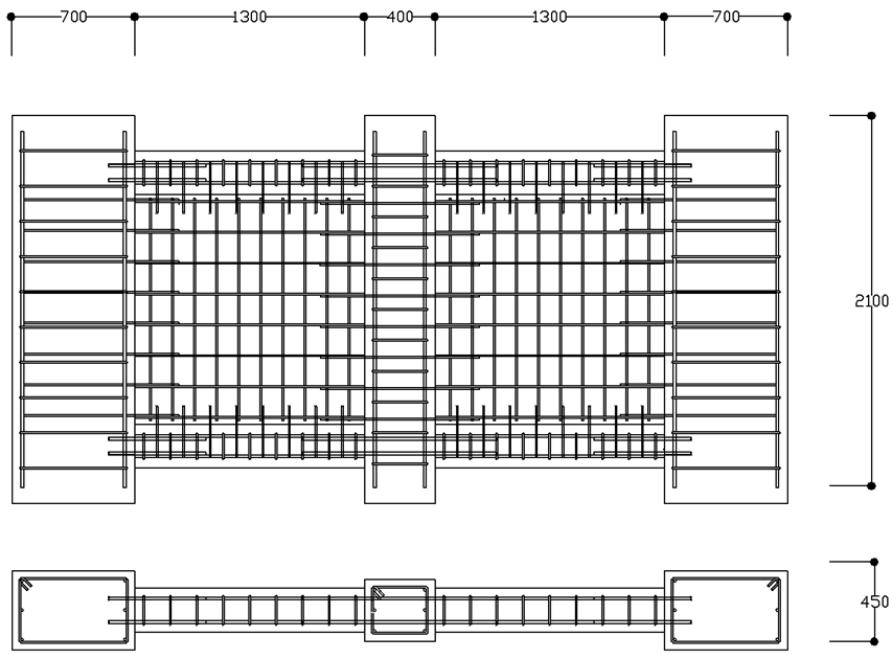

b) Specification of W2

Fig. 2-3 Specification of specimens (W1 & W2)

Table 1 Properties of specimens

	W1	W2	Column (W2)
f_c (Nominal)	24 MPa		30 MPa
f_y (Nominal)	400 MPa (SS400)		
Transverse Rebar	HD10@125 mm		HD10@175 mm
Longitudinal Rebar	HD10@175 mm		4-HD16
Dowel Bar (Transverse)	None	HD10 @ 150 mm	

2.1.4 Retrofitting sequence of W2

The retrofitting sequence of W2 is abided by manual of manufacturing company of epoxy; HILTI Corporation.

The first process is interface roughening to prevent unexpected interface failure. In the site level, Sand-blast is usually used for this process; however, since transverse dowel bars are used in the specimen W2, surface of the wall panel's end region is roughened by using concrete drill. After the roughening process is done, drilling process is proceeded to insert the dowel bars. The depth of the hole is determined from the manual of HILTI Corporation. The depth of the hole for the vertical dowel bar (HD16) is 150 mm, and that for the transverse dowel bar (HD10) is 100 mm. The next process is settlement of dowel bars by using epoxy. After cleaning in the hole, epoxy HIT-RE500 often used in the construction site is injected in the hole, and dowel bars are installed into the hole. Since hardening time is needed to fix the dowel bars' location, the reinforcements of the column component are arranged 24 hours later. After that, concrete for the column is casted. All the processes are illustrated in **Fig. 2-4.**

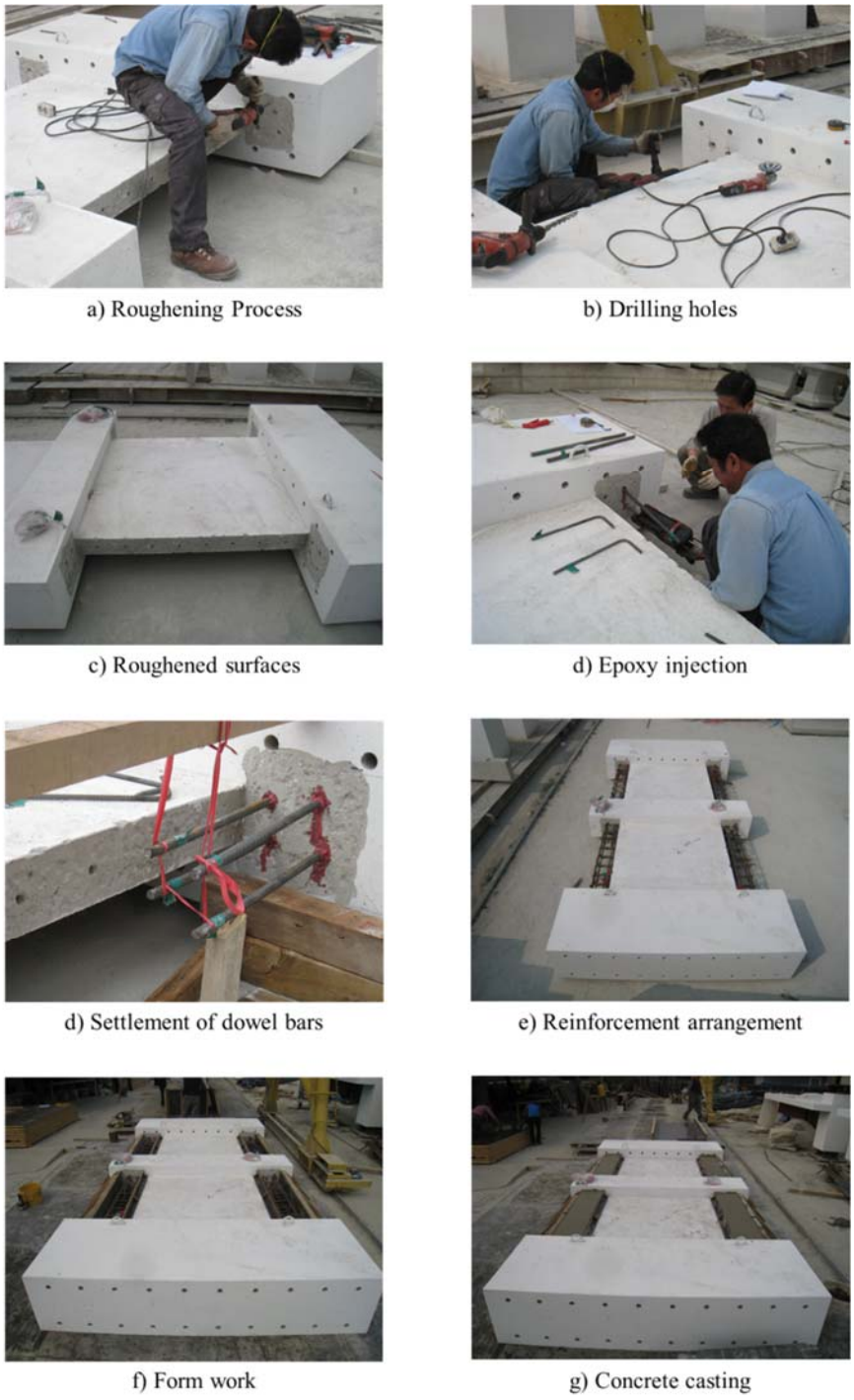

a) Roughening Process

b) Drilling holes

c) Roughened surfaces

d) Epoxy injection

d) Settlement of dowel bars

e) Reinforcement arrangement

f) Form work

g) Concrete casting

Fig. 2-4 Retrofitting sequence

2.1.5 Result of material property test

The mixture proportions of concrete with nominal compressive strength of 24 MPa used for the specimens and 30 MPa used for the retrofitting column component are shown in **Table 2**. The concrete cylinders of them were casted with 100 mm$\times$200 mm size according to KS F 2403 provision. The actual compressive strength, f_c of each nominal compressive strength was measured from average value of direct compressive test results of 3 cylinders. The direct compression test was performed according to KS F 2405 provision. The yield strength of the reinforcements of the wall panel, f_y was measured from direct tension test. The test results are tabulated in **Table 3.**

Table 2 Mixture portions of concrete

Nominal strength (MPa)	W/C (%)	S/a (%)	Unit weight(kgf/m^3)				
			W	C	S	G	Ad
24	49.4	47.5	162	328	869	979	3.50
30	44.2	46.9	165	373	837	966	1.87

Table 3 Strength of concrete and reinforcement

	Concrete (f_c)		Reinforcement (f_y)
Nominal strength	24 MPa	30 MPa	400 MPa
Actual strength (Average value)	26 MPa	25 MPa	488 MPa

2.1.6 Test set-up

Both end boundary elements of the specimens were fixed by using 200 mm diameter bolts to make fixed boundary condition. Each specimen was subjected to monotonic load until the specimen failed by using 200 ton actuator. Moreover, six LVDTs were installed under the specimen to measure force-directional deformation of the specimen. The test set-up and location of each LVDT are shown in **Fig. 2-5.**

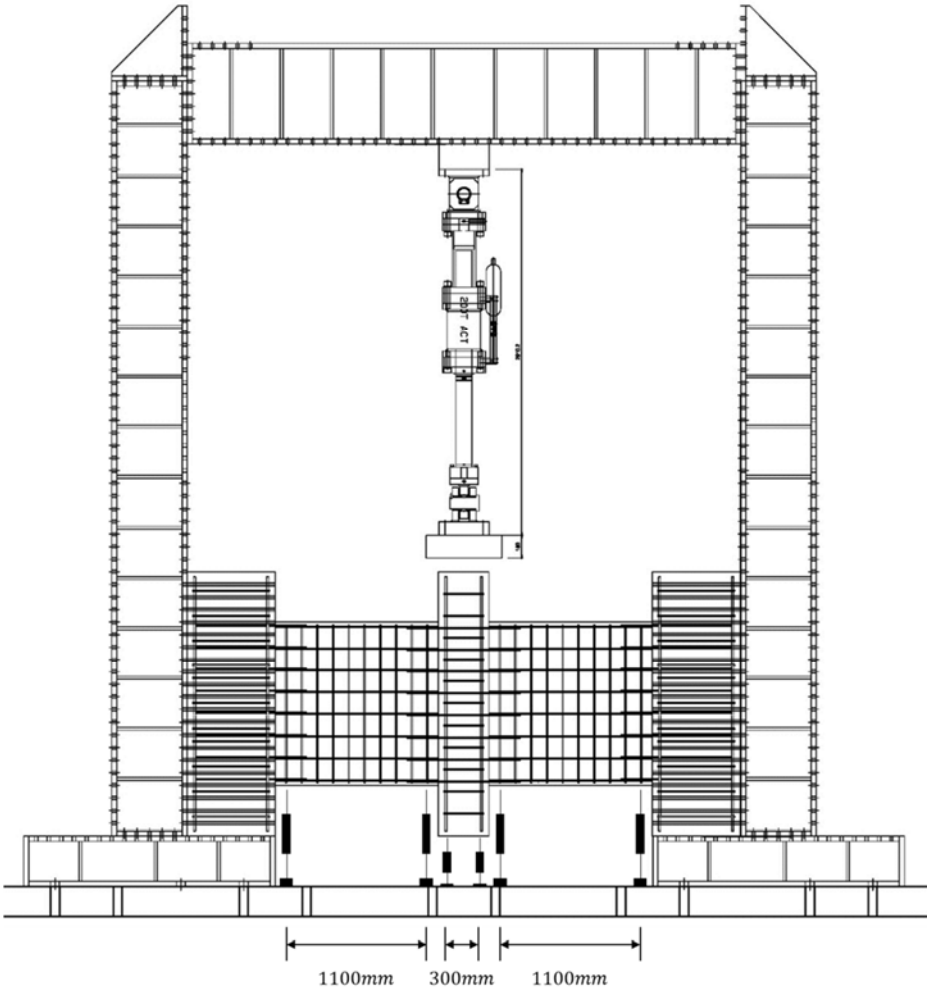

Fig. 2-5 Test set-up (W1 & W2)

In addition, 5 mm steel strain gauges are adhered to vertical and transverse reinforcement of the wall panel to identify whether they are yielded or not. The locations of them are shown in **Fig. 2-6.**

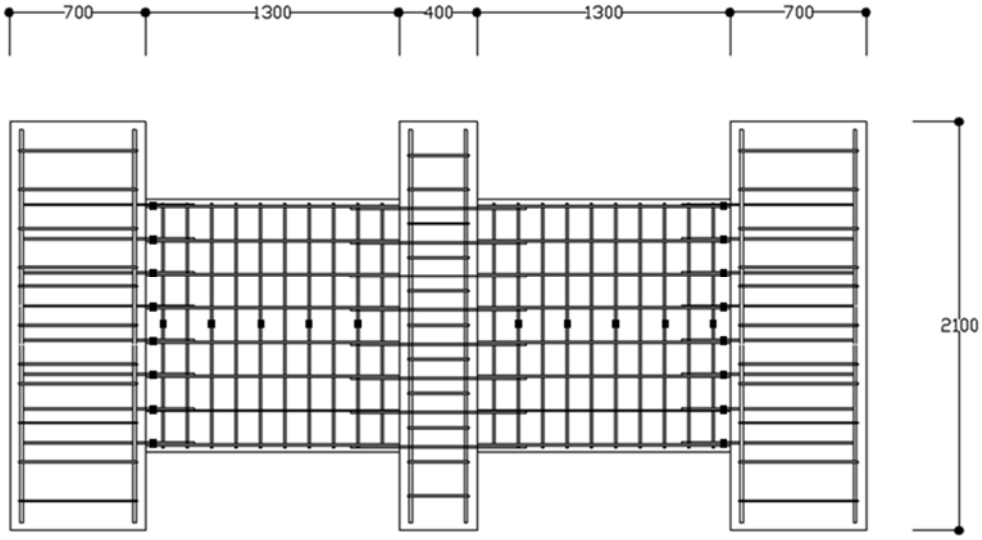

a) Locations of steel strain gauges (W1)

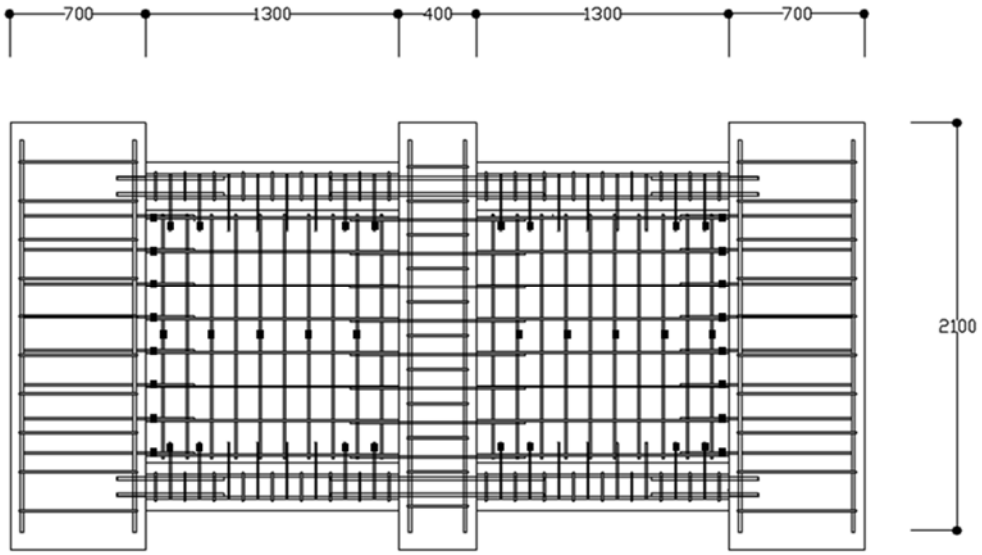

b) Locations of steel strain gauges (W2)

Fig. 2-6 Locations of steel strain gauges (W1 & W2)

2.1.7 Modification factor to derive shear strength of wall panel

Although each specimen of this test is consist of two wall panels, failure of the specimen does not accompanied with failure of two wall panels. The failure of the wall panel cracked in advance is accelerated with load increasing than the other one. After all, the specimen is failed by collapse of the wall panel cracked earlier. However, since the other one also contribute to strength of the specimen some extent, it is need to modify the strength of the specimen to that of the one wall panel. Although comparing transverse reinforcement's strain is rational way to consider shear force contribution of each wall panel, since lots of strain gauges were damaged by an unknown reason, alternative way was needed. Therefore, this study considered the failed wall panel stands at least nominal shear strength of RC squat wall failed by diagonal tension failure, V_n from FEMA 306[4)]. Therefore, this research defined the modification factor, η. (**Equation (1)**)

$$\eta = \frac{V_n}{V_{u,W1}} \qquad (1)$$

where

$V_{u,W1}$ = ultimate strength of W1 from test result (N)

V_n = nominal shear strength of wall failed by diagonal tension failure from FEMA 306 (N)

The nominal shear strength of RC squat wall failed by diagonal tension failure from FEMA 306 can be calculated from below equations. (**Equation (2) or (3)**)

In the case of $h_w / l_w > 2.0$;

$$V_n = A_{cv}(0.17\sqrt{f_c} + \rho_t f_{ty}) \quad (2)$$

In the case of $h_w / l_w < 1.5$;

$$V_n = A_{cv}(0.25\sqrt{f_c} + \rho_t f_{ty}) \quad (3)$$

where

h_w = height of wall section (mm)

l_w = length of wall section (mm)

A_{cv} = net area of concrete section bounded by web thickness and length of section in the direction of shear force considered (mm^2)

ρ_t = transverse reinforcement ratio of wall

f_{ty} = yield strength of shear reinforcement (MPa)

By calculating nominal shear strength of the wall panel of W1 (Aspect ratio=1.0), V_n by using **Equation (3)**, and the ultimate strength of W1, $V_{u,W1}$ from the test result of W1, it is able to derive modification factor, η from **Equation (1)**. Therefore, the shear strength of the end retrofitted single-layered squat wall can be easily derived from the modification factor, η by the ultimate strength of W2, $V_{u,W2}$ from the test result of W2.

2.2 Test results

2.2.1 Test result of W1 (Non-retrofitted single-layered squat wall)

The test result of W1 is shown in **Fig. 2-7**. The ultimate strength of W1, $V_{u,W1}$ is 1,011.24 kN and deformation at that time, $\Delta_{u,W1}$ is 3.92 mm. Since failure of the specimen is accompanied with diagonal tension failure of only one wall panel cracked first as expected, actual shear strength carried by one wall panel is at least nominal shear strength derived from FEMA 306, V_n (559.20 kN). Based on this concept, the modification factor, η could be determined as 0.55 (559.20/1,011.24) from **Equation (1)**. This value can also apply to W2 to determine actual shear strength carried by end retrofitted single-layered squat wall.

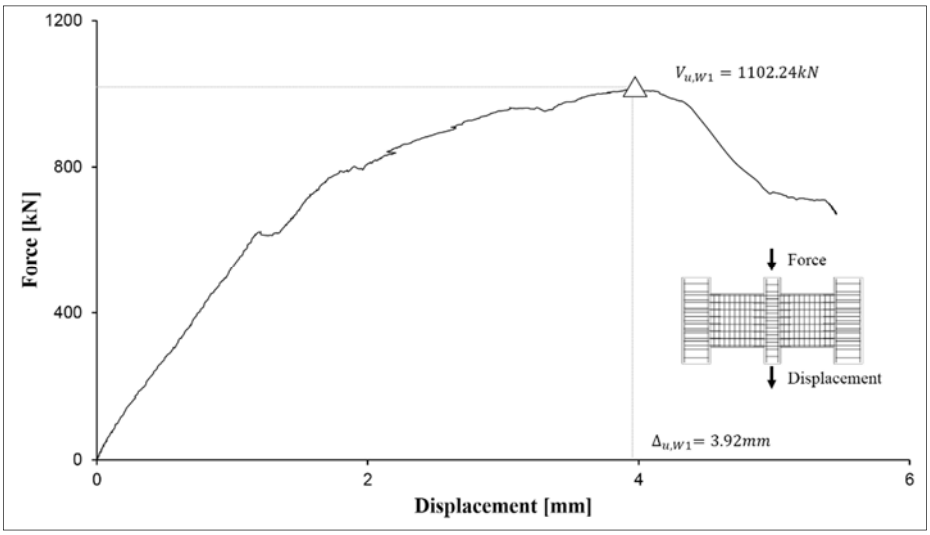

Fig. 2-7 Load-deflection curve of W1

W1 behaved elastically until load reached to about 620 kN without any

crack occurred. After that, major diagonal crack occurred at left side wall panel, and smaller diagonal crack occurred at right side wall panel. Strain of the transverse reinforcement experienced very little change, and had negative values until the diagonal cracks occurred at the wall panels. They behaved elastically after the major diagonal crack is occurred. As load increasing, several fine diagonal cracks forming diagonal strut were propagated at the right wall panel, while there were few small cracks occurred at the right wall panel. From then, there did not arise any cracks at the wall panels, and the deformation was increased with widening the major diagonal crack width occurred at the left wall panel. Finally, W1 failed suddenly accompanied with yielding of transverse reinforcement of right wall panel. The strain variation according to load applied to W1 is shown in **Fig. 2-8,** and crack pattern of W1 at failure is shown in **Fig. 2-9.** However, since several gauges of W1 were damaged, there were limitations to express all strain variations.

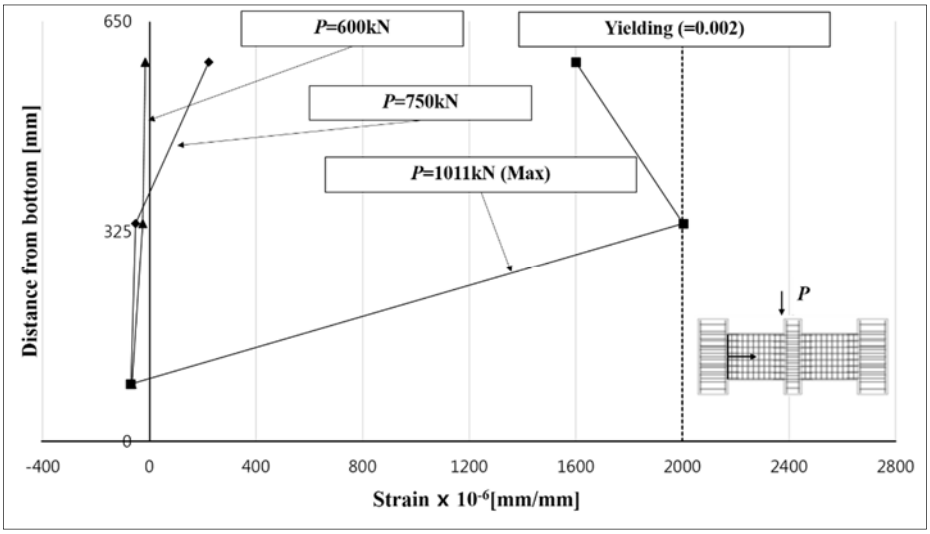

Fig. 2-8 Measured strains of transverse reinforcement in W1

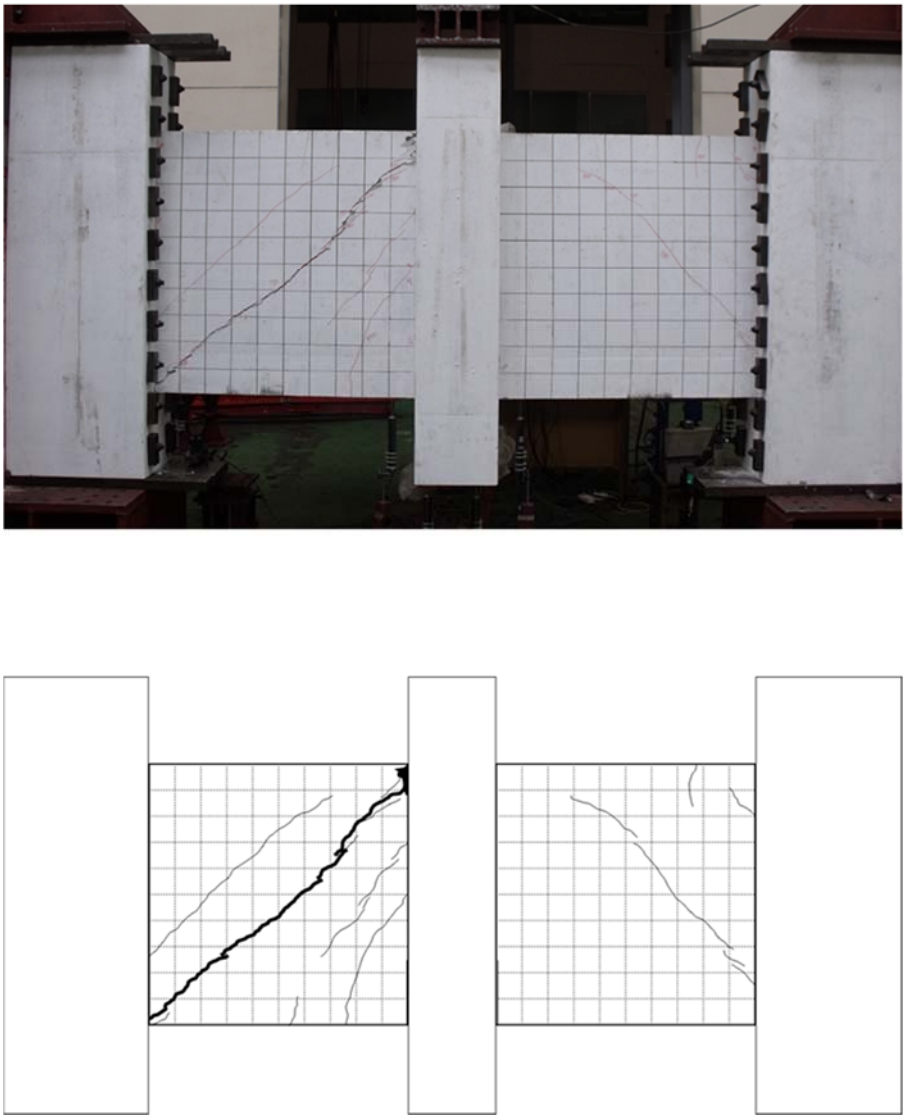

Fig. 2-9 Crack pattern of W1

2.2.2 Test result of W2 (End retrofitted single-layered squat wall)

The test result of W2 is shown in **Fig. 2-10**. The ultimate strength of W2, $V_{u,W2}$ is 1,903.11 kN, and deformation at that time, $\Delta_{u,W2}$ is 6.36 mm. Since failure of the specimen is accompanied with failure of only one wall panel cracked first similar to that of W1, the modification factor, η (=0.55) derived from W1's result can be used to determine shear force carried by one retrofitted single-layered squat wall by multiplying η and $V_{u,W2}$. Therefore, it is able to verify the shear strength of the retrofitted single-layered squat wall is 1,046.71 kN (=0.55×1,903.11).

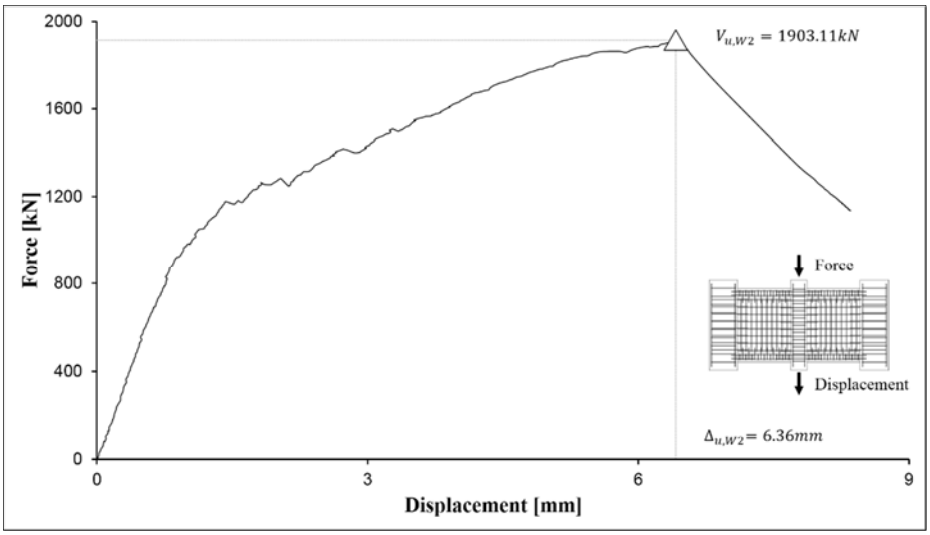

Fig. 2-10 Load-deflection curve of W2

W2 behaved elastically until the load reached to about 900 kN without any crack occurred. After that, major diagonal crack occurred at both side wall panels. Strain of transverse reinforcement experienced very little change until the major diagonal cracks occurred at the wall panels, similar to W1's result. Different from the behavior of W1, deformation of the specimen was increased

with occurrence of many diagonal cracks forming several diagonal struts in the both wall panels instead of widening major diagonal crack width. Moreover, few flexural cracks were occurred at the center of the retrofitting column after the several diagonal cracks were fully formed at the wall panels. Finally, shear cracks are occurred at the end of retrofitting column forming diagonal strut at the wall panel, and W2 suddenly failed with widening width of major diagonal crack of the left wall panel and shear crack of retrofitting column. Until W2 failed, there did not arise any interface failure between the retrofitting columns and the wall panels. The strain variation according to load applied to W2 is shown in **Fig. 2-11,** and crack pattern of W2 at failure is shown in **Fig. 2-12.** Similar to the case of W1, since several gauges of W2 were damaged, there were limitations to express all strain variations.

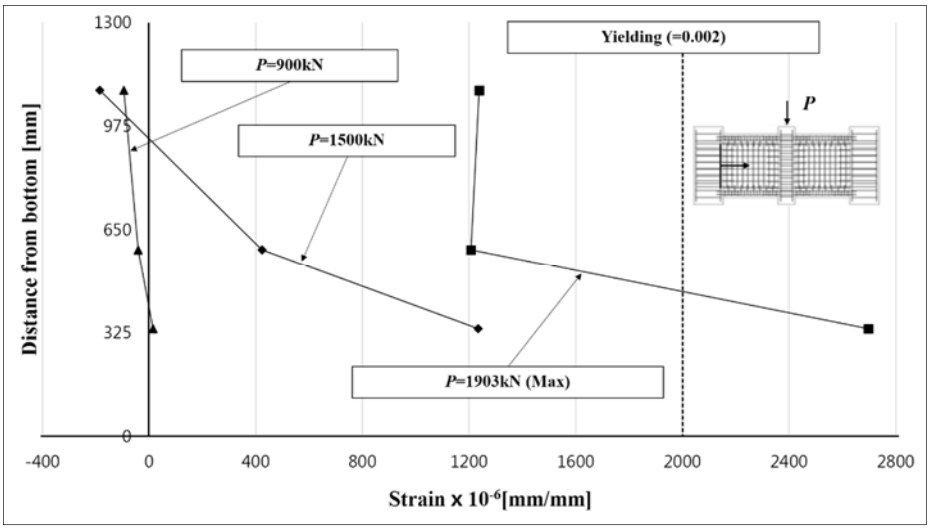

Fig. 2-11 Measured strains of transverse reinforcement in W2

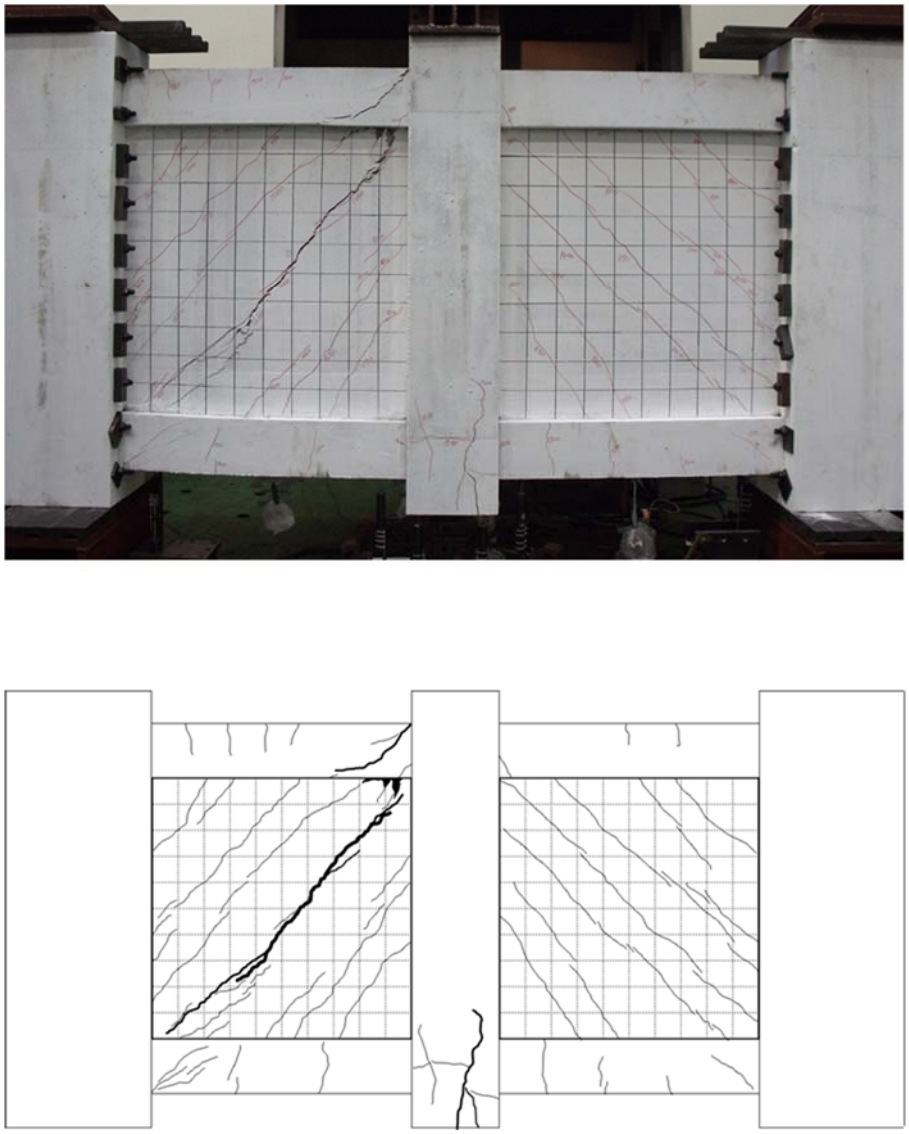

Fig. 2-12 Crack pattern of W2

However, when the load reached over 1,500 kN, a large flexural crack occurred at bottom face of the boundary element located at the center of the specimen. It is due to that there was no flexural reinforcement at the bottom face of the center boundary element where the maximum moment was applied when W2 begin to behave in beam-behavior. This flexural crack propagated to upside until W2 failed. The propagated flexural crack is shown in **Fig. 2-13.**

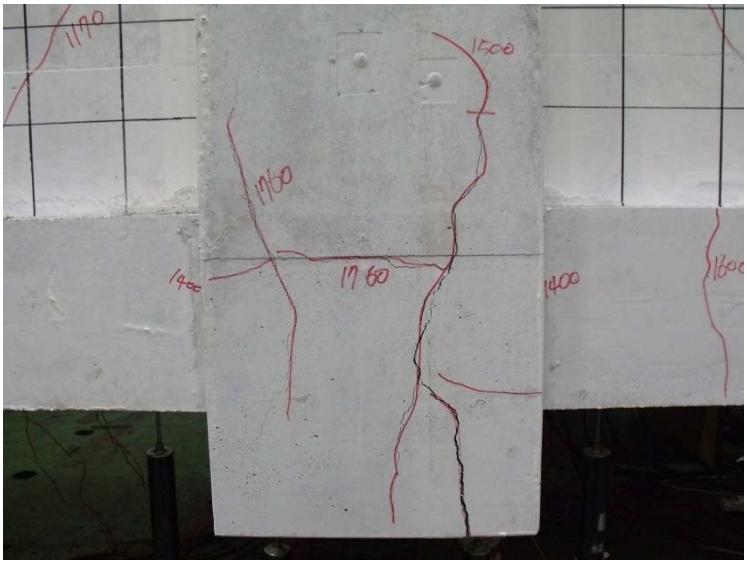

Fig. 2-13 Flexural cracks occurred at boundary element (W2)

There were no interface failure between the squat wall and the retrofitting column until the failure of W2. Therefore, it was confirmed that the existing provision for the shear friction reinforcement can prevent interface failure of end retrofitted squat wall.

2.2.3 Retrofitting effect of end retrofitting method

The comparison result between W1 and W2 is shown in **Fig. 2-14**. The initial stiffness of the specimen is measured from linear portion of the test result. That comparison result shows that end retrofitting method almost doubled non retrofitted single layered squat wall's initial stiffness and ultimate strength. Moreover, end retrofitting column can enhance deformation ability a little with prevent immediate diagonal tension failure accompanied with yielding of transverse reinforcement occurred in W1 though the failure mode of W2 was also governed with diagonal tension failure. However, the transverse reinforcement of W2 could experience more strain beyond its yield strain by retrofitting column members placed at the both ends of the squat wall as shown in **Fig. 2-8** and **Fig. 2-11**. Therefore, more distributed struts occurred in W2 can be explained by this strain behavior.

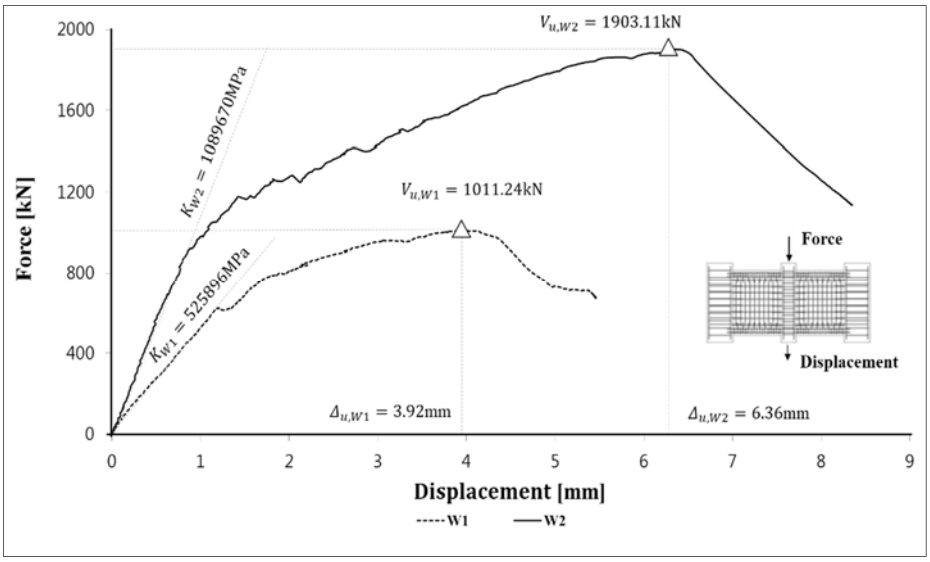

Fig. 2-14 Comparison result (W1 & W2)

.

2.3 Proposed equation to evaluate shear strength of end retrofitted single-layered squat wall

2.3.1 Existing provisions (ACI318-11)

There exist several provisions to evaluate shear strength of squat wall existing provisions. ACI318-11[5)], the most general provision used to evaluate shear strength of squat wall suggests two types of equations for this purpose. One is for general shear wall without considering seismic details; boundary elements. (**Equation (4)**) Another one is for shear wall with seismic details; therefore, it considers squat wall's aspect ratio in the equation. (**Equation (6)**)

$$V_n = V_c + V_s \tag{4}$$

$$V_c = 0.28\sqrt{f_c}\,t_w d + \frac{N_u d}{4l_w} \tag{5a}$$

$$V_s = \frac{A_{vh} f_y d}{s_h} \tag{5b}$$

$$V_n = A_{cv}(\alpha_c \sqrt{f_c} + \rho_t f_y) \tag{6}$$

where,

V_c = nominal shear strength provided by concrete (N)

V_s = nominal shear strength provided by shear reinforcement (N)

t_w = thickness of wall (mm)

d = effective length of wall section ($= 0.8l_w$, ACI 349-06) (mm)

N_u = factored axial force applied to wall section (N)

A_{vh} = area of transverse reinforcement (mm^2)

s_h = spacing of transverse reinforcement (mm^2)

α_c = coefficient determined by aspect ratio of wall

(1/4 for $h_w / l_w \leq 1.5$, and 1/6 for $h_w / l_w \geq 2.0$)

Since these equations proposed by not only ACI318-11, also FEMA306 do not have any terms about retrofitting column's detail, they cannot be used directly for the end retrofitted squat wall. However, this study tried to apply these equations to the test result of W2 for verifying applicability of these equations to the end retrofitted squat wall by neglecting reinforcement details of retrofitting column component. The comparison result is shown in **Table 4**.

Table 4 Nominal shear strength of existing provisions

	$\eta V_{u,W2}$ (kN)	ACI318-11 (kN) (General wall) (Eq. (4))	ACI318-11 (kN) (Wall with seismic detail) (Eq. (6))	FEMA306 (kN) (Diagonal tension failure) (Eq. (2) or (3))
V_n	1,046.71	645.86	1,007.28	1,076.21
$\eta V_{u,W2}$	1.00	0.62	0.96	1.03

Table 4 shows the proposed equation of squat wall with seismic detail from ACI318-11 and squat wall failed with diagonal tension failure from FEMA306 can predict shear strength of W2. However, since they does not consider shear strength of retrofitting column, new analytical model considering not only shear strength of squat wall, also detail of retrofitting column. Therefore, this study suggested a new analytical model for evaluating shear strength of retrofitted squat wall with considering these contributions.

2.3.2 Proposed analytical model

To propose a new analytical model to evaluate end retrofitted squat wall with considering detail of retrofitting column member, this study revised existing analytical model for analyzing the retrofitted squat wall. The existing model used for it has to be referred first.

Hwang et al.[6)] proposed analytical flow chart using strut-and-tie load paths that shows how lateral force transfer within the RC shear wall. This load paths is consist of 3 strut mechanisms; diagonal strut mechanism, flat strut mechanism, and steep strut mechanism. The diagonal strut mechanism is consist of only a single diagonal compression strut, and its strut width, a_s is same as the depth of the compression zone at the base of the wall. The flat strut mechanism includes one transverse tie and two flat struts, and the steep strut mechanism is composed of one vertical tie and two steep struts. These strut mechanisms are behaved with same strut width, a_s as shown in **Fig. 2-15**. Moreover, Hwang et al. used stiffness ratios between these mechanisms, R_d, R_h, R_v and this study used them to calculate shear force carried by the squat wall.

However, since validity of the existing model was verified only for general type of shear wall that has boundary elements, the end retrofitted single layered squat wall cannot be analyzed directly by using this model. There does not also exist any terms related with details of retrofitting column in this model. Moreover, the existing model used the strut width, a_s as the depth of the flexural compression zone of an elastic column from Paulay and Priestley's equation. Therefore, this study assumed the length h_s that shear deformation of column is occurred intensively, and used this length for compatibility condition between the column and the squat wall. The length h_s satisfied this condition can be used for computing the width of the strut width, a_s.

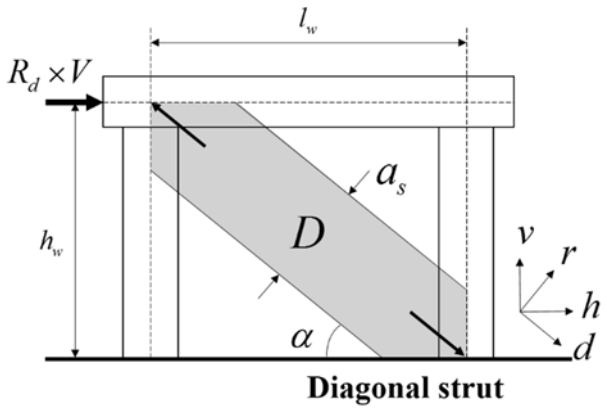

a) Diagonal strut mechanism

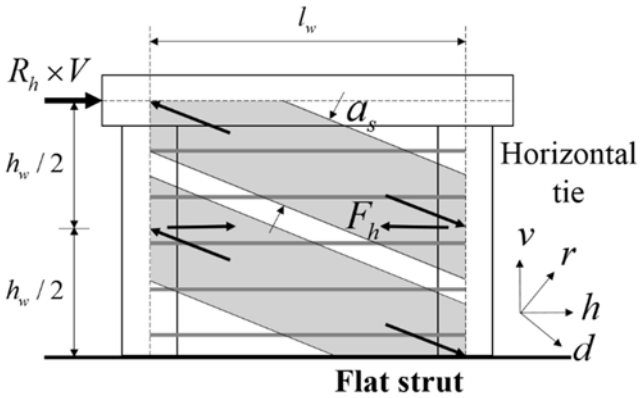

b) Flat strut mechanism

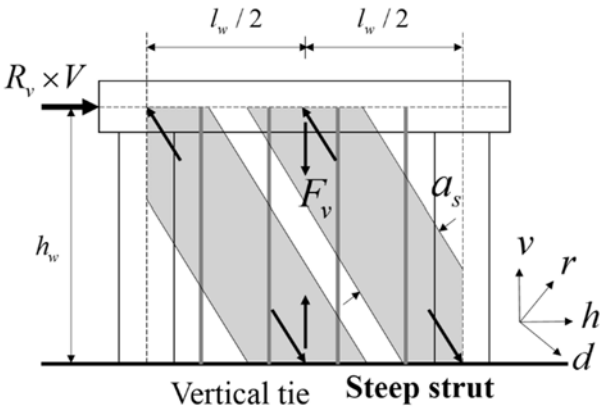

c) Steep strut mechanism

Fig. 2-15 Wall shear resisting mechanisms (Shyh-Jiann Hwang et al., 2001)

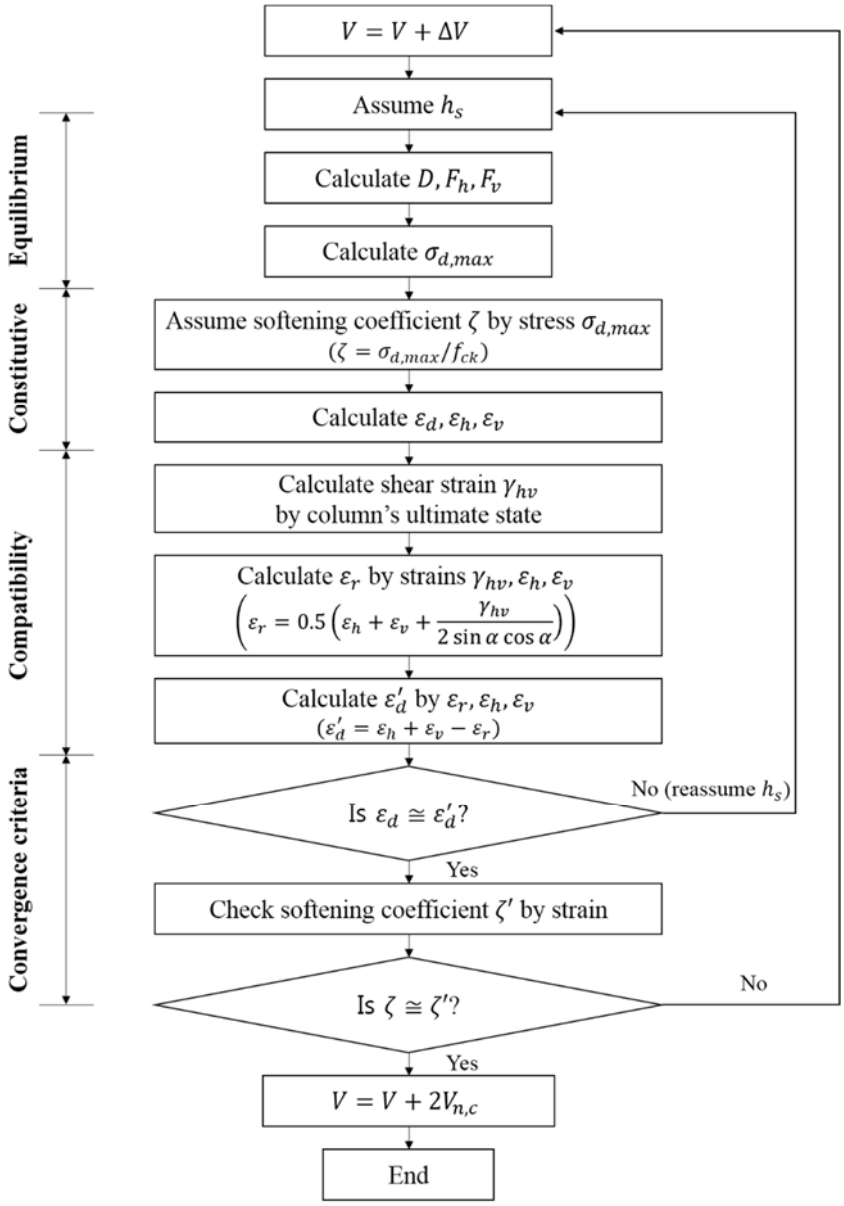

Fig. 2-16 Proposed flow chart to analyze end retrofitted squat wall considering detail of column

Based on these studies, this study proposed a flow chart to evaluate shear strength of the end retrofitted single-layered squat wall as shown in **Fig. 2-16**. The equilibrium conditions, constitutive relationships, and compatibility conditions used in this model are summarized in the below.

a) Equilibrium conditions

For the assumed ultimate shear force carried by the squat wall V and the length h_s of the concentrated shear deformation of the column is occurred, it is able to compute shear strength contributions of three strut mechanisms; horizontal portion of diagonal compression, D from diagonal strut mechanism, tension applied to transverse tie, F_h from the flat strut mechanism, and horizontal portion of tension applied to vertical tie, F_v of the steep strut mechanism as shown in below equilibrium equation (**Equation (7)**).

$$V = -D\cos\alpha + F_h + F_v \cot\alpha \qquad (7)$$

where

D = strength of diagonal strut from diagonal strut mechanism (N)

F_v = strength of vertical tie from steep strut mechanism (N)

F_h = strength of horizontal tie from flat strut mechanism (N)

Moreover, since relative stiffness ratio between these three strut mechanisms were already suggested as below equations depending on aspect ratio of the squat wall, (**Equation (8a~8c)**) it is able to compute shear strength contributions of three strut mechanisms.

$$-D\cos\alpha : F_h : F_v \cot\alpha = R_d : R_h : R_v \qquad (12a)$$

$$\frac{R_h}{R_d} = \frac{\gamma_h}{1-\gamma_h} \qquad (12b)$$

$$\frac{R_v}{R_d} = \frac{\gamma_v}{1-\gamma_v} \qquad (12c)$$

where

$\frac{R_h}{R_d}$ = relative stiffness ratio between horizontal and diagonal mechanism

$\frac{R_v}{R_d}$ = relative stiffness ratio between vertical and diagonal mechanism

γ_h = fraction of horizontal shear transferred by the horizontal tie in absence of the vertical tie $\left(= \frac{2\tan\alpha - 1}{3}\right)$

γ_v = fraction of vertical shear transferred by the vertical tie in absence of the horizontal tie $\left(= \frac{2\cot\alpha - 1}{3}\right)$

α = angle of diagonal strut formed in squat wall ($\tan^{-1}\left(h_w / l_w\right)$) (rad)

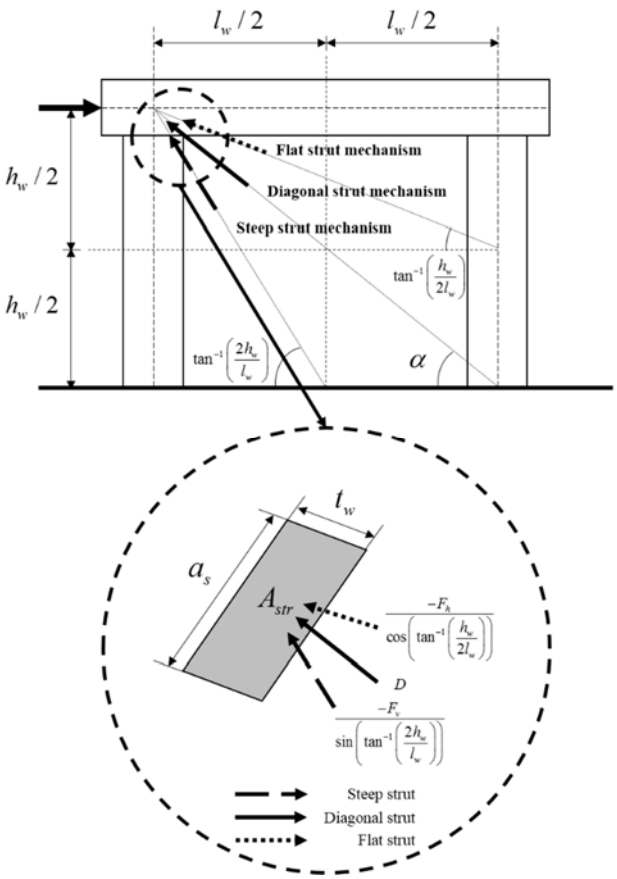

Fig. 2-17 Applied forces to strut section

Based on the forces carried by each strut mechanism, it is able to determine the forces applied to the strut section area A_{str} orthogonal to d -direction as shown in **Fig. 2-17**. The strut section area A_{str} can be computed by thickness of the squat wall, t_w times the strut width, a_s. Therefore, the ultimate compressive stress applied in d – direction, $\sigma_{d,\max}$ when the ultimate shear force V is carried by the squat wall can be computed by below equation.

$$\sigma_{d,\max} = \frac{1}{A_{str}}\left\{ D - \frac{\cos\left(\alpha - \tan^{-1}\left(\frac{h_w}{2l_w}\right)\right)}{\cos\left(\tan^{-1}\left(\frac{h_w}{2l_w}\right)\right)} F_h - \frac{\cos\left(\tan^{-1}\left(\frac{2h_w}{l_w}\right) - \alpha\right)}{\sin\left(\tan^{-1}\left(\frac{2h_w}{l_w}\right)\right)} F_v \right\} \quad (13)$$

where

$\sigma_{d,\max}$ = ultimate compressive stress applied in d – direction (MPa)

A_{str} = area of strut section $\left(= a_s \times t_w\right)$ (mm^2)

b) Constitutive relationships

The constitutive relationship of the cracked concrete used Zhang and Hsu's model considering softening coefficient. Since this model is aimed to derive the ultimate shear strength of the squat wall, only ascending branch of the model is used.

In the case of $\frac{-\varepsilon_d}{\zeta\varepsilon_0} \le 1.0$

$$\sigma_d = -\zeta f_c \left[2\left(\frac{-\varepsilon_d}{\zeta\varepsilon_0}\right) - \left(\frac{-\varepsilon_d}{\zeta\varepsilon_0}\right)^2 \right] \quad (14)$$

where,

ζ = softening coefficient considering cracking of concrete

ε_d = d – directional strain (r – d coordinate : principal coordinate)

ε_0 = strain at peak stress f_c $\left(=0.002+0.001\left(\frac{f_c-20}{80}\right)\right)$

The softening coefficient ζ can be computed by using compressive strength of the concrete, f_{ck} and r – directional strain values as below equation.

$$\zeta=\frac{5.8}{\sqrt{f_c}}\frac{1}{\sqrt{1+400\varepsilon_r}}\leq\frac{0.9}{\sqrt{1+400\varepsilon_r}} \tag{15}$$

where

ε_r = r – directional strain (r – d coordinate : principal coordinate)

Moreover, the constitutive relationship of the reinforcement used bilinear assumption. These relationships can be applied to compute forces carried by horizontal and vertical tie of flat and steep strut mechanisms.

In the case of $\varepsilon_s < \varepsilon_y$

$$f_s = E_s\varepsilon_s \tag{16a}$$

In the case of $\varepsilon_s \geq \varepsilon_y$

$$f_s = f_y \tag{16b}$$

where

ε_s = strain of reinforcement (arranged in $h - v$ coordinate)

E_s = young's modulus of reinforcement (MPa)

f_s = stress of reinforcement (MPa)

f_y = yield stress of reinforcement (MPa)

When computing the cross area of the horizontal tie A_{th}, it is assumed that the horizontal shear reinforcement within the center half of the squat wall is fully effective, and the other horizontal reinforcement is included as 50% effective. The cross area of the vertical tie A_{tv}, includes only the vertical shear reinforcement within the squat wall web and excludes without boundary elements. For a squat wall without boundary elements, the vertical shear reinforcement within the central portion of $0.8l_w$ is considered effective to constitute the vertical tie. Therefore, the forces carried by the horizontal and the vertical tie, F_h and F_v can be computed by below equations.

$$F_h = A_{th} E_s \varepsilon_h \leq F_{yh} \tag{17}$$

$$F_v = A_{tv} E_s \varepsilon_v \leq F_{yv} \tag{18}$$

where,

A_{th} = area of effective transverse reinforcement (mm^2)

A_{tv} = area of effective vertical reinforcement (mm^2)

c) Compatibility conditions

The compatibility relationship between the strains in the principle coordinate of RC element (r – d coordinate) and the arranged reinforcement coordinate (h – v coordinate) can be expressed in below equations. This model assumed that the principle direction of RC element is same as that of the diagonal strut.

$$\varepsilon_v = \varepsilon_r \cos^2 \alpha + \varepsilon_d \sin^2 \alpha \tag{19}$$

$$\varepsilon_h = \varepsilon_r \sin^2 \alpha + \varepsilon_d \cos^2 \alpha \tag{20}$$

$$\frac{\gamma_{hv}}{2} = (\varepsilon_r - \varepsilon_d) \sin \alpha \cos \alpha \tag{21}$$

where

γ_{hv} = h – v directional shear strain

The first strain invariant can be derived by summing the **Equation (19)** and **Equation (20)**. That condition implies the strain relationship between the strains of the r – d coordinate and that of the h – v coordinate regardless of the angle of the principle coordinate, α.

$$\varepsilon_r + \varepsilon_d = \varepsilon_h + \varepsilon_v \tag{22}$$

Moreover, this study suggested additional compatibility condition considering monolithic behavior of end retrofitted member. The shear deformation of the retrofitting column is concentrated in the length h_s due to strut action of the squat wall as shown in **Fig. 2-18**. Since this length forms strut width formed in the squat wall by monolithic behavior, it's able to compute strut width a_s by using h_s.

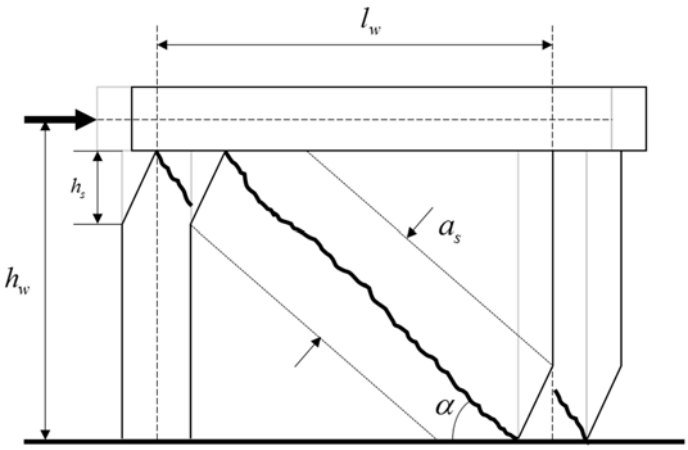

Fig. 2-18 Deformed shape of retrofitted squat wall

$$a_s = 2h_s \cos\alpha \tag{23}$$

The concentrated shear deformation Δ_s occurred in the length h_s from the nominal shear strength of the retrofitting column $V_{n,c}$ from ACI318-11 (**Equation (4)**) can be computed from the below equation[7)].

$$\Delta_s = V_{n,c} h_w \left(\frac{\kappa}{GA_{eff}} \right) \tag{24}$$

where

Δ_s = concentrated shear deformation occurred in length h_s (mm)

$V_{n,c}$ = nominal shear strength of retrofitting column (N) (ACI318-11)

κ = coefficient determined by shape of section (rectangular = 1.2)

GA_{eff} = effective shear stiffness of retrofitting column (MPa)

Since the effective shear stiffness considers cracking of concrete section, this study assumed that reduction degree of the shear stiffness of the

retrofitting column section is same as that of the flexural stiffness of the section due to concrete cracking. The effective flexural stiffness EI_{eff} can be expressed for yield moment – yield curvature ratio from the moment – curvature relationship of the column section. Therefore, the effective shear stiffness can be computed based on this assumption.

$$GA_{eff} = \frac{A_c}{2(1+\nu)} \frac{EI_{eff}}{I_c} \tag{25}$$

where

A_c = area of retrofitting column section (mm^2)

ν = poisson's ratio of concrete (=0.2)

EI_{eff} = effective flexural stiffness considering cracking concrete (MPa)

($EI_{eff} = M_y / \phi_y$)

I_c = moment of inertia of retrofitting column section (mm^4)

From the **Equation (24)** to **Equation (25)**, the concentrated shear deformation of the column Δ_s can be derived. This deformation can be used for computing the shear strain γ_{hv} occurred in the retrofitting column as shown in the below equation.

$$\gamma_{hv} = \frac{\Delta_s}{h_s} \tag{26}$$

As shown in **Fig. 2-18**, this study assumed that both the squat wall and the retrofitting column reaches the ultimate state simultaneously, the shear strain of the strut formed in the squat wall is also same as γ_{hv}. Therefore, it is

able to compute r – directional strain ε_r from the shear strain γ_{hv}, ε_h, and ε_v by summing two compatibility equations (**Equation (21)** and **Equation (22)**).

$$\varepsilon_r = 0.5\left(\varepsilon_h + \varepsilon_v + \frac{\gamma_{hv}}{2\sin\alpha\cos\alpha}\right) \tag{26}$$

Based on the computed r – directional strain ε_r, d – directional strain ε_d' for verifying validity of the assumed length can be computed by using the first strain invariant (**Equation (22)**).

$$\varepsilon_d' = \varepsilon_h + \varepsilon_v - \varepsilon_r \tag{27}$$

where

ε_d' = d – directional strain computed from compatibility conditions

d) Convergence criteria

To verify validity of the assumed values (V and h_s), this study suggested two convergence criteria. The first convergence criteria compared d – directional strain ε_d and ε_d' computed from different equations. The former value, ε_d is derived from the constitutive relationship of the concrete (**Equation (14)**), and the latter value, ε_d' is derived from the compatibility condition computed from ε_r, ε_h, and ε_v (**Equation (14)**). If difference between these two values does not become to be zero, the length h_s which concentrated shear deformation is occurred has to be reassumed. If the difference becomes to be zero, the second convergence criteria has to be proceeded.

The second convergence criteria compared the softening coefficient ζ and ζ' computed from different equations similar to the process of the first convergence criteria. The former value, ζ is derived from the d – directional stress occurred in the squat wall, $\sigma_{d,\max}$ divided by the concrete compressive strength of the squat wall, f_c. The latter value, ζ' is derived from the r – directional strain, ε_r and the concrete strength of the squat wall, f_c (**Equation (15)**). If difference between these two values does not become to be zero, the shear force carried by the squat wall, V has to be reassumed. If the difference becomes to be zero, the shear strength of the end retrofitted squat wall, V can be computed by summing shear strength of the retrofitting column, $V_{n,c}$ twice.

e) Initial stiffness of end retrofitted squat wall

Initial stiffness of the end retrofitted squat wall can be easily computed by transferring end retrofitted squat wall's resisting mechanism against lateral force to the single diagonal strut mechanism. The initial stiffness of the single diagonal strut, K can be computed by below equation[8)].

$$K = \frac{E_c^w a_s' t_w}{\sqrt{h_w^2 + l_w^2}} \cos^2 \alpha \qquad (28)$$

where

E_c^w = young's modulus of squat wall's concrete (MPa)

a_s' = modified width of single diagonal strut (mm)

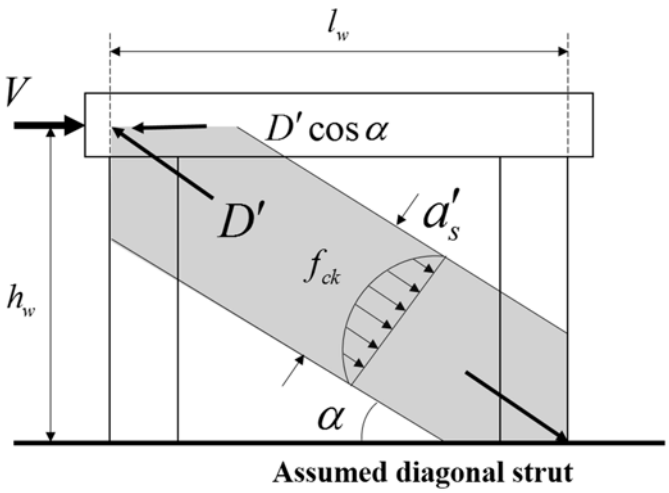

Fig. 2-19 Assumed diagonal strut model for computing initial stiffness of retrofitted squat wall

When shear strength of the end retrofitted squat wall, V is computed from the flow chart of this study as shown in **Fig. 2-16**, modification process is needed to transfer resisting three strut mechanisms to the modified single diagonal strut with strut width, a'_s as shown in **Fig. 2-19**. Since the assumed resisting mechanism of the retrofitted squat wall is the modified single diagonal strut, horizontal portion of the strength of the modified diagonal strut, $D'\cos\alpha$ is same as V from the result of this study's flow chart. The strength of the modified diagonal strut, D' can be computed by below equation.

$$D' = 0.65 f_{ck} a'_s t_w \tag{29}$$

Therefore, the width of the modified single diagonal strut, a'_s can be derived from V and D'.

$$a'_s = \frac{V}{0.65 f_{ck} t_w \cos\alpha} \tag{30}$$

2.3.3 Validity of proposed model

This study also confirmed validity of the proposed model for evaluating retrofitting effect of end retrofitted squat wall. Therefore, this study evaluated shear strength and initial stiffness of the end retrofitted squat wall by using the proposed model of this study, and compared it with the experimental results of W2 and that of the existing provisions; ACI318-11, FEMA306, and the proposed model by Hwang et al. These results are shown in **Table 5**.

Table 5 Comparison results (End retrofitted squat wall)

	$\eta V_{u,W2}$ (kN)	Proposed Method (kN) (Eq. 14)	ACI318 (kN) (Eq. (4))	ACI318 (kN) (Eq. (6))	FEMA306 (kN) (Eq. (2) or (3))	Shyh-Jiann Hwang et al. (kN)
V	1,046.71	998.26	645.86	1,007.28	1,076.21	636.41
$\frac{V}{\eta V_{u,W2}}$	1.00	0.95	0.62	0.96	1.03	0.61

a) Shear strength

	Experimental (K_e) (MPa)	Analytical (K) (MPa)
K_e	587,508	572,086
K / K_e	1.0	0.97

b) Initial stiffness

As shown in **Table 5**, proposed model can predict not only shear strength, also initial stiffness of the end retrofitted squat wall closely than the other methods. Moreover, the proposed model of this study has the merit of reflecting the details of the retrofitting column than existing models. By using the computed shear strength and initial stiffness from the proposed model, it's able to plot bilinear capacity curve. Although the ultimate deformation is not expressed in this bilinear curve, it's able to verify the validity of the proposed method visually by using this curve as shown in **Fig. 2-20**.

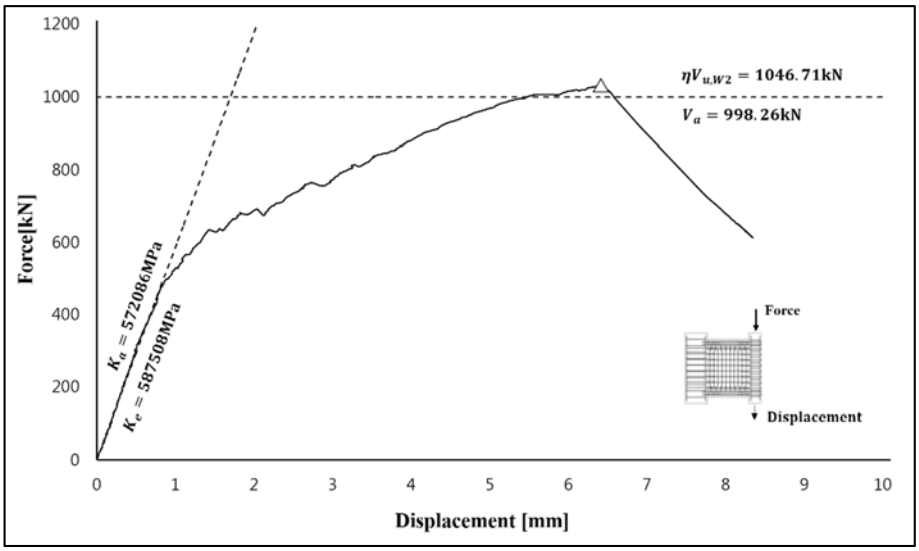

Fig. 2-20 Validity of proposed method

2.3.4 Applying proposed model to RC squat wall infilled RC frame (Example of the proposed model)

Since the concrete section enlargement retrofitting method is opposite concept of the infilled retrofitting in RC frame, this study used the proposed model to test result of RC squat wall infilled RC frame specimen of previous study applied to cyclic loading, and checked validity of this method again. To clarify the analytical process of the proposed model of this study, the analytical process to determine the ultimate shear strength of the infilled squat wall of the previous study[9)] is computed step by step following the flow chart (**Fig. 2-16**). The details and the material properties used in the previous study is shown in **Table 6**, and specifications of the specimen are shown in **Fig. 2-21**.

Table 6 Properties of infilled squat wall specimen

	RC column	Infilled RC squat wall
Section dimension	3760 mm × 133 mm	304.8 mm × 304.8 mm
Height	2134 mm	
Concrete compressive strength	23 MPa	
Yield strength of reinforcement	420 MPa	
Transverse reinforcement	HD10 @ 304.8mm	HD13 @ 304.8 mm
Vertical reinforcement	4 – HD22	HD13 @ 304.8 mm

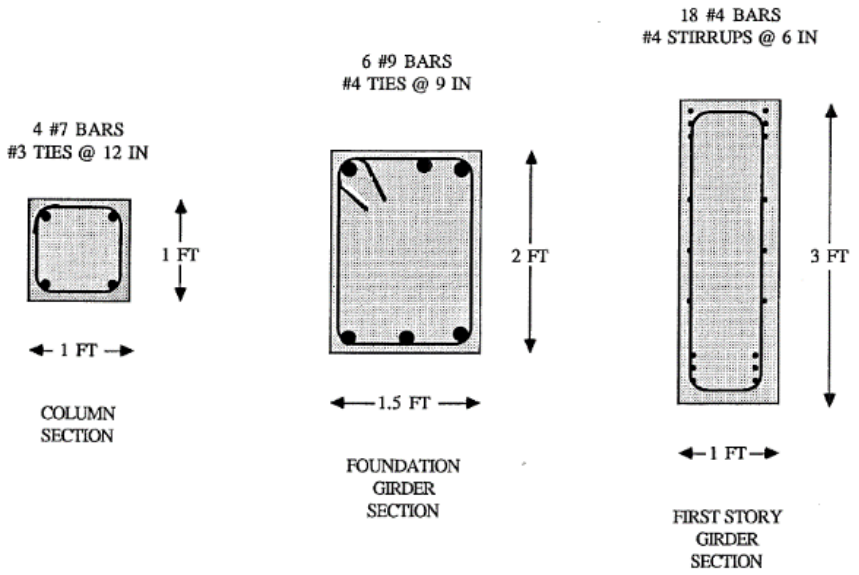

a) Frame member cross sections of the specimen

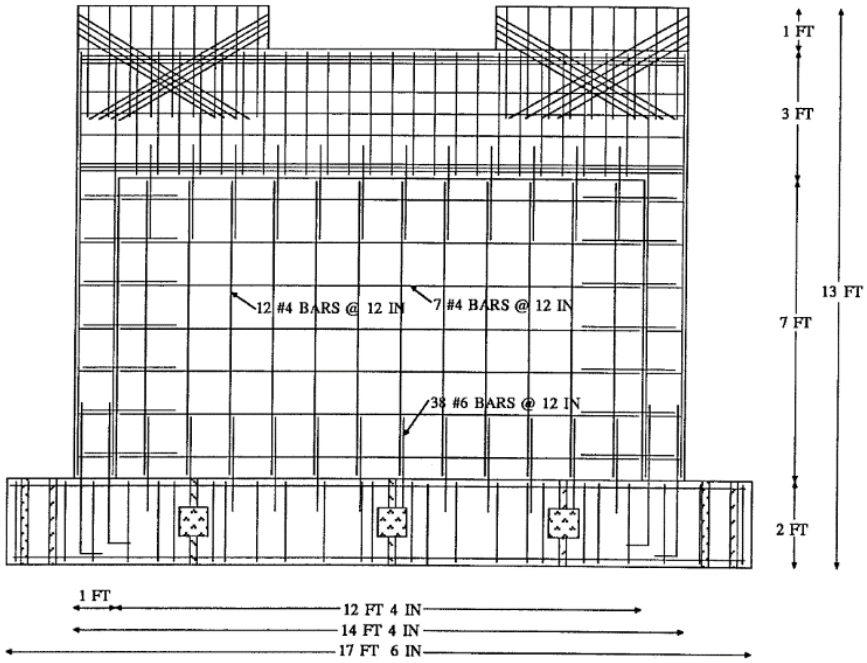

b) Reinforcement layout of the specimen

Fig. 2-21 Specification of the specimen (Patrica Jean Gaynor, 1988)

As shown in the **Fig. 2-16**, the shear force carried by the infilled squat wall V has to be assumed first for analysis, and this study assumed the value as 1,111 kN. In addition, the length h_s where the concentrated shear deformation of the column is occurred also has to be assumed, and this study assumed it as 305 mm. Based on these values, it is able to compute not only the strut width a_s by the assumed h_s, also D, F_h, and F_v by the stiffness ratios, R_h / R_d and R_v / R_d depending on the aspect ratio of the infilled squat wall.

$$a_s = 2h_s \cos\alpha = 530.33mm \qquad (\text{I})$$

$$\frac{R_h}{R_d} = \frac{\gamma_h}{1-\gamma_h}\left(\gamma_h = \frac{2\tan\alpha - 1}{3} = 0.045\right) = 0.047 \qquad (\text{II})$$

$$\frac{R_v}{R_d} = \frac{\gamma_v}{1-\gamma_v}\left(\gamma_v = \frac{2\cot\alpha - 1}{3} = 0.84\right) = 5.30 \qquad (\text{III})$$

$$\begin{cases} -D\cos\alpha = 175.06kN \\ F_h = 8.26kN \\ F_v \cot\alpha = 1635.17kN \end{cases} \qquad (\text{IV})$$

Therefore, it is able to compute the ultimate *d* – directional stress, $\sigma_{d,\max}$ by computing the **Equation (13)**.

$$\sigma_{d,\max} = -12.38MPa \qquad (\text{V})$$

Based on the computed stress, the softening coefficient ζ can be computed by using the compressive strength of the concrete used for the infilled squat wall.

$$\zeta = \frac{\sigma_{d,\max}}{f_{ck}} = 0.54 \qquad \text{(VI)}$$

By using the constitutive relationship of the concrete considering the softening effect, the *d* – directional strain, ε_d can be derived as -0.00109. In addition, the area of the effective reinforcement in vertical and transverse direction, A_{tv} and A_{th} are 650 mm^2 and 1,300 mm^2, respectively. Therefore, the *v* – and *h* – directional strain are 0.00335 and 0.00006, respectively based on the constitutive relationship of the reinforcement.

The shear strength of the specimen's column section, $V_{n,c}$ is 147.49 kN according to the ACI provision (**Equation (4)**). In addition, the effective flexural stiffness of the cracked column section, EI_{eff} is computed as 30 % of the flexural stiffness of the non-cracked column section, EI from the section analysis. Therefore, the shear deformation of the column concentrated in the length h_s can be computed. Since the specimen's column section is rectangular shaped, the κ value uses 1.2.

$$\Delta_s = V_{n,c} h_w \left(\frac{\kappa}{GA_{eff}} \right) = 1.47 \text{ mm} \qquad \text{(VII)}$$

The shear strain considering the monolithic behavior of the retrofitted member, γ_{hv} can be computed as below.

$$\gamma_{hv} = \frac{\Delta_s}{h_s} = 0.0048 \qquad \text{(VIII)}$$

The *r* – directional strain ε_r can be computed from the derived *v* –, *h* – directional strains, and the shear strain γ_{hv} by summing the strain

compatibility equation and the first strain invariant (**Equation (26)**).

$$\varepsilon_r = 0.5\left(\varepsilon_h + \varepsilon_v + \frac{\gamma_{hv}}{2\sin\alpha\cos\alpha}\right) = 0.0045 \qquad \text{(IX)}$$

Therefore, the d – directional strain ε_d' from the derived strain values can be computed by the first strain invariant.

$$\varepsilon_d' = \varepsilon_v + \varepsilon_h - \varepsilon_r = -0.00109 \qquad \text{(X)}$$

The d – directional strain value from the constitutive relationship, ε_d and that from the compatibility condition, ε_d' have to be compared to verify the first assumed the length, h_s.

$$\varepsilon_d(-0.00109) = \varepsilon_d'(-0.00109) \qquad \textbf{[O.K]}$$

In addition, the softening coefficient can be calculated from the r – directional strain value, ε_r.

$$\zeta = \frac{5.8}{\sqrt{f_c}}\frac{1}{\sqrt{1+400\varepsilon_r}}\left(=0.72\right) \le \frac{0.9}{\sqrt{1+400\varepsilon_r}}\left(=0.54\right) \text{(XI)}$$

The softening coefficient calculated from the compressive strength of the concrete, ζ and that from the r – directional strain value, ε_r have to be compared to verify the first assumed shear force carried by the infilled squat wall, V.

$$\zeta(0.54) = \zeta'(0.54) \qquad \textbf{[O.K]}$$

Therefore, the first assumed length h_s = 305 mm and the first assumed shear force carried by the infilled squat wall, V = 1,111 kN are valid, and the retrofitted member's total shear capacity can be calculated by summing the shear strength of the column section twice.

$$V = V + 2V_{n,c} = 1,406.35 \text{ kN} \qquad \text{(XII)}$$

To compute the initial stiffness of the infilled squat wall, the modified strut width, a_s' can be derived by the Equation (30).

$$a_s' = \frac{V}{0.65 f_{ck} t_w \cos\alpha} = 815 \text{ mm} \qquad \text{(XIII)}$$

Therefore, the initial stiffness of the retrofitted can be computed by using the modified strut width, a_s'.

$$K = \frac{E_c^w a_s' t_w}{\sqrt{h_w^2 + l_w^2}} \cos^2\alpha = 643,244 \text{ MPa} \qquad \text{(XIV)}$$

The test result is shown in **Fig. 2-22**, and comparison of the experimental result, existing provisions (ACI318-11, FEMA306, and the proposed model by Hwang et al.), and the proposed model is shown in **Table 7**.

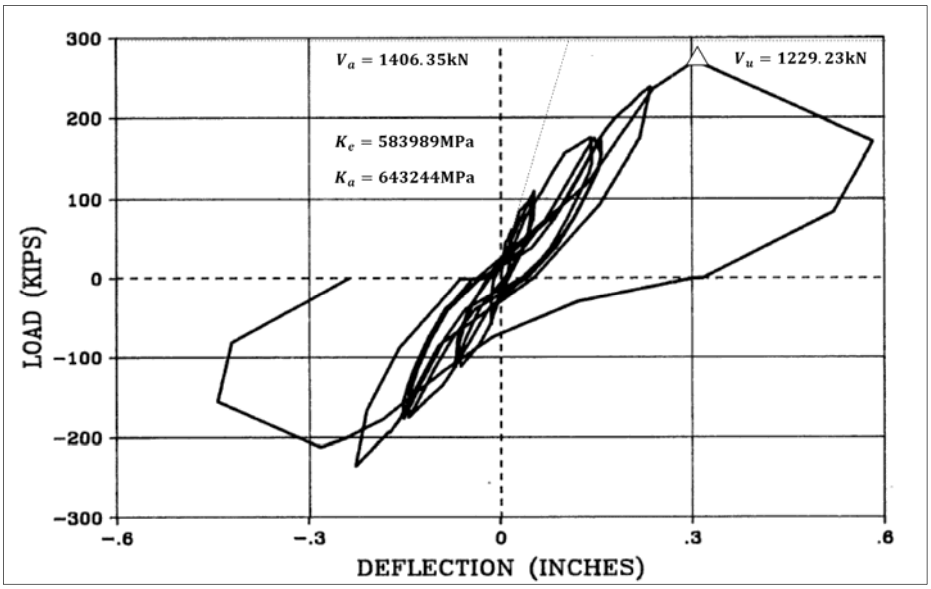

Fig. 2-22 Load-deflection of the specimen (Patrica Jean Gaynor, 1988)

Table 7 Comparison results (Infilled squat wall)

	V_u (kN)	Proposed method (kN) (Eq. 14)	ACI318 (kN) (Eq. (4))	ACI318 (kN) (Eq. (6))	FEMA306 (kN) (Eq. (2) or (3))	Shyh-Jiann Hwang et al. (kN)
V	1,229.23	1,406.35	1,232.94	1,720.67	2,699.03	1,987.44
$\frac{V}{V_u}$	1.00	1.14	0.99	1.40	2.20	1.62

a) Shear strength

	Experimental (K_e) (MPa)	Analytical (K) (MPa)
K_e	583,989	643,244
K / K_e	1.00	1.10

b) Initial stiffness

While the existing provisions cannot predict shear strength of the specimen, the proposed model can also predict not only shear strength, also initial stiffness of the RC squat wall infilled RC frame considering the details of the column section closely to the test result as shown in the **Table 7**. Therefore, it's able to confirm the validity of the proposed model by this comparison result.

Since the infilled RC squat wall retrofitting in RC frame method is widely used for seismic retrofitting method to RC frame, it is the result of great significant to evaluate retrofitting effect of not only the end retrofitted squat wall with concrete section enlargement retrofitting method, also the RC squat wall infilled RC frame by the proposed model of this study.

Chapter 3. UHPFRC web retrofitted single-layered squat wall

3.1 Experimental program

3.1.1 Material & reinforcement detail of retrofitting target

Similar to Chapter 2, material properties and reinforcement detail of the single-layered squat wall are based on the structural drawing of the existing shear wall type low – rise building built in 1980's. Therefore, retrofitting target used material properties and reinforcement ratios same with that of the Chapter 2. The compressive strength of the concrete is 24 MPa, SS400 is used for the reinforcement, and the reinforcement ratio of the vertical and transverse direction are 0.33 % and 0.47 %, respectively.

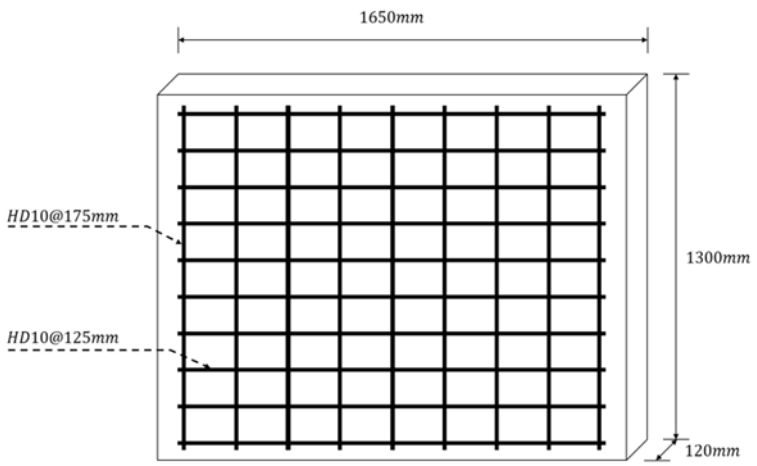

Fig. 3-1 Specification of retrofitting target (for UHPFR web retrofitting)

However, since the purpose of this experiment is verifying shear retrofitting effect of the UHPFRC web retrofitting, this study planned the retrofitting target wall with 0.8 aspect ratio. Other scale geometric properties are also same as that of the Chapter 2.

3.1.2 Material properties & detail of retrofitting UHPFRC section

Since performance of the UHPFRC is different depending on its mixture proportions, there are several types of the UHPFRC under investigation depending on mixture proportions of the UHPFRC around the globe. This study used Kang, and Hong's mixture proportions for the UHPFRC web retrofitting as shown in **Table 8**. It's expected compressive strength is 150 MPa, and flexural tensile strength is 60 MPa according to previous studies[10)].

Table 8 Mixture proportion of UHPFRC

Classification	Cement	Silica fume	Sand	Filler	Super plasticizer	Water	Steel fiber (vol. %)
Mixture proportion	1	0.23	1.1	0.39	0.02	0.19~0.25	2.0±0.5

The thickness of the retrofitting UHPFRC section is 30 mm for constructability and retrofitting efficiency. To evaluate net retrofitting effect of the web UHPFRC retrofitting to the squat wall, there does not exist any tensile member like wire mesh or reinforcement in the retrofitting section. The width of the UHPFRC retrofitting section is same as that of retrofitting target's web; however, the height of the UHPFRC retrofitting section is 200 mm larger than that of retrofitting target's web. This is the reason to prevent rocking failure of the UHPFRC retrofitting section by inserting it into the foundations of the retrofitting target.

3.1.3 Specification of test specimens

To evaluate shear retrofit efficiency of the UHPFRC web retrofitting method, this study planned two types of specimens; one is non retrofitted single-layered squat wall (WN), another UHPFRC web retrofitted single-layered squat wall (WR).

The test specimens also consist of the three boundary element, and the two wall panel elements similar to the specimens of the Chapter 2. However, since purpose of this test was verifying shear retrofitting effect against to the cyclic loading, this study arranged eight through HD24 SS520 reinforcements with screw at the both ends into the middle boundary element. Moreover, flexural reinforcements were arranged at the topmost and bottommost face of the middle boundary element to prevent unexpected flexural crack occurred in the test of the Chapter 2. In addition, the 100 mm depth grooves for casting UHPFRC were made in the each boundary element of the specimen WR, and interface of the retrofitted specimen WR was roughened by using roller after normal strength concrete casting had finished. The details of the specimens are shown in **Fig. 3-2** and **Table 9**. Furthermore, the grooves and the interface condition are shown in **Fig. 3-3** and **Fig. 3-4**, respectively.

Table 9 Properties of specimens

		WN	WR
Normal strength concrete	f_c (Nominal)	24 MPa	
	f_y (Nominal)	400 MPa (SS400)	
Transverse reinforcement		HD10 @ 125 mm	
Longitudinal reinforcement		HD10 @ 175 mm	
UHPFRC	Thickness	None	30 mm
	Compressive strength		150 MPa
	Flexural tensile strength		60 MPa

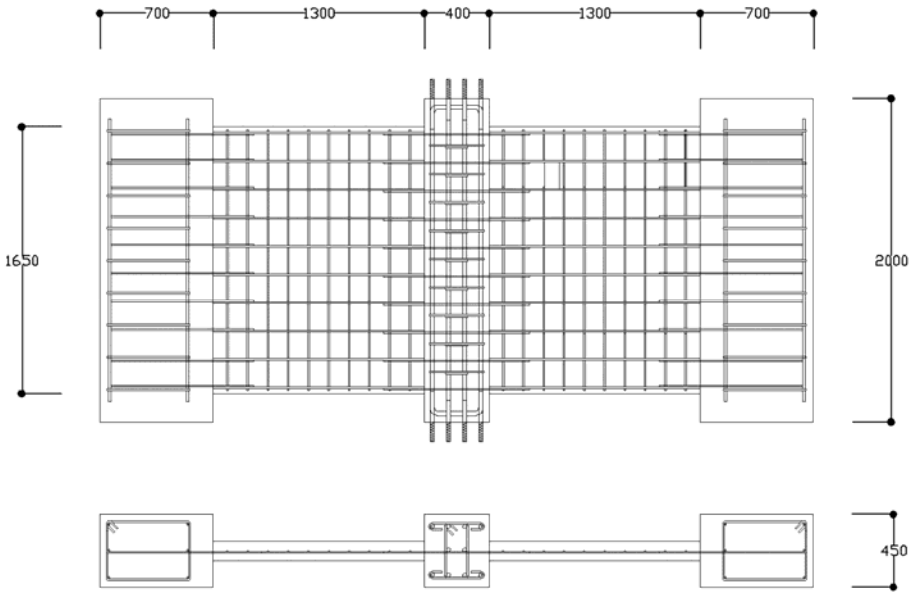

a) Specification of WN

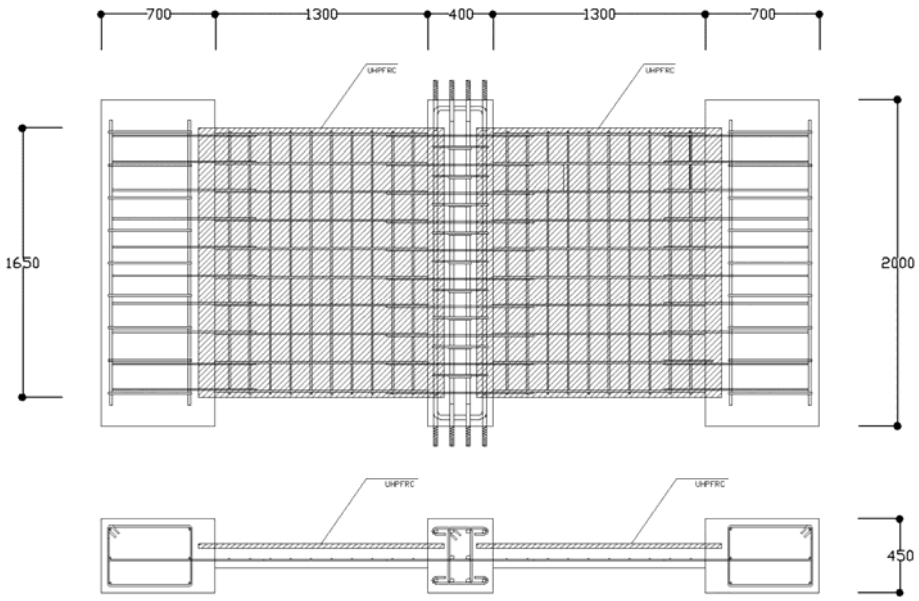

b) Specification of WR

Fig. 3-2 Specification of specimens (WN & WR)

Fig. 3-3 100mm depth groove in WR

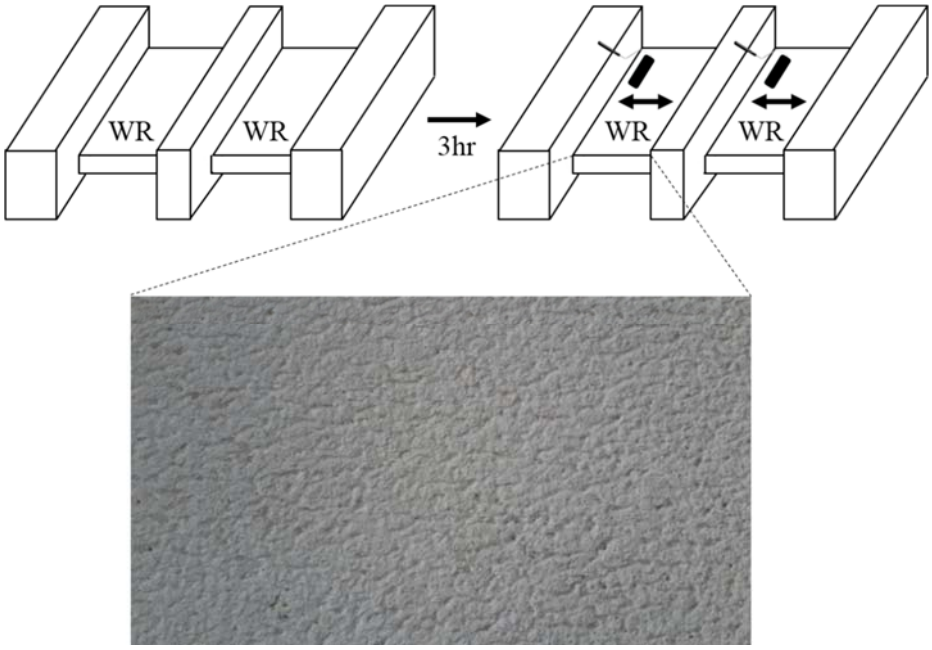

Fig. 3-4 Interface condition of WR

3.1.4 Retrofitting sequence of WR

Since working place of manufacturing WR was located far away from materials for the UHPFRC and a concrete mixer located in the laboratory, premixing work was preceded in the laboratory before casting the UHPFRC. The premixing work is mixing binding materials (cement, silica fume, fine aggregate, and filler) and packing water-reducing agent. This procedure make it easy to cast the UHPFRC in working place. Moreover, since casting capacity of the concrete mixer is only 30 L, it was impossible to cast UHPFRC panel (about 75 L; 1650 mm × 1500 mm × 30 mm) at a time. Therefore, premixing packing of one UHPFRC retrofitting section was divided into three sets; 25 L amount of the UHPFRC. Therefore, six premixed sets were prepared before the casting work. The formulation of them are shown in **Table 10**.

After the premixing packing procedure had finished, they were delivered to the working place. Since the interface roughening had finished before, UHPFRC casting work was proceeded. First, premixed binding materials, water and half amount of water-reducing agent were poured into the concrete mixer, and activated it. About few minutes later, the rest of water-reducing agent was poured into the mixer by several times, then the mixed materials in the mixer became well mixed. Afterward, fibers were poured into the mixer, and mixing one UHPFRC premixed pack process was finished. This process was repeated six times to cast two UHPFRC retrofitting section (about 150 L). The discharged UHPFRC was sealed with vinyl until mixing of the next premixed pack is finished. The sequence of this process is shown in **Fig. 3-5**. The retrofitted specimen was 90 degrees Celsius steam-cured about three days to reveal its strength.

Table 10 Premix setting (6 sets)

No.	Premix	Casting amount	Premix sack	Binder & aggregates (kg)				Water & Super plasticizer & steel fiber (g)				
		L	kg	Sand	Silica Fume	Cement	Filler	Water	Super plasticizer	Water + Super plasticizer	Super plasticizer2	Steel fiber
1	1650A-1	24	64.80	26.40	6.00	24.00	8.40	5280	480	5760	480	4894
2	1650A-2	24	64.80	26.40	6.00	24.00	8.40	5280	480	5760	480	4894
3	1650A-3	24	64.80	26.40	6.00	24.00	8.40	5280	480	5760	480	4894
4	1650B-1	24	64.80	26.40	6.00	24.00	8.40	5280	480	5760	480	4894
5	1650B-2	24	64.80	26.40	6.00	24.00	8.40	5280	480	5760	480	4894
6	1650B-3	24	64.80	26.40	6.00	24.00	8.40	5280	480	5760	480	4894

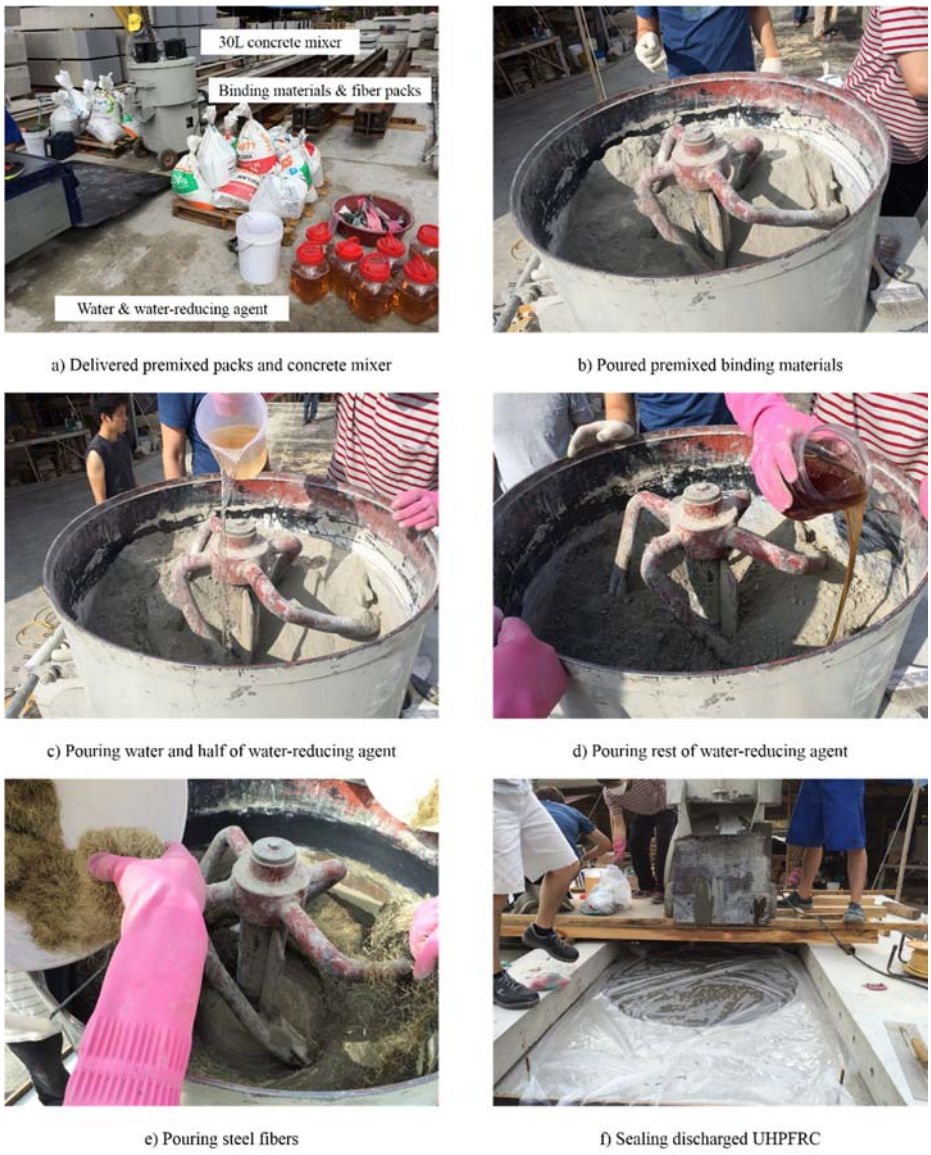

a) Delivered premixed packs and concrete mixer

b) Poured premixed binding materials

c) Pouring water and half of water-reducing agent

d) Pouring rest of water-reducing agent

e) Pouring steel fibers

f) Sealing discharged UHPFRC

Fig. 3-5 Mixing procedure of one premixed UHPFRC pack

3.1.5 Result of material property test

The mixture proportion of the normal strength concrete with nominal compressive strength of 24 MPa used for the specimens is same as that of the Chapter 2. The mixture proportion of the UHPFRC is shown in **Table 8**. The cylinders of the normal strength concrete and that of the UHPFRC were casted with 100 mm × 200 mm size according to KS F 2403 provision. The actual compressive strength, f_c of each nominal compressive strength was measured from average value of direct compressive test results of the three cylinders. The direct compression test was performed according to KS F 2405 provision. Since the reinforcements used for the wall panel was also same as that of the Chapter 2, the yield strength of the reinforcements of the wall panel is 488 MPa, derived from the result of the previous material property test. The test results are tabulated in **Table 11**.

Table 11 Strength of concrete and reinforcement

	Concrete (f_{ck})	UHPFRC		Reinforcement (f_y)
		Compressive (f_{ck}^{UHPC})	Flexural tensile	
Nominal strength	24 MPa	150 MPa	60 MPa	400 MPa
Actual strength (Average value)	30 MPa	100 MPa	29.5 MPa	488 MPa

As shown in the **Table 11**, the compressive strength and the flexural tensile strength of the UHPFRC is lower than the expected strength. The reason of this distinction is supposed that moisture in the air was penetrated into the premixed pack, but it lacks confirmation. Therefore, this strength degradation of previous study's UHPFRC mixture proportions caused by casting with premixed materials has to be more researched later. This study did not deal with this problem.

3.1.6 Test set-up

The basic setting of this test is same as that of the Chapter 2. However, since this test is planned to apply cyclic loading to the specimens, jigs were fastened to the eight through reinforcements of the middle boundary element. Moreover, two 200 ton UTM were used for equipment to apply cyclic loading, and five LVDTs were installed under the specimen to measure force-directional deformation of the specimen. In addition, four LVDTs were also installed to the surface of the wall panel in diagonal direction to measure shear deformation of the specimen. The test set-up and location of each LVDT are shown in **Fig. 3-6**.

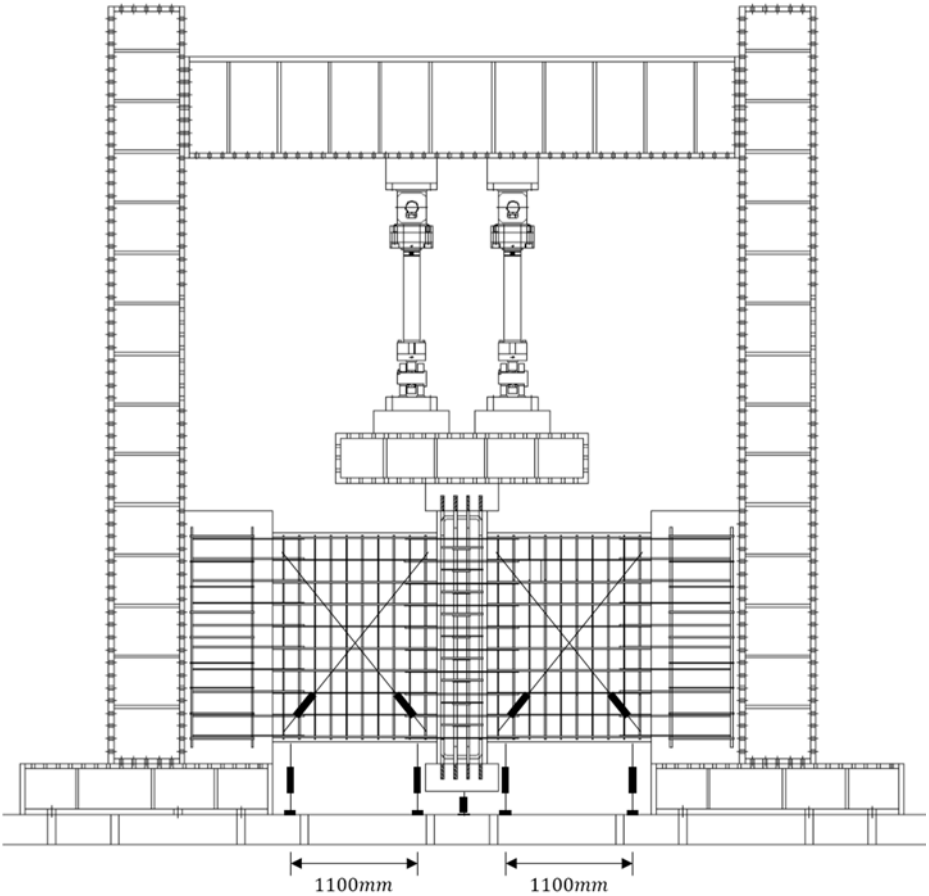

Fig. 3-6 Test set-up (WN & WR)

The cyclic loading test was performed by displacement-controlled loading abided by manual of test method for precast concrete structural wall[11)]. The test sequence is expressed in terms of drift ratio, and the initial drift ratio shall be within the essentially elastic response range of the specimen. In addition, subsequent drift ratios shall be to values not less than 5/4 times, and not more than 3/2 times, the previous drift ratio. According to these limitations, load profile of the cyclic loading was determined as shown in **Fig. 3-7**.

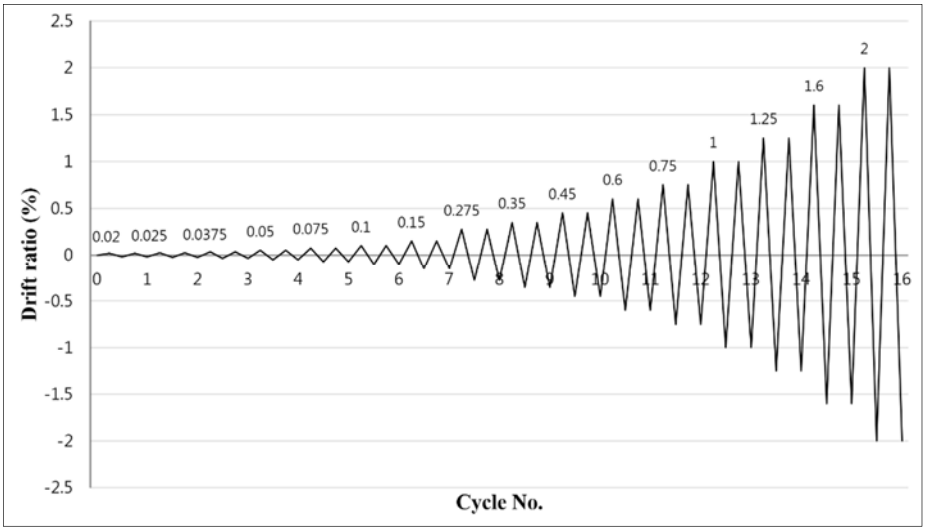

Fig. 3-7 Lateral loading protocol

In addition, 5 mm steel strain gauges are adhered to vertical and transverse reinforcement of the wall panel to identify whether they are yielded or not. The locations of them are shown in **Fig. 3-8.**

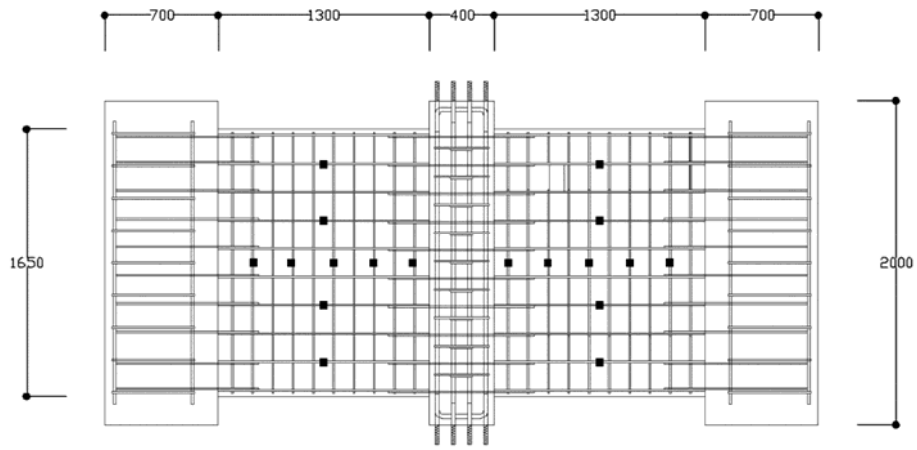

a) Locations of steel strain gauges (WN)

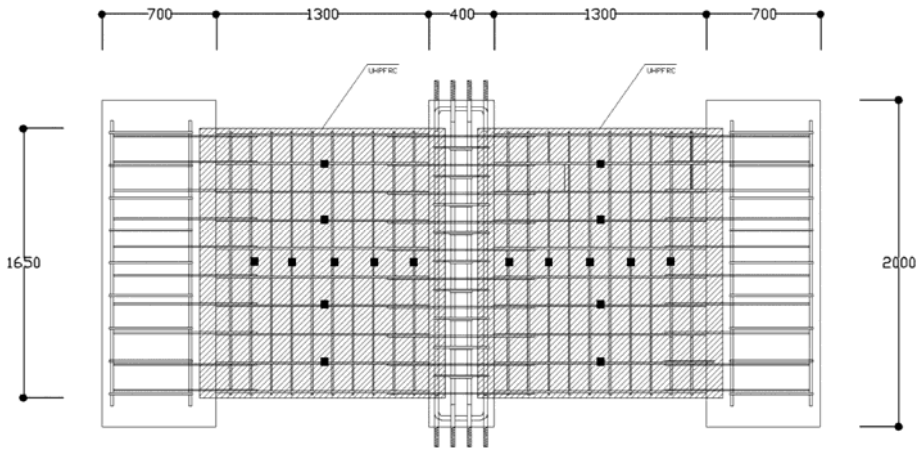

b) Locations of steel strain gauges (WR)

Fig. 3-8 Locations of steel strain gauges (WN & WR)

3.2 Test results

3.2.1 Test result of WN (Non-retrofitted single-layered squat wall)

The total cyclic response of WN is shown in **Fig. 3-9**. The failure of WN was accompanied with yielding of the transverse reinforcements in the both wall panels of the specimen. The failure mode of WN was governed by diagonal tension failure of the only wall panel in WN. The ultimate strength of WN in positive direction, $V_{u,WN}^{+}$ is 1,618.41 kN, and drift ratio at that time is 0.56 % ($\Delta_{u,WN}^{+}$ =7.31 mm). The ultimate strength of WN in negative direction, $V_{u,WN}^{-}$ is -832.02 kN, and drift ratio at that time is 0.38% ($\Delta_{u,WN}^{-}$ =4.99 mm). The crack pattern of WN after the test was finished is shown in **Fig. 3-10**.

Since the transverse strains measured through the cyclic loading showed that the both left and right wall panel contributed almost same portion to the behavior of the specimen as shown in **Fig. 3-11**. Therefore, it is reasonable to consider that the cyclic behavior of the one wall panel is same as that of the specimen with half strength. However, there exists some gap between the positive directional strength and the negative directional strength of the specimen. The strength of the positive direction is almost 95 % larger than that of the negative direction. The reason of this imbalance phenomenon is supposed that there occurred some gap between the both boundary elements and the foundation frame when the negative directional load was applied to the specimen.

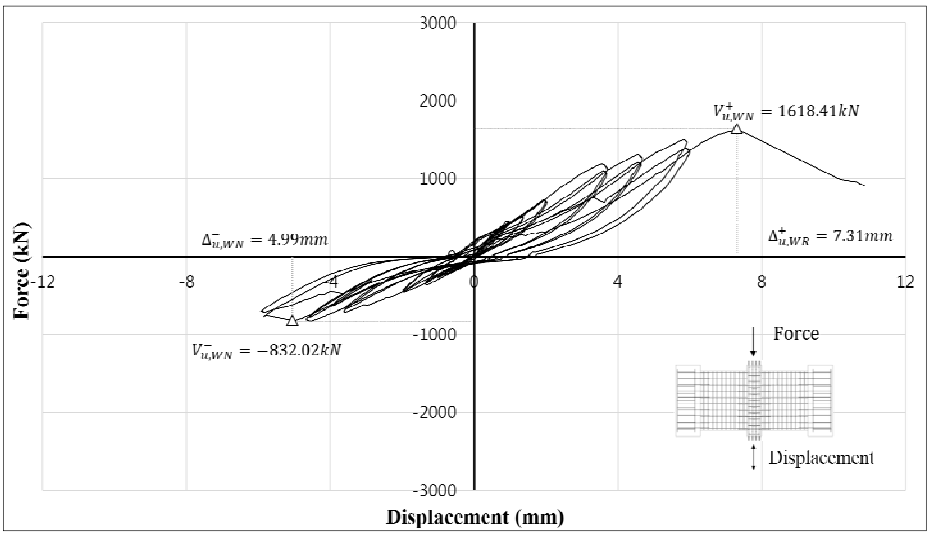

Fig. 3-9 Total cyclic behavior of WN

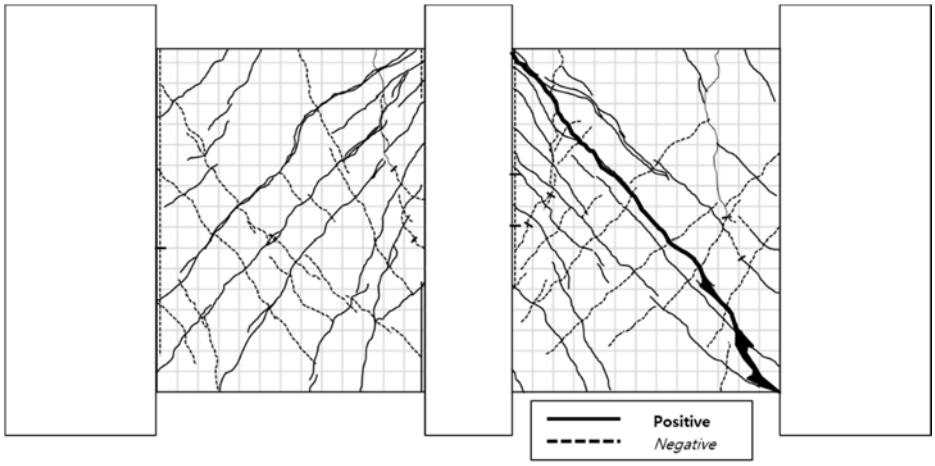

Fig. 3-10 Crack pattern of WN (0.56 % drift ratio)

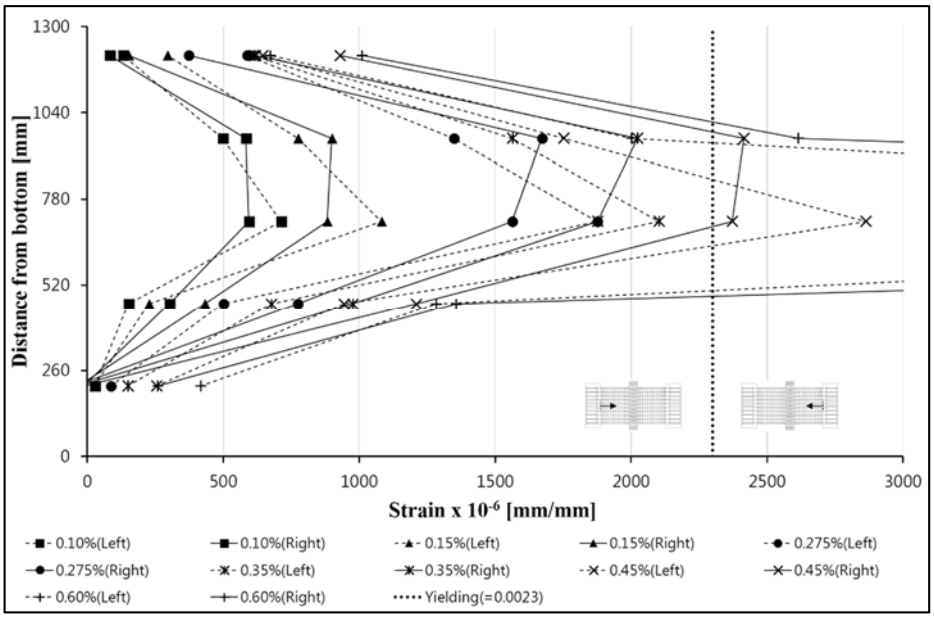

Fig. 3-11 Comparison result of both wall panels in WN (Strains of transverse reinforcement)

3.2.2 Test result of WR (UHPFRC web retrofitted single-layered squat wall)

Since there occurred some unexpected problems during the test, WR could not reach its ultimate state. The strength and the deformation in the negative direction could not be measured after the 9th cycle (0.35 % drift ratio), because some through reinforcements were fractured due to high tensile force applied to the specimen. In addition, There occurred distortion of the middle boundary element during the first cycle of the 12nd cycle (0.75 % drift ratio), and the test was re-conducted after readjusting the distorted middle boundary element from the 12nd cycle. However, there did not occurred any specific damage in the specimen, and the specimen could not reach its ultimate state due to interface failure between the squat wall and the UHPFRC panel at the modified 14th cycle (1.25 % drift ratio) as shown in **Fig. 3-13**.

To consider the total cyclic behavior of the specimen after readjusting the middle boundary element had done, deformation of the specimen measured

from modified 12nd cycle to modified 14th cycle is reduced about 4.09 mm. The total cyclic response of WR considering this modification is shown in **Fig. 3-13**. The maximum strength of WR in positive direction, $V^{+}_{u,WR}$ is 2,427.92 kN, and drift ratio at that time is 0.60% ($\Delta^{+}_{u,WR}$ =7.75mm). In addition, cracking of the UHPFRC panel did not occurred before the 12nd cycle, though lots of cracks occurred in the normal strength concrete wall panel at that time. The crack pattern of WR after the test was finished is shown in **Fig. 3-14**.

Similar to the case of WN, since the transverse strains measured through the cyclic loading showed that the both left and right wall panel contributed almost same portion to the behavior of the specimen. Therefore, it is also reasonable to the cyclic behavior of the one wall panel is same as that of the specimen with half strength.

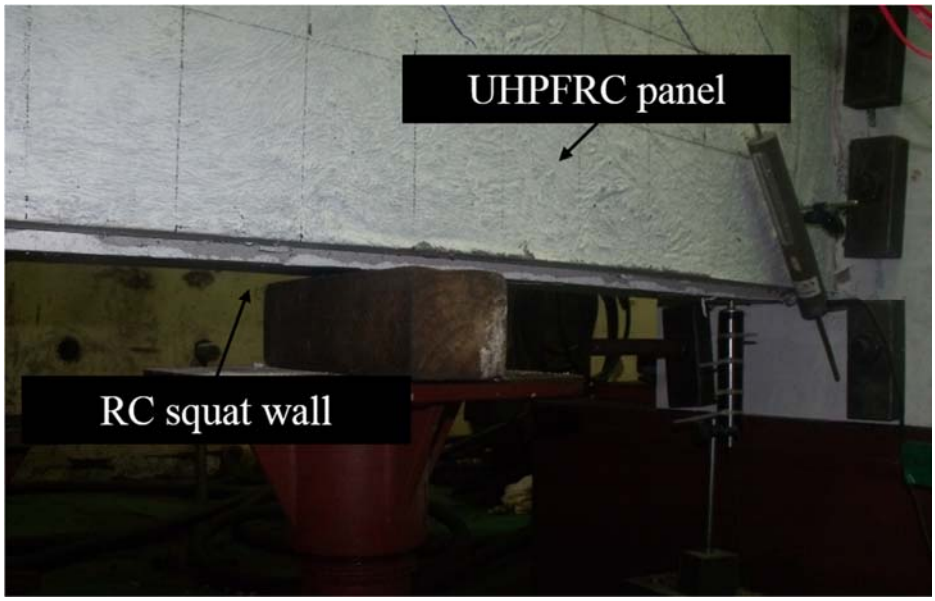

Fig. 3-12 Interface failure of WR (Modified 14th cycle)

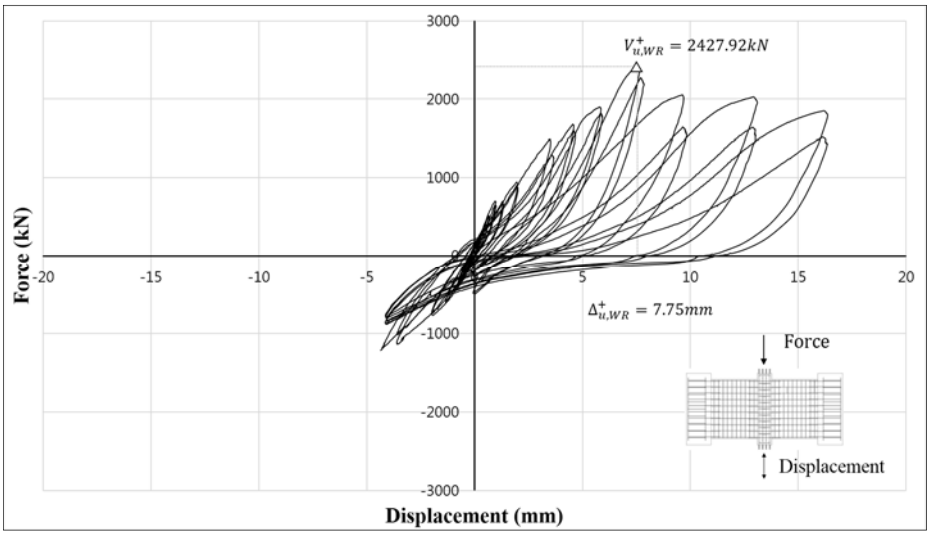

Fig. 3-13 Total cyclic behavior of WR

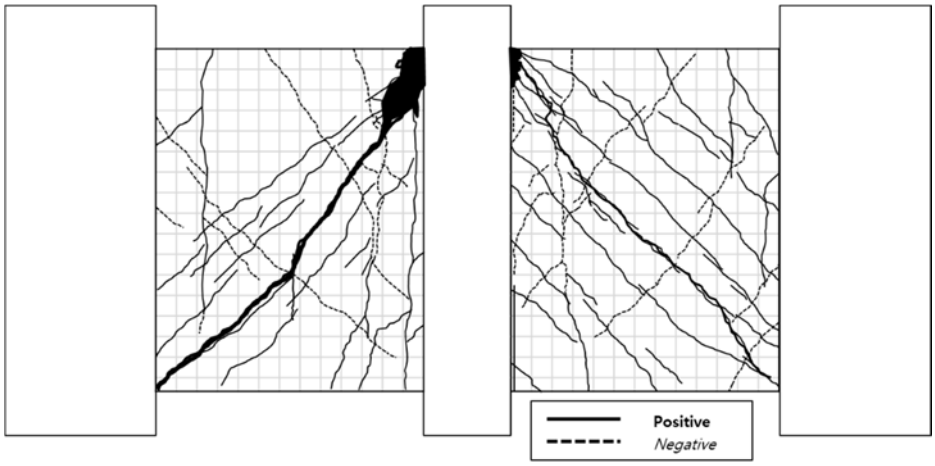

a) Crack pattern of RC squat wall

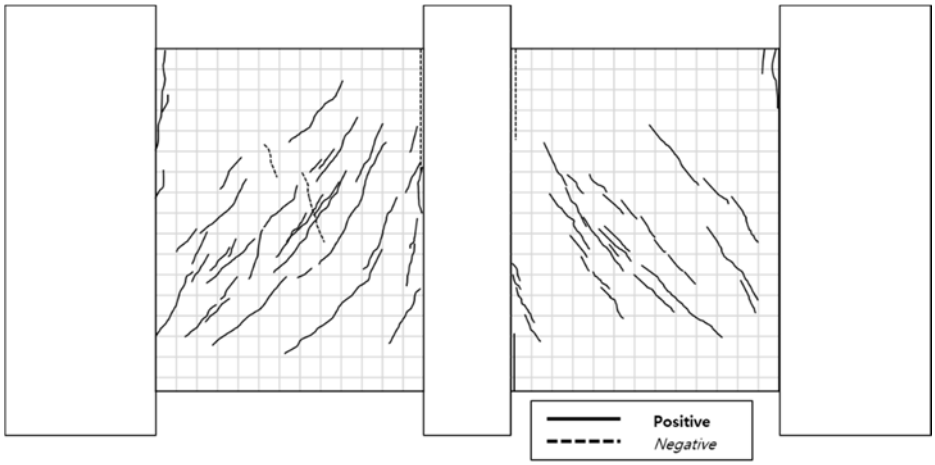

b) Crack pattern of UHPFRC panel

Fig. 3-14 Crack pattern of WR (1.25% drift ratio)

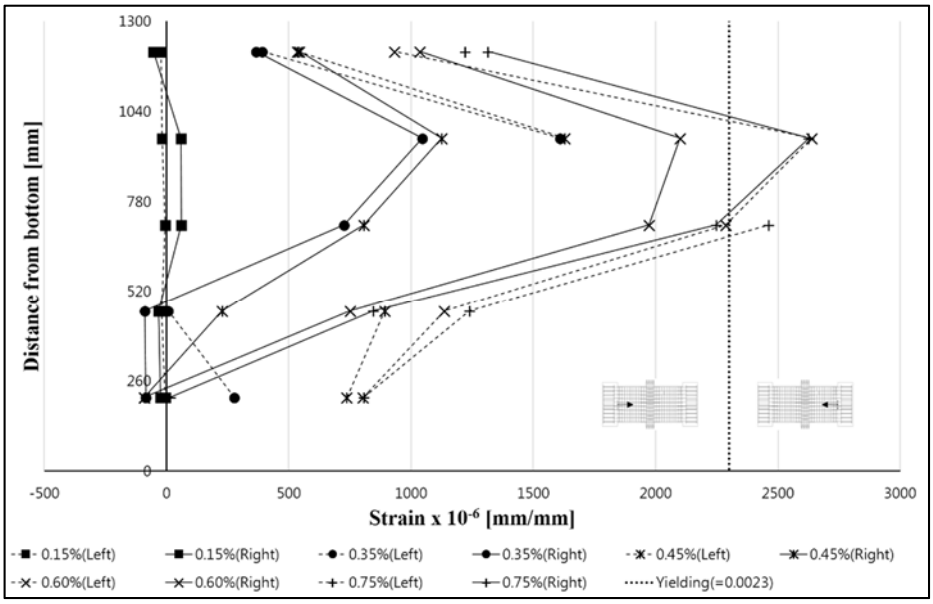

Fig. 3-15 Comparison result of both wall panels in WR (Strains of transverse reinforcement)

3.2.3 Retrofitting effect of UHPFRC web retrofitting method

Since the specimens were subjected to the cyclic loading, it is convenient to verify retrofitting effect of UHPFRC web retrofitting by using positive directional backbone curves of them as shown in **Fig. 3-16**.

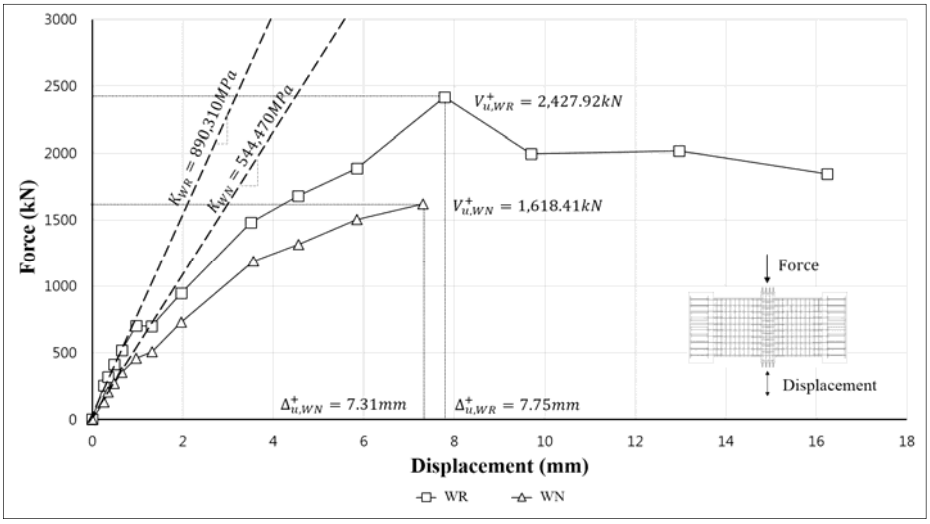

Fig. 3-16 Comparison result (Backbone curve of WN & WR)

Although WR could not be tested until the ultimate state, it is able to confirm that about 60% of initial stiffness and about 50% of ultimate strength are enhanced by 40mm UHPFRC web retrofitting without any reinforcement in the retrofitting section. Moreover, the UHPFRC panel restraints the strain increment of the transverse reinforcements. This fact can be confirmed by the strain distribution of the both specimens at the 10th cycle when the transverse reinforcement of WN yielded as shown in **Fig. 3-17**. Nevertheless, the comparison result of dissipated energy derived from the area of the positive directional cycles between WN and WR shows conflicting this fact. The dissipated energy of WR is always larger than that of WN at every load cycles as shown in **Fig. 3-18**. This contradiction can be explained by energy dissipation contribution of the UHPFRC panel. Therefore, it is able to delay yielding of the transverse reinforcement, and increase the dissipated energy than the single-layered squat wall by the UHPFRC panel at the same load cycle.

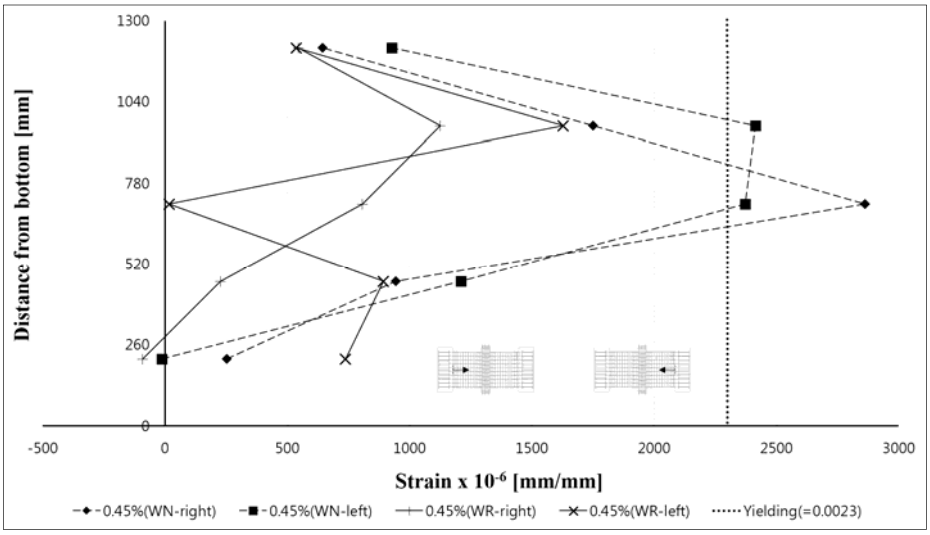

Fig. 3-17 Restrained strain of transverse reinforcement at 0.45% drift ratio (WN & WR)

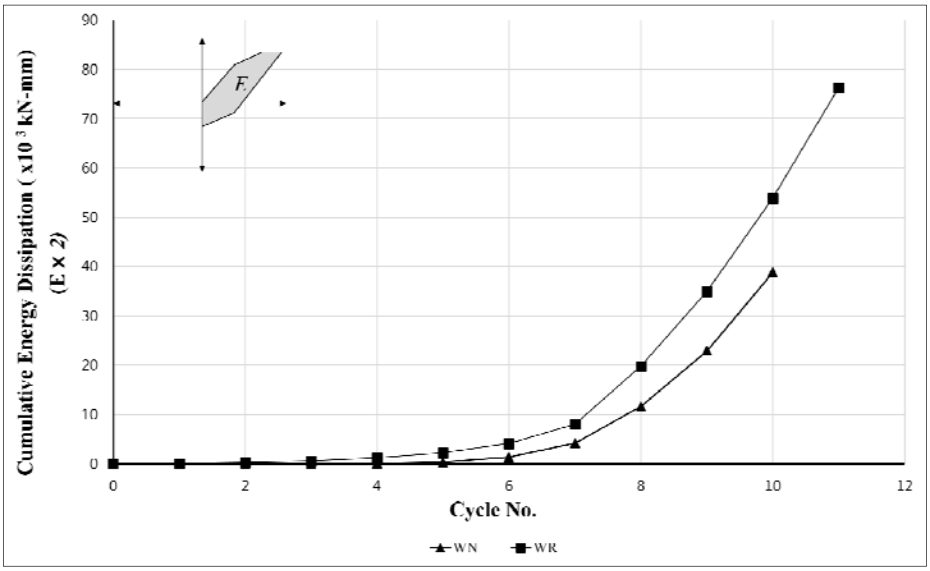

Fig. 3-18 Dissipated energy of the specimens (~ 11st cycle)

3.3 Proposed method to evaluate behavior of UHPFRC web retrofitted single-layered squat wall

3.3.1 Shear strength from existing provisions (FEMA 306, K-UHPC)

Although the ultimate failure mode of retrofitted specimen, WR could not be clearly determined from the test, it can be supposed as diagonal tension failure based on the WR's crack pattern. When considering the wall panel and UHPFRC panel in parallel, it's able to apply the existing provisions to derived retrofitted member's shear strength.

FEMA 306 proposed shear strength of the wall failed by diagonal tension failure, and it can be computed by using **Equation (2)** or **Equation (3)**. Moreover, KCI proposes structural provision for K-UHPC[12)], a kind of the UHPFRC mixed with specific mix proportion. There exists proposed equations for predicting shear strength of beam casted with K-UHPC expressed as the sum of matrix, fiber, shear reinforcement, and prestressing contributions. Since the UHPFRC panel used in this study does not have any shear reinforcement and prestressing steel, shear strength of the UHPFRC panel can be computed by **Equation (18)**.

$$V_d = V_{rpcd} + V_{fd} \tag{18}$$

$$V_{rpcd} = \phi_b (0.18\sqrt{f_{cd}}\, b_w d) \tag{18a}$$

$$V_{fd} = \phi_b (f_{vd} / \tan \beta_u) b_w z \tag{18b}$$

where

V_{rpcd} = nominal shear strength provided by matrix (N)

V_{fd} = nominal shear strength provided by fiber (N)

b_w = width of the web (mm)

ϕ_b = reduction factor (0.77)

f_{cd} = nominal compressive strength of K-UHPC (MPa)

f_{vd} = average tensile stress occurred in right angle of diagonal crack (MPa)

β_u = formed angle between axial direction and diagonal crack

(45 degree is assumed in this study)

z = distance from location of compressive resultant is applied and

center of tensile reinforcement ($d/1.15$ is assumed, (mm))

To calculate the shear strength of the retrofitted squat wall by using existing provisions, conditions of the WR are used for these equations. f_{cd} of the **Equation (18a)** is 100 MPa based on the material test of this study, and since this study did not plan any direct tensile test specimen, f_{vd} is 9 MPa computed from the below equation, tension softening curve of K-UHPC provision as shown in **Fig. 3-19**.

$$f_{vd} = \frac{1}{w_u}\int_0^{w_u} \phi_c \sigma_k(w)dw \qquad (19)$$

where

w_u = crack width when UHPFRC's ultimate tensile stress is occurred (mm)

ϕ_c = material reduction factor (=0.8)

$\sigma_k(w)$ = tension softening curve of UHPFRC depending on crack width (MPa)

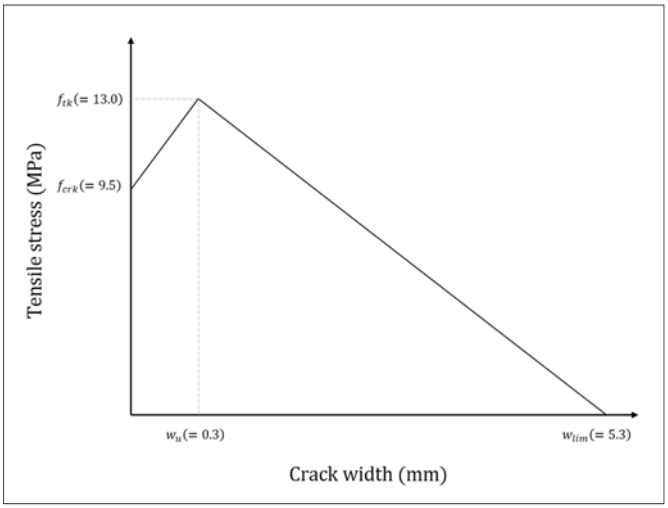

Fig. 3-19 Tension softening curve (K-UHPC provision, 2012)

The shear strength contribution of the single layered RC squat wall computed from FEMA 306 (**Equation (3)**) is 777.04 kN, and that of the UHPFRC panel computed from K-UHPC (**Equation (18)**) is 391.36 kN. Therefore, it is able to verify the shear strength of the UHPFRC web retrofitted single-layered RC squat wall is 1168.40 kN (= 777.04 + 391.36) from the point of parallel view, and this value is very close to the test result, expressed to half value of the ultimate strength of WR (1213.96 kN = 2427.92 / 2). However, it is not sure that the ultimate state of the RC wall and the UHPFRC panel occurred at the same time. Moreover, since the test result of WR could not verify the UHPFRC web retrofitted wall's failure mode clearly, it needs to be verified.

Therefore, this study proposed analytical approach to predict behavior of the UHPFRC web retrofitted squat wall subjected to pure shear by using the softened membrane model (SMM), and check the validity of the point of parallel view using the existing provisions.

3.3.2 Softened membrane model (SMM) of RC 2-D element

There were lots of shear theories had been studied by lots of researchers[14]. Veccihio and Collins (1986) developed the modified compression field theory (MCFT), so it could predict post-cracking behavior of the RC 2-D element. However, Hsu (1998) had pointed out its conceptual errors, and proposed the rotating-angle softened-truss model (RA-STM), and the fixed-angle softened-truss model (FA-STM) more developed and complicated than RA-STM. However, the RA-STM and the FA-STM can only predict the ascending branch of the RC 2-D element. The former one is based on the assumption that the direction of cracks coincides with that of the principal compressive stress in cracked concrete, and later one is based on the assumption that the direction of cracks is defined by the angle in the principal coordinate of applied stresses to the RC element as shown in **Fig. 3-20.**

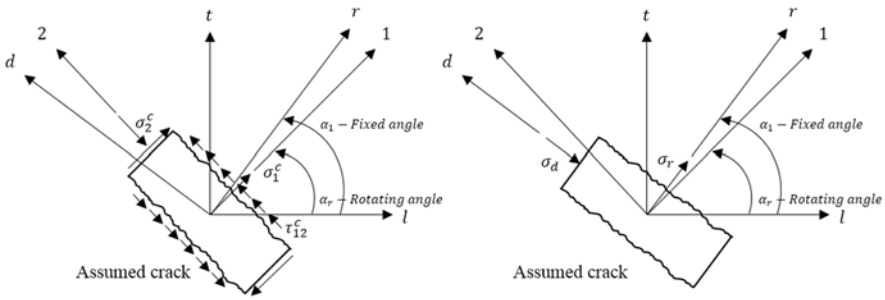

a) Fixed-angle theory b) Rotating-angle theory

Fig. 3-20 Stress states in fixed-angle theory and rotating angle theory (Hsu, 2010)

In addition, Hsu and Zhu[15] (2000) developed FA-STM, and proposed the softened membrane model (SMM) considering Hsu/Zhu ratios defined as the poisson ratios of cracked reinforced concrete to predict post-peak behavior of the RC 2-D element. The flow chart of the SMM is shown in **Fig. 3-21**. By following this sequence, it is able to compute every strains and stresses applied to the RC 2-D element for selected 2-directional uniaxial strain of the principal coordinate of applied stresses to the RC element, $\overline{\varepsilon}_2$. Each step of the flow chart can be summarized in this study step by step.

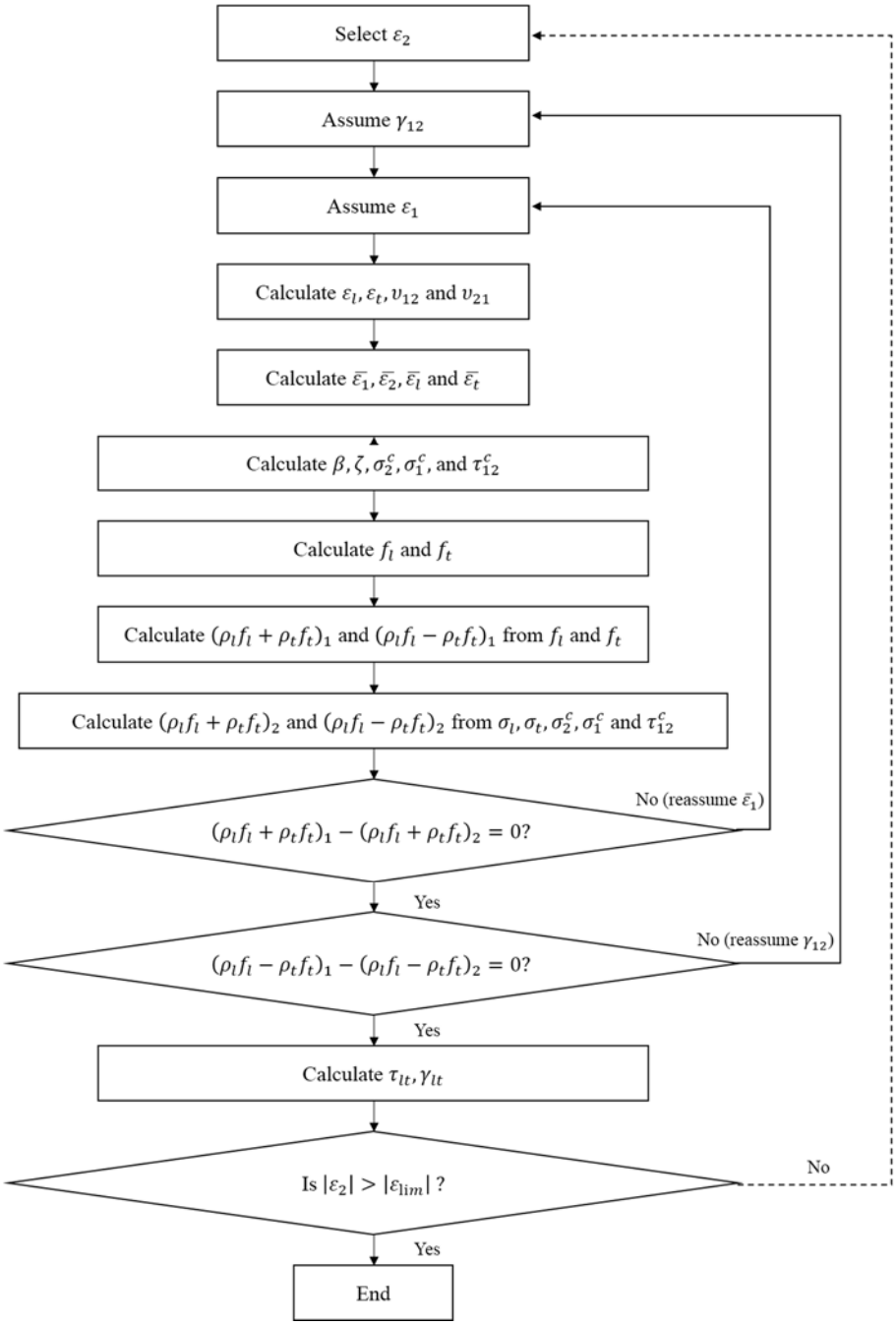

Fig. 3-21 Flow chart of solution procedure for SMM (Hsu, 2010)

a) Calculate ε_l, ε_t, ν_{12}, and ν_{21}

Before beginning the flow chart, it is recommended to establish stress equilibrium equations and strain compatibility equations of the RC element. Since the RC element is consist of the concrete part and reinforcements assumed as smeared steel for the SMM, the Mohr stress circle of the RC element subjected to the external stresses (σ_l, σ_t, and τ_{lt}) can be divided into that of the concrete element and that of the smeared steel (**Fig. 3-22**).

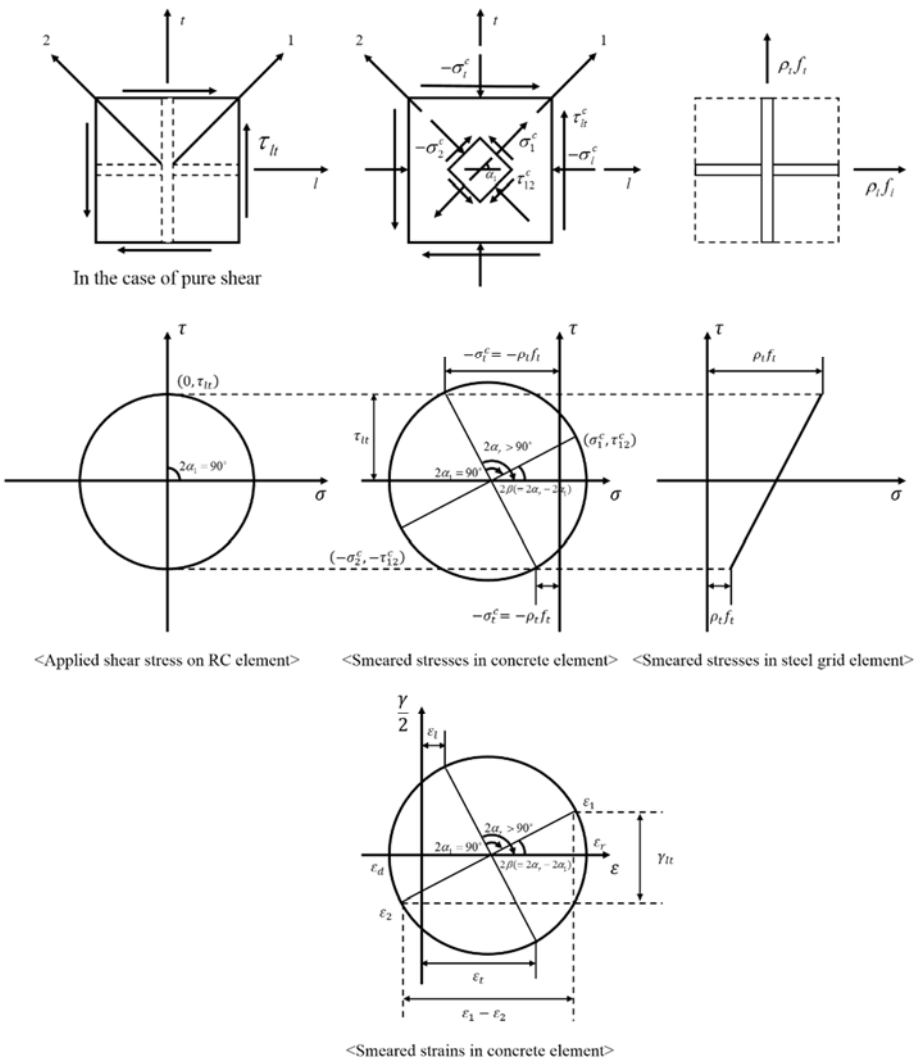

Fig. 3-22 Mohr circles for smeared stresses and strains in 2-D RC element under pure shear (Hsu, 2010)

According to the **Fig. 3-22**, the stress equilibrium equations and strain compatibility equations can be derived as below equations.

Stress equilibrium equations

$$\sigma_l = \sigma_1^c \cos^2 \alpha_1 + \sigma_2^c \sin^2 \alpha_1 - \tau_{12}^c 2 \sin \alpha_1 \cos \alpha_1 + \rho_l f_l \tag{20}$$

$$\sigma_t = \sigma_1^c \sin^2 \alpha_1 + \sigma_2^c \cos^2 \alpha_1 + \tau_{12}^c 2 \sin \alpha_1 \cos \alpha_1 + \rho_t f_t \tag{21}$$

$$\tau_{lt} = (\sigma_1^c - \sigma_2^c) \sin \alpha_1 \cos \alpha_1 + \tau_{12}^c (\cos^2 \alpha_1 - \sin^2 \alpha_1) \tag{22}$$

Strain compatibility equilibrium equations

$$\varepsilon_l = \varepsilon_1 \cos^2 \alpha_1 + \varepsilon_2 \sin^2 \alpha_1 - \frac{\gamma_{12}}{2} 2 \sin \alpha_1 \cos \alpha_1 \tag{23}$$

$$\varepsilon_t = \varepsilon_1 \sin^2 \alpha_1 + \varepsilon_2 \cos^2 \alpha_1 + \frac{\gamma_{12}}{2} 2 \sin \alpha_1 \cos \alpha_1 \tag{24}$$

$$\frac{\gamma_{lt}}{2} = (\varepsilon_1 - \varepsilon_2) \sin \alpha_1 \cos \alpha_1 + \frac{\gamma_{12}}{2} (\cos^2 \alpha_1 - \sin^2 \alpha_1) \tag{25}$$

where

ε_1, ε_2, ε_l, ε_t = biaxial strains in 1 – 2 & l – t coordinate

ρ_l = longitudinal reinforcement ratio of wall

α_1 = angle of applied principal compressive stress (2-axis) with respect to longitudinal steel reinforcements (*l*-axis)

Therefore, ε_l and ε_t can be computed by the strain compatibility equations (**Equation (23) ~ (25)**) from assumed ε_1, and assumed γ_{12} for the selected ε_2. Moreover, Hsu/Zhu ratios (ν_{12} and ν_{21}) can be derived by the determined strain in the reinforcement that yields first, ε_{sf} (ε_l or ε_t) as;

In the case of $\varepsilon_{sf} \le \varepsilon_y$;

$$\nu_{12} = 0.2 + 850\varepsilon_{sf} \tag{26a}$$

In the case of $\varepsilon_{sf} > \varepsilon_y$;

$$\nu_{12} = 1.9 \tag{26b}$$

$\nu_{21} = 0$ after cracking, $\nu_{21} = 0.2$ before cracking (27)

b) Calculate $\overline{\varepsilon_1}$, $\overline{\varepsilon_2}$, $\overline{\varepsilon_l}$, and $\overline{\varepsilon_t}$

The uniaxial strain of 1-2 coordinate, $\overline{\varepsilon_1}$ and $\overline{\varepsilon_2}$ derived from the Hsu/Zhu ratios and biaxial strains of 1-2 coordinate determined earlier;

$$\overline{\varepsilon_1} = \frac{1}{1-\nu_{12}\nu_{21}}\varepsilon_1 + \frac{\nu_{21}}{1-\nu_{12}\nu_{21}}\varepsilon_2 \tag{28}$$

$$\overline{\varepsilon_2} = \frac{\nu_{21}}{1-\nu_{12}\nu_{21}}\varepsilon_1 + \frac{1}{1-\nu_{12}\nu_{21}}\varepsilon_2 \tag{29}$$

Then, it is able to compute uniaxial strain of *l*-*t* coordinate, $\overline{\varepsilon_l}$ and $\overline{\varepsilon_t}$ using strain compatibility equations;

$$\overline{\varepsilon_l} = \overline{\varepsilon_1}\cos^2\alpha_1 + \overline{\varepsilon_2}\sin^2\alpha_1 - \frac{\gamma_{12}}{2}2\sin\alpha_1\cos\alpha_1 \tag{30}$$

$$\overline{\varepsilon_t} = \overline{\varepsilon_1}\sin^2\alpha_1 + \overline{\varepsilon_2}\cos^2\alpha_1 + \frac{\gamma_{12}}{2}2\sin\alpha_1\cos\alpha_1 \tag{31}$$

c) Calculate β, ζ, σ_1^c, and σ_2^c

The deviation angle, β is the difference between the angle α_1 of the applied principal stresses in the 1-2 coordinate and the angle α_r of the principal concrete stresses in the *r-d* coordinate. It also can be derived from the below equation that is induced from the point of geometric view of the Mohr strain circle as shown in **Fig. 3-22**;

$$\beta = \frac{1}{2}\tan^{-1}\left[\frac{\gamma_{12}}{(\varepsilon_1 - \varepsilon_2)}\right] \tag{32}$$

Since the strains of the concrete element and reinforcements, $\overline{\varepsilon_1}$, $\overline{\varepsilon_2}$ are determined in the previous equations, stresses applied to the concrete element can be computed by using constitutive relationship of the concrete element.

Constitutive relationship of concrete element

The compressive stress–strain curve of concrete in a 2-D element subjected to shear exhibits three characteristics. First, the peak point is softened in both stress and strain. Second, the pre-peak ascending curve is found to be parabolic. Third, the post-peak descending curve is also a parabolic curve, but the gently sloping curve intersects the horizontal axis at a large strain of $4\varepsilon_0$, four times the strain at the peak stress, f_c as shown in **Fig. 3-23**. Based on this figure, the constitutive relationships of concrete compressive stress σ_2^c and the uniaxial compressive strain $\overline{\varepsilon_2}$, are given as follows;

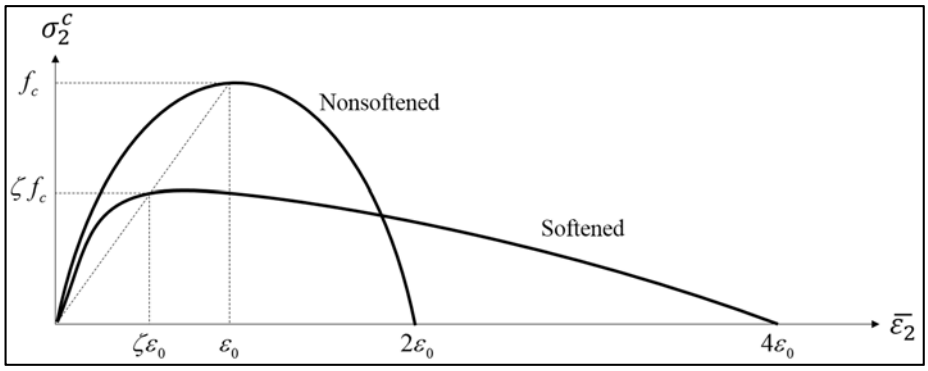

Fig. 3-23 Compressive stress–strain curve of concrete (Hsu, 2010)

In the case of $\overline{\varepsilon_2} / \zeta\varepsilon_0 \le 1$;

$$\sigma_2^c = \zeta f_c \left[2\left(\frac{\overline{\varepsilon_2}}{\zeta\varepsilon_0}\right) - \left(\frac{\overline{\varepsilon_2}}{\zeta\varepsilon_0}\right)^2 \right] \tag{33a}$$

In the case of $\overline{\varepsilon_2} / \zeta\varepsilon_0 \ge 1$;

$$\sigma_2^c = \zeta f_c \left[1 - \left(\frac{\overline{\varepsilon_2} / \zeta\varepsilon_0 - 1}{4/\zeta - 1}\right)^2 \right] \tag{33b}$$

The softening coefficient ζ is affected by three parameters; the uniaxial tensile strain $\overline{\varepsilon_1}$ in the perpendicular direction, the concrete compressive strength f_c, and the deviation angle β as below equation.

$$\zeta = f_1\left(\overline{\varepsilon_1}\right) f_2\left(f_{ck}\right) f_3\left(\beta\right) \tag{34}$$

where

$$f_1\left(\overline{\varepsilon_1}\right)=\frac{1}{\sqrt{1+400\overline{\varepsilon_1}}}$$

$$f_2\left(f_c\right)=\frac{5.8}{\sqrt{f_c}}\leq 0.9 \quad (f_c \text{ in MPa})$$

$$f_3\left(\beta\right)=1-\frac{|\beta|}{24^\circ}$$

The tensile stress–strain curve of concrete in a 2-D element consists of two distinct branches. Before cracking, the stress–strain relationship is essentially linear. After cracking, however, a drastic drop of strength occurs and the descending branch of the curve become concave as shown in **Fig. 3-24**. Based on this figure, the constitutive relationships of concrete tensile stress σ_1^c and the uniaxial tensile strain $\overline{\varepsilon_1}$, are given as follows;

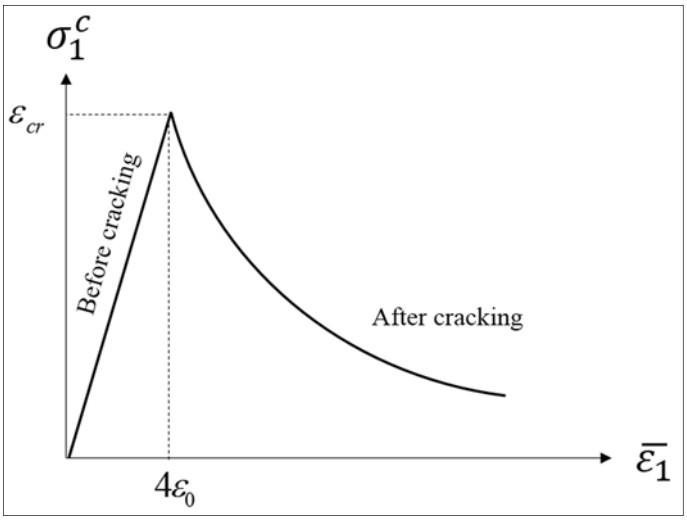

Fig. 3-24 Tensile stress–strain curve of concrete (Hsu, 2010)

In the case of $\overline{\varepsilon_1} \le \varepsilon_{cr}$;

$$\sigma_1^c = E_c \overline{\varepsilon_1} \tag{35a}$$

In the case of $\overline{\varepsilon_1} > \varepsilon_{cr}$;

$$\sigma_1^c = f_{cr} \left(\frac{\varepsilon_{cr}}{\overline{\varepsilon_1}} \right)^{0.4} \tag{35b}$$

where,

E_c = young's modulus of concrete (MPa)

ε_{cr} = cracking strain of concrete, taken as 0.00008 (mm / mm)

f_{cr} = cracking stress of concrete, taken as $0.31\sqrt{f_c}$ (MPa)

Based on the Mohr circle for stresses and strains in **Fig. 3-22**, and assuming that the direction of the principal stress of concrete coincides with the principal strain, smeared stress–strain relationships of concrete in shear can be obtained as below equations.

$$\tau_{12}^c = \frac{\sigma_1^c - \sigma_2^c}{2} \tan 2\beta \tag{36}$$

$$\gamma_{12} = \left(\varepsilon_1 - \varepsilon_2 \right) \tan 2\beta \tag{37}$$

d) Calculate f_l and f_t

Since the strains of the concrete element and reinforcements, $\overline{\varepsilon_l}$, and $\overline{\varepsilon_t}$ are determined in the previous equations, stresses applied to the reinforcements can be computed by using constitutive relationship of the reinforcement.

Constitutive relationship of smeared reinforcement

The smeared tensile stress–strain relationship of reinforcement embedded in concrete is determined bilinear model considering strain hardening as shown in **Fig. 3-25**. The constitutive relationships are given as follows;

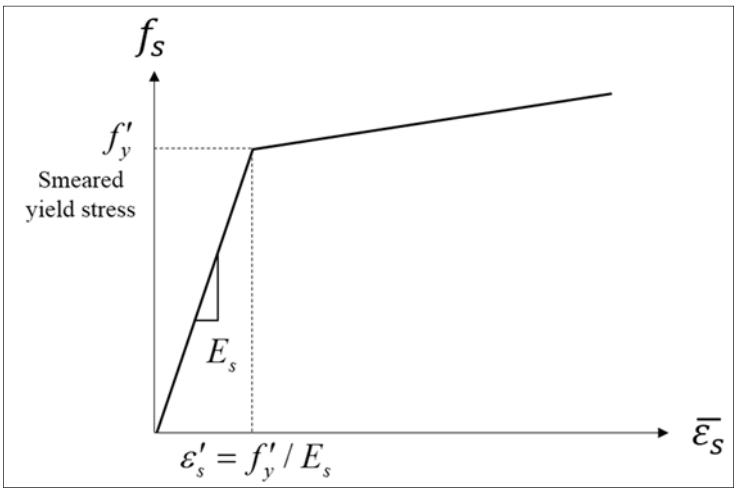

Fig. 3-25 Stress–strain relationship for reinforcement using bilinear model

In the case of $\overline{\varepsilon_s} \le \varepsilon'_y$;

$$f_s = E_s \overline{\varepsilon_s} \tag{38a}$$

In the case of $\overline{\varepsilon_s} > \varepsilon'_y$;

$$f_s = \left(0.91 - 2B\right) f_y + \left(0.02 + 0.25B\right) E_s \overline{\varepsilon_s} \tag{38b}$$

where

f'_y = smeared yield stress of reinforcement $\left(= \left(0.93 - 2B\right) f_y\right)$

$$B = \frac{1}{\rho_s}\left(\frac{f_{cr}}{f_y}\right)^{1.5}$$

$\overline{\varepsilon_s}$ = strain of longitudinal or transverse reinforcement ($\overline{\varepsilon_l}$ or $\overline{\varepsilon_t}$)

ρ_s = ratio of longitudinal or transverse reinforcement (ρ_l or ρ_t)

e) Solution algorithm using $\rho_l f_l$ and $\rho_t f_t$

For the selected biaxial 2-directional strain ε_2, it needs to be verified the validity of the assumed strains ε_1 and γ_{12}. SMM modified the first two equilibrium equations (**Equation (20) ~ (21)**) to make two equations for the convergence criteria by summing up and subtracting them as below;

$$\left(\rho_l f_l + \rho_t f_t\right)_2 = \left(\sigma_l + \sigma_t\right) - \left(\sigma_1^c + \sigma_2^c\right) \tag{39}$$

$$\left(\rho_l f_l - \rho_t f_t\right)_2 = \left(\sigma_l - \sigma_t\right) - \left(\sigma_1^c - \sigma_2^c\right)\cos 2\alpha_1 + 2\tau_{12}^c \sin 2\alpha_1 \tag{40}$$

Since the smeared stress in the longitudinal and transverse reinforcement f_l and f_t can be determined by **Equation (38a) ~ (38b)**, $\left(\rho_l f_l + \rho_t f_t\right)_1$ and $\left(\rho_l f_l + \rho_t f_t\right)_2$ can be computed directly. By comparing $\left(\rho_l f_l + \rho_t f_t\right)_1$ with $\left(\rho_l f_l + \rho_t f_t\right)_2$, and $\left(\rho_l f_l - \rho_t f_t\right)_1$ with $\left(\rho_l f_l - \rho_t f_t\right)_2$, it is able to confirm the validity of the assumed strains ε_1 and γ_{12}.

f) Calculate τ_{lt} and γ_{lt}

The shear stress τ_{lt} and the shear strain γ_{lt} for the selected can be calculated from the equilibrium equation and the compatibility equation. (**Equation (22) and (25)**) After the completing the iterative process in the flow chart by selecting a series of ε_2 values, it is able to plot the $\tau_{lt} - \gamma_{lt}$ curves.

3.3.3 Analysis of WN using SMM

Although the SMM had been proved its reliability on the analysis of the

RC 2-D membrane element by lots of researchers, the applicability of applying SMM to the test specimens of this study has to be reviewed, because the test set-up is not general test set-up of the squat wall testing.

The SMM have to solve 19 unknown variables (6 stresses, 10 strains, the deviation angle, the softening coefficient, and the 2 Hsu/Zhu ratios) with 19 equations. Therefore, it is need to develop the program for the iterative analysis, and tried to make it with MATLAB. However, the divergence result was often occurred due to inappropriate initially assumed values ε_1 and γ_{12} for the selected ε_2. That shows the weakness of the SMM that is significantly dependent on the initially assumed values ε_1 and γ_{12}. To resolve this weakness, this study made an iterative macrocode with Microsoft Excel. The advantage of this macrocode is showing the convergence value according to the initially assumed values ε_1 and γ_{12} for the selected ε_2 intuitively as shown in **Fig. 3-26**.

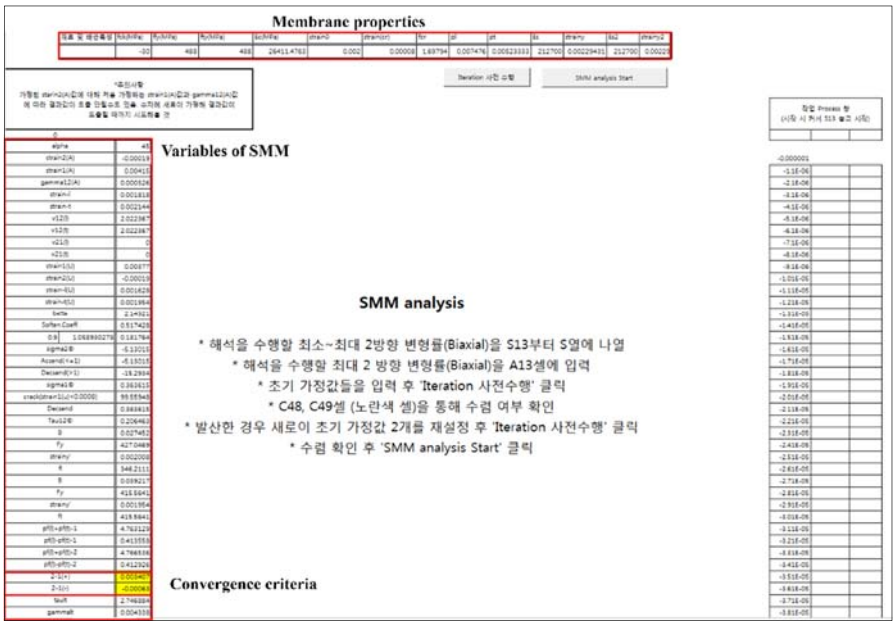

Fig. 3-26 Iterative macrocode of SMM by Excel

By using this macrocode, it is able to determine shear stress–shear strain curve of WN, membrane element with single-layered reinforcement. Moreover,

to prove the accuracy of the SMM, this study also analyzed WN with the modified compression field theory, and RA-STM with MEMBRANE 2000 published by the University of Toronto. The comparison result of the test and that of the analysis are shown in **Fig. 3-27**.

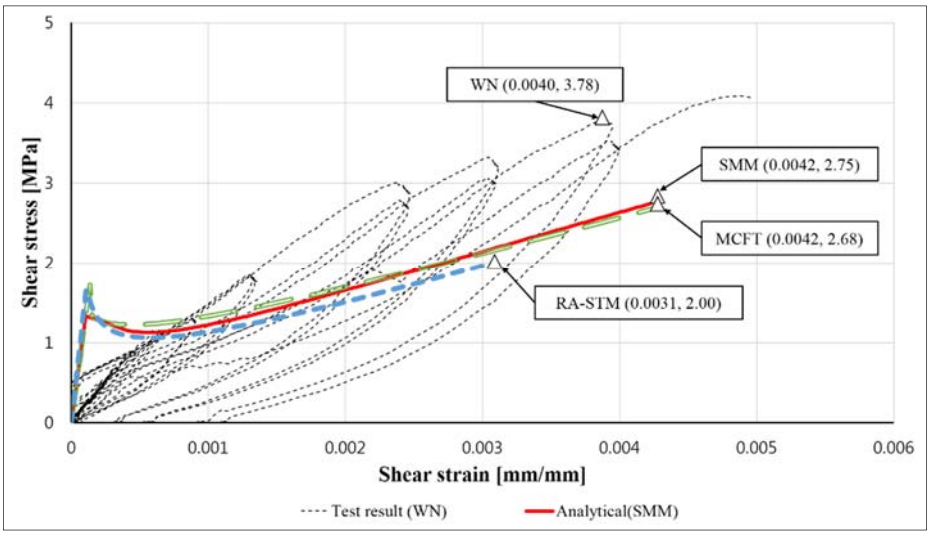

Fig. 3-27 Comparison of the result of WN and analytical methods

The shear strain of WN is measured by ratio of the displacement to the height of the wall panel. The comparison result shows that the SMM and the MCFT can expect yielding point of WN accurately. However, analytical shear stresses when the transverse reinforcement yielded derived from the MCFT and the SMM are almost 75% of the test result. The reason of this distinction is supposed that the unusual test setting of this study would affect the behavior of the specimen. However, since the SMM can expect the shear strain when transverse yielding is occurred in WN accurately, and shear stress almost close to that of WN at that time than the other methods (MCFT, RA-STM), this study used the SMM to analyze the UHPFRC web retrofitted single-layered RC squat wall.

3.3.4 Analysis of WR using SMM

To analyze the UHPFRC web retrofitted squat wall with the SMM, this

study assumed three basic assumptions. First, the RC squat wall and the UHPFRC behaved with the same strain values ε_1, ε_2, γ_{12} at the same time. Second, the UHPFRC panel and the RC squat wall have the same strut angle, α_1. Third, since the softening behavior of the UHPFRC has not be studied before, this study assumed that existing softening coefficient ζ for the normal strength concrete also can be used for strength of the UHPFRC.

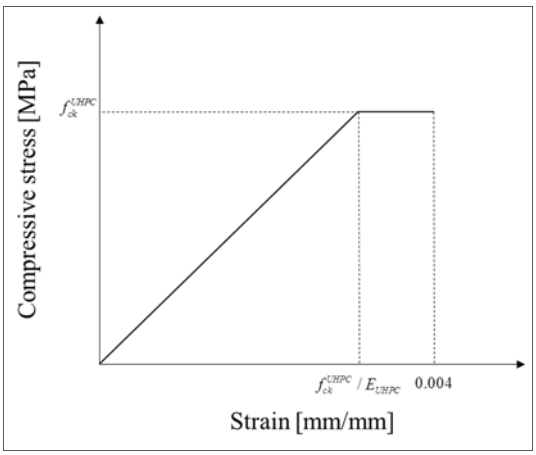

Fig. 3-28 Compressive stress–strain relationship for K-UHPC

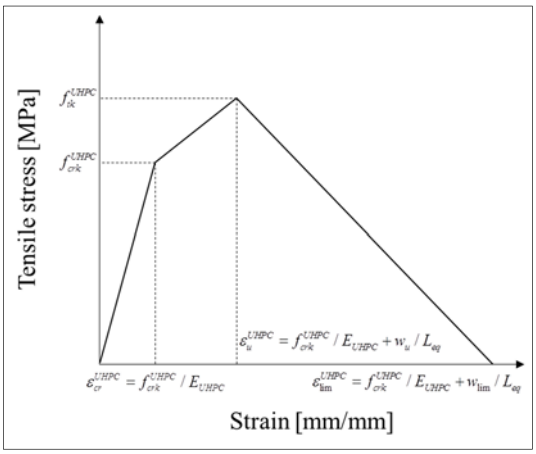

Fig. 3-29 Tensile stress–strain relationship for K-UHPC

The constitutive relationships of the UHPFRC are assumed to be same as that of the K-UHPC provision as shown in **Fig. 3-28** and **Fig. 3-29**. Based on the material test results of this study, the constitutive relationships of the UHPFRC

compressive stress σ_2^{UHPC} and the uniaxial compressive strain $\overline{\varepsilon_2}$, can determined as follows;

In the case of $\overline{\varepsilon_2} \le f_c^{UHPC} / E_{UHPC}$;

$$\sigma_2^{UHPC} = \zeta E_{UHPC} \overline{\varepsilon_2} \tag{41a}$$

In the case of $\overline{\varepsilon_2} > f_c^{UHPC} / E_{UHPC}$;

$$\sigma_2^{UHPC} = \zeta f_c^{UHPC} \tag{41b}$$

where

f_c^{UHPC} = compressive strength of UHPFRC (in this study, 100 MPa)

E_{UHPC} = young's modulus of UHPFRC (40,000 MPa)

The constitutive relationships of the UHPFRC tensile stress σ_1^{UHPC} and the uniaxial tensile strain $\overline{\varepsilon_1}$, are determined from direct tension test of UHPFRC dog bone specimen; however, this study did not plan direct tension test. Therefore, since the K-UHPC uses 1.5% fiber, this study used the constitutive relationships of UHPFRC tensile stress σ_1^{UHPC} and the uniaxial tensile strain $\overline{\varepsilon_1}$ of the K-UHPC provision directly.

In the case of $\overline{\varepsilon_1} \le f_{crk}^{UHPC} / E_{UHPC}$;

$$\sigma_1^{UHPC} = E_{UHPC} \overline{\varepsilon_1} \tag{42a}$$

In the case of $f_{crk}^{UHPC} / E_{UHPC} \le \overline{\varepsilon_1} \le f_{crk}^{UHPC} / E_{UHPC} + w_u / L_{eq}$;

$$\sigma_1^{UHPC} = f_{crk}^{UHPC} + \left(\frac{(f_{crk}^{UHPC} - f_{crk}^{UHPC})}{w_u / L_{eq}} \right) \left(\overline{\varepsilon_1} - \frac{f_{crk}^{UHPC}}{E_{UHPC}} \right) \tag{42b}$$

In the case of $f_{crk}^{UHPC} / E_{UHPC} + w_u / L_{eq} \le \overline{\varepsilon_1} \le f_{crk}^{UHPC} / E_{UHPC} + w_{\lim} / L_{eq}$;

$$\sigma_1^{UHPC} = f_{tk}^{UHPC} - \left(\frac{f_{tk}^{UHPC}}{\left(w_{\lim} - w_u \right) / L_{eq}} \right) \left(\overline{\varepsilon_1} - \left(\frac{f_{crk}^{UHPC}}{E_{UHPC}} + \frac{w_u}{L_{eq}} \right) \right) \qquad (42c)$$

where

f_{crk}^{UHPC} = cracking tensile stress of K-UHPC (9.5 MPa)

f_{tk}^{UHPC} = nominal tensile stress of K-UHPC (13 MPa)

$w_{\lim}$ = maximum crack width of UHPFRC (5.3 mm)

$L_{eq} = 0.8 l_w \left[1 - 1 / (1.05 + 6 l_w / l_{ch})^4 \right]$

l_{ch} = characteristic length (1.01×10^4 mm)

Based on these relationships, it is able to define stress equilibrium equations due to uniaxial strains $\overline{\varepsilon_1}$, $\overline{\varepsilon_2}$, and γ_{12} of the UHPFRC panel.

Stress equilibrium equations (UHPFRC panel)

$$\sigma_l^{UHPC} = \sigma_1^{UHPC} \cos^2 \alpha_1 + \sigma_2^{UHPC} \sin^2 \alpha_1 - \tau_{12}^{UHPC} 2 \sin \alpha_1 \cos \alpha_1 \qquad (43)$$

$$\sigma_t^{UHPC} = \sigma_1^{UHPC} \sin^2 \alpha_1 + \sigma_2^{UHPC} \cos^2 \alpha_1 + \tau_{12}^{UHPC} 2 \sin \alpha_1 \cos \alpha_1 \qquad (44)$$

$$\tau_{lt}^{UHPC} = (\sigma_1^{UHPC} - \sigma_2^{UHPC}) \sin \alpha_1 \cos \alpha_1 + \tau_{12}^{UHPC} (\cos^2 \alpha_1 - \sin^2 \alpha_1) \qquad (45)$$

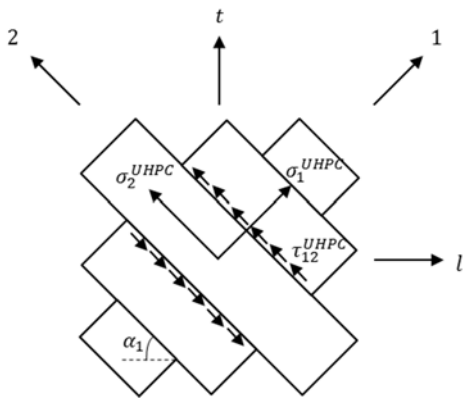

Fig. 3-30 Stress equilibrium of the retrofitting UHPFRC panel

Since the retrofitted member is subjected to the pure shear in this study, force equilibrium considering the stresses of the RC squat wall and the UHPFRC panel (**Equation (20) ~ (21)**, and **(43) ~ (44)**) and the thickness of them also has to be included.

$$\sigma_l t_w + \sigma_l^{UHPC} t_{UHPC} = 0 \tag{46a}$$

$$\sigma_t t_w + \sigma_t^{UHPC} t_{UHPC} = 0 \tag{46b}$$

Based on these equations, it is able to define modified convergence criteria of the SMM considering the stresses and the thickness of the UHPFRC panel by summing up and subtracting the **Equation (46a)** and the **Equation (46b)** as below;

In the case of pure shear;

$$\left(\rho_l f_l + \rho_t f_t\right)_2 = \left(\sigma_1^c + \sigma_2^c\right) - \frac{t_{UHPC}}{t_w}\left(\sigma_1^{UHPC} + \sigma_2^{UHPC}\right) \tag{47}$$

$$\left(\rho_l f_l - \rho_t f_t\right)_2 = -\left(\sigma_1^c - \sigma_2^c\right)\cos 2\alpha_1 + 2\tau_{12}^c \sin 2\alpha_1 \tag{48}$$

$$-\frac{t_{UHPC}}{t_w}\left[\left(\sigma_1^{UHPC} - \sigma_2^{UHPC}\right)\cos 2\alpha_1 + 2\tau_{12}^{UHPC} \sin 2\alpha_1\right]$$

Therefore, it is able to follow the flow chart of the SMM considering the UHPFRC panel behaved with the same strain conditions of the RC squat wall. The failure mode of the web UHPFRC retrofitted RC squat wall also can be verified. The shear stress–shear strain curve of the UHPFRC web retrofitted RC squat wall plotted from the modified SMM as shown in **Fig. 3-31.**

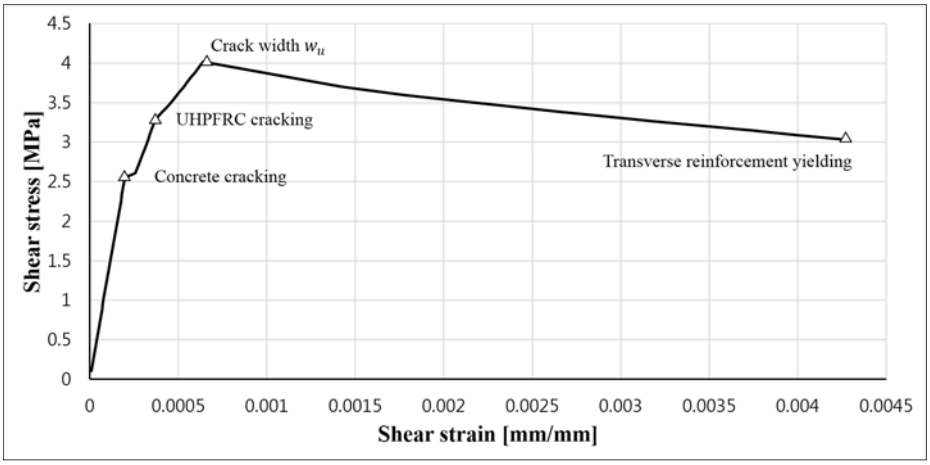

Fig. 3-31 Analytical result of the web UHPFRC retrofitted RC squat wall (Modified SMM)

According to the analytical result of the modified SMM, the failure mode of the UHPFRC web retrofitted RC squat wall can be arranged with some specific events. After the normal strength concrete cracking is occurred, stiffness does not decreased so much different from the case of the RC squat wall. When the UHPFRC panel is cracked, bridging action is started by fibers. The maximum shear stress is appeared when the crack width of the UHPFRC panel reaches w_u. Beyond the maximum shear stress, linearly descending branch is formed by fibers of the UHPFRC panel. Finally, yielding of the transverse reinforcement causes diagonal tension failure. The comparison result between the test result of WR and the analytical result is shown in **Fig. 3-32**. The shear strain of WR is measured from its diagonally installed LVDTs until the 12nd cyclic loading; the distortion of the middle boundary element was occurred.

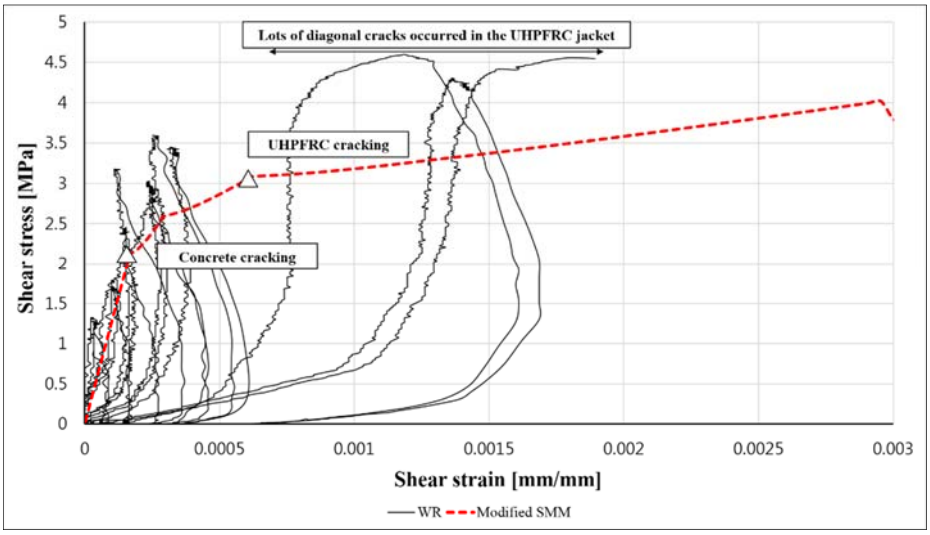

Fig. 3-32 Comparison result of WR & modified SMM

The analytical maximum shear stress of the UHPFRC web retrofitted squat wall is about 70 % of that of the test result, similar to the case of WN. Although the test result crack widening of the UHPFRC could not follow that of the RC wall due to lack of the interface shear, and the ultimate failure of the test could not be determined, there are some evidences that can support the validity of the analytical result. First, the overall appearance of the test result is similar to that of the analytical result. Second, the restraint of the strain of the transverse reinforcement at the earlier cycles shows that the RC squat wall and the UHPFRC panel behaved with the same strains. Third, occurrence of the lots of diagonal cracks at the test (11st ~ 12nd cycle) within the region from the point of the UHPFRC cracking to the point of the UHPFRC crack width reaches w_u. Therefore, it's able to conclude the validity of the proposed method, a certain extent.

3.3.5 Retrofitting effect depending on t_{UHPC}/t_w ratio

The retrofitting efficiency of web retrofitting method could be diverse depending on the retrofitting thickness ratio. Since the material property of the retrofitting material is distinct to that of the retrofitting target, the UHPFRC web retrofitting method especially needs consideration about this problem. Therefore, this study compared the shear stress–strain curves of the UHPFRC web retrofitted RC squat walls retrofitted with different t_{UHPC}/t_w ratios (t_w =120 mm) by the modified SMM. The comparison result is shown in **Fig. 3-33**.

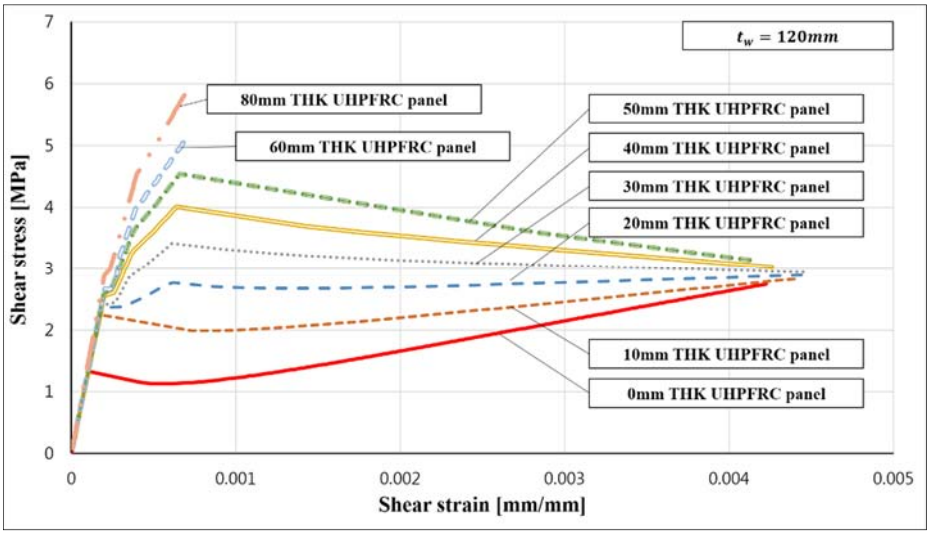

Fig. 3-33 Shear stress–shear strain curve depending on thickness of UHPFRC panel

The UHPFRC panel enhances the post-cracking behavior of the retrofitted member, and shows linearly descending branch. However, when the t_{UHPC}/t_w ratio is increased over 0.5 (in this study, 60 mm), the linearly descending branch is disappeared, and the transverse reinforcement yielded suddenly after the peak stress. **Table 12** shows the state of the stresses in the UHPFRC web retrofitted squat wall computed from the modified SMM according to the state of the member.

Table 12 Stresses computed from modified SMM

Retrofitting	State	γ_{lt}	τ_{lt}(RC wall) [MPa]	τ_{lt}(UHPFRC) [MPa]	f_t [MPa]
0mm THK UHPFRC ($t_{UHPC}/t_w = N/A$)	UHPFRC crack width 0.3mm	0.0042	2.75	N/A	409
	Ultimate				
10mm THK UHPFRC ($t_{UHPC}/t_w = 0.083$)	UHPFRC crack width 0.3mm	0.00064	1.62	6.44	57
	Ultimate	0.0044	2.88	2.23	415
20mm THK UHPFRC ($t_{UHPC}/t_w = 0.17$)	UHPFRC crack width 0.3mm	0.00062	2.08	6.88	38
	Ultimate	0.0044	2.88	2.56	418
30mm THK UHPFRC ($t_{UHPC}/t_w = 0.25$)	UHPFRC crack width 0.3mm	0.00061	2.47	7.18	30
	Ultimate	0.0044	2.95	2.91	418
40mm THK UHPFRC ($t_{UHPC}/t_w = 0.33$)	UHPFRC crack width 0.3mm	0.00064	2.83	7.65	27
	Ultimate	0.0042	2.89	3.47	396
50mm THK UHPFRC ($t_{UHPC}/t_w = 0.42$)	UHPFRC crack width 0.3mm	0.00066	3.04	8.12	25
	Ultimate	0.0039	2.82	3.93	383
60mm THK UHPFRC ($t_{UHPC}/t_w = 0.5$)	UHPFRC crack width 0.3mm	0.00068	3.25	8.64	23
	Ultimate				
80mm THK UHPFRC ($t_{UHPC}/t_w = 0.67$)	UHPFRC crack width 0.3mm	0.00069	3.37	9.48	22
	Ultimate				

The **Table 12** shows that if there is a big difference between the shear stress carried by the RC squat wall and that of the UHPFRC panel, the transverse reinforcement yielded suddenly. Therefore, the t_{UHPC}/t_w ratio of 0.17 to 0.25 is recommended in retrofitting WN with the UHPFRC web retrofitting of this study to prevent sudden yielding of transverse reinforcement with sufficient retrofitting effect. Therefore, the shear strength summing up the existing provisions (**Equation (3)** and **Equation (18)**) is not valid for predicting the UHPFRC web retrofitted squat wall.

3.3.6 Computation of interface stress $\tau_{interface}$ under pure shear

This study assumed the interface element with zero thickness located between the UHPFRC panel and the RC squat wall to determine the design interface stress $\tau_{interface}$ preventing the interface failure occurred in WR as shown in **Fig. 3-34**. Since the failure mode of the UHPFRC retrofitted RC squat wall investigated in the previous part, it is able to determine the ultimate stress applied to the interface element. The interface element has to transfer the maximum shear stress caused by one element to the other element. There are two stresses control the maximum shear stress applied to the interface element. First one is yield stress of the transverse and the vertical reinforcement (f_{ty} and f_{ly}). The other one is the ultimate tensile stress of the UHPFRC panel (f_{tk}^{UHPC}). The force applied to the interface element is controlled by the former stress when t_{UHPC}/t_w is very low, and the later stress when t_{UHPC}/t_w is high. Based on these facts, this study suggested the equations for calculating $\tau_{interface}$ as below;

$$\tau_{interface} = \max\left(\frac{\sqrt{\left(A_t f_{ty}\right)^2 + \left(A_l f_{ly}\right)^2}}{A_{interface}}, \frac{\sqrt{2}\min(s_l, s_t) t_{UHPC} f_{tk}^{UHPC}}{A_{interface}} \right) \quad (49)$$

where,

s_l = spacing of the longitudinal reinforcement (mm)

A_l = area of the longitudinal reinforcement in the spacing s_l (mm^2)

f_{ly} = yield strength of the longitudinal reinforcement (MPa)

$A_{interface}$ = triangular area formed by diagonal crack in interface element (mm^2)

$$\left(= \frac{\left(\min(s_l, s_t)\right)^2}{2} \right)$$

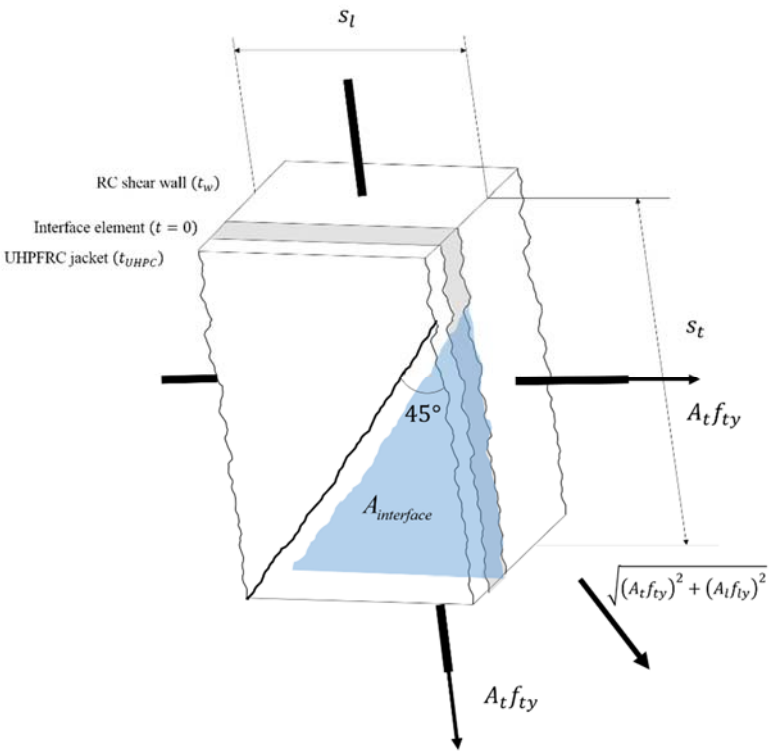

a) Interface shear controlled by yielding of the reinforcements

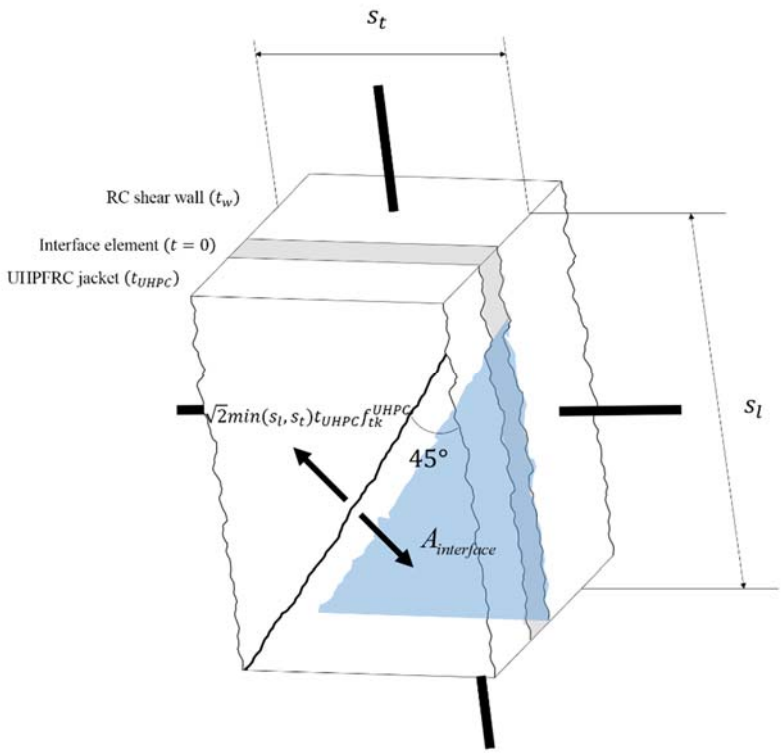

b) Interface shear controlled by tensile stress of the UHPFRC

Fig. 3-34 Computation of interface shear with the assumed interface element

Therefore, based on the suggested equation for computing the interface stress $\tau_{interface}$, it is able to compute the design interface stress for WR as 11.7 MPa (max (6.27 MPa, 11.77 MPa)). Therefore, since required shear stress for the one side web retrofitting with thickness of the UHPFRC panel as t_{UHPC}, it is recommended to retrofit the RC squat wall with the UHPFRC panel at the both web surfaces with thickness of the UHPFRC panel as $t_{UHPC}/2$ to make them behave monolithically.

3.3.7 Validity of the proposed method

The proposed model of this study for deriving shear stress – shear strain result of the UHPFRC web retrofitted RC squat wall can be verified its validity by comparing the analytical result between the single – layered squat wall retrofitted with single – layered RC web section enlargement method and double – layered squat wall behaved monolithically. Therefore, this study assumed two squat walls as shown in **Fig. 3-35**.

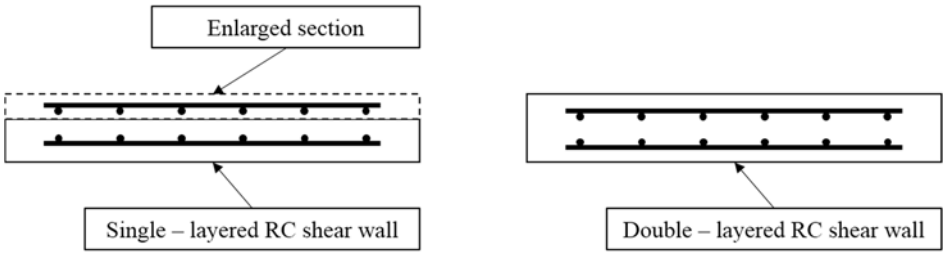

(a) Web retrofitted single –layered squat wall (b) Double – layered squat wall

Fig. 3-35 Assumed sections to verify the validity of the modified SMM

As shown in the Fig., the web retrofitted single – layered squat wall and the double – layered squat wall have not only same sectional dimensions, also same reinforcement ratio. Therefore, these two members are actually behave in same behavior, and have same shear stress – shear strain result. If the modified SMM is valid for analyzing the web retrofitted squat wall, the shear stress – shear strain curve derived from it of web retrofitted single – layered squat wall and the double – layered squat wall have to be same. The details of them are tabulated in **Table 13**. The material properties used in them are same as that of WR.

By using these details and the material properties, this study analyzed the web retrofitted single – layered squat wall with the modified SMM proposed in this study and the double – layered squat wall with the SMM proposed by Hsu and Zhu (2000). The shear stress – shear strain results of them are compared in **Fig. 3-36**.

Table 13 Details of the assumed sections

	Properties	Web retrofitted single – layered squat wall	Double – layered squat wall
Retrofitting target	$l_w \times t_w$	1300 mm × 80 mm	1300 mm × 120 mm
	ρ_l	0.56 % (HD10 @ 175 mm)	0.75 % (2 – HD10 @ 175 mm)
	ρ_t	0.79% (HD10 @ 125 mm)	1.05 % (2 – HD10 @ 125 mm)
Retrofitting panel	$l_w \times t_w$	1300 mm × 40 mm	N.A
	ρ_l	1.12 % (HD10 @ 175 mm)	
	ρ_t	1.57 % (HD10 @ 125 mm)	

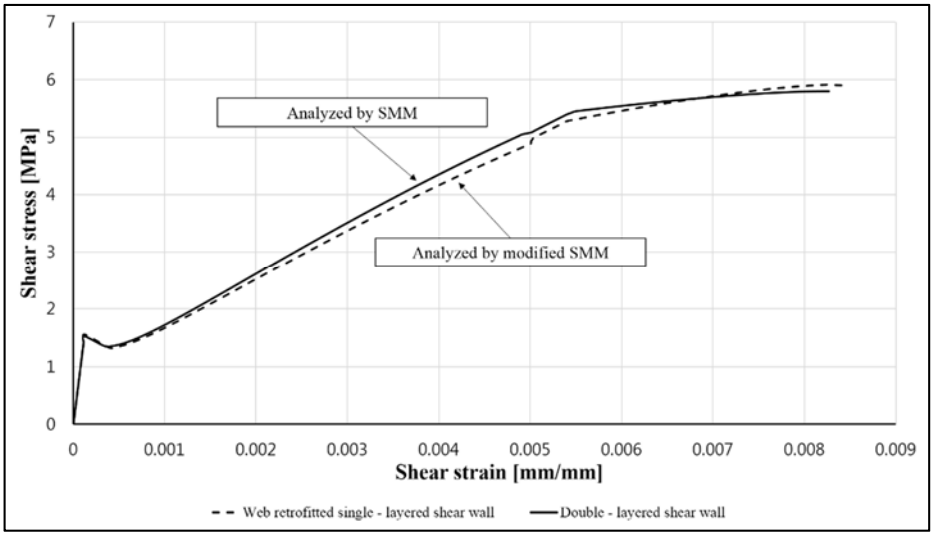

Fig. 3-36 Comparison result of the assumed sections

By the comparison result, it is able to verify the validity of the modified SMM proposed in this study. Moreover, it is confirmed that the modified SMM also can be used for the case of the web section enlargement retrofitting with RC panel usually used in structural remodeling site. Therefore, if there exist precise constitutive relationships of materials that used for the web retrofitting, it is able to determine shear retrofitting effect by deriving the shear stress – shear strain relationship of the web retrofitted squat wall with the modified SMM.

Chapter 4. Conclusions

This study planned experimental programs and proposed analytical methods to predict the ultimate shear strength and behavior of the retrofitted single-layered squat wall by section enlargement retrofitting method.

In the Chapter 2, the end retrofitted single-layered squat wall by providing column element as additional boundary element was analyzed in the experimental and analytical way. Therefore, it is able to determine the retrofitting effect of this method by using the proposed analytical model almost same as that of the test result. The conclusions of this chapter are summarized below.

(1) Compared to the non-retrofitted specimen, the strain of the transverse reinforcement experienced larger value beyond its yield strain due to the retrofitting column located at the both ends of the squat wall.

(2) Failure of the end retrofitted specimen is accompanied with yielding of transverse reinforcements and shear failure of retrofitting column.

(3) The proposed model includes not only the components of the details of the end retrofitting column, and that of the squat wall by assuming the length, h_s where the concentrated shear deformation of the retrofitting column is occurred. It is able to consider monolithic behavior of the end retrofitted squat wall with this length. By using the proposed model, it is able to predict the ultimate shear strength of the end retrofitted squat wall close to that of the test result.

(4) It is able to derive the initial stiffness of the end retrofitted squat wall close to that of the test result by transferring member's resisting mechanism to the single diagonal strut mechanism. The initial stiffness of the modified diagonal strut can be derived by the modified strut computed from the derived retrofitted squat wall's ultimate shear strength of this study.

(5) The proposed method of this study also can analytically predict the ultimate shear strength and the initial stiffness of the infilled RC squat wall in RC frame close to the test result of it.

In the Chapter 3, the UHPFRC web retrofitted single-layered squat wall was analyzed in experimental and analytical way. Although the test result was not good enough to prove the retrofitting effect of the UHPFRC web retrofitting method, it is able to determine the failure mode of the retrofitted squat wall by modified SMM proposed in this study. The conclusions of this chapter are also summarized below.

(1) Compared to the non-retrofitted specimen, the retrofitting UHPFRC panel restraints strain increment of the transverse reinforcements. This fact can be confirmed by the comparison results of the strain distribution between the specimens; WN and WR.

(2) The dissipated energy of WR is always larger than that of WN at every load cycles. Based on this fact, it is able to confirm the energy dissipation contribution of the retrofitting UHPFRC panel.

(3) Since WR could not reach its ultimate state, the softened membrane model (SMM), reliable model for analyzing 2-D RC membrane element was modified in this study to consider the retrofitting effect of the UHPFRC panel with considering the thickness ratio t_{UHPC} / t_w.

Based on the similarities found between the both experimental and analytical results, it is confirmed that the modified SMM can predict the UHPFRC web retrofitted squat wall conservatively.

(4) Based on the analytical results from the modified SMM, the failure mode of the UHPFRC web retrofitted squat wall in the case of thickness of the retrofitting UHPFRC panel is 40mm, one third of the thickness of the retrofitting target can be determined.

(5) The comparison results analyzed from the modified SMM with changing the thickness ratio t_{UHPC}/t_w shows that larger t_{UHPC}/t_w result in brittle failure mechanism due to the great difference between the shear stress carried by the RC squat wall and that by the UHPFRC panel derived from the modified SMM. The most ideal failure mechanism is occurred when the shear stress carried by the RC squat wall and that by the UHPFRC panel are almost equal.

(6) The interface stress occurred between the RC squat wall and the retrofitting UHPFRC panel can be computed based on the determined failure mode of the UHPFRC web retrofitted squat wall from the modified SMM. This study assumed the zero thickness interface element to determine interface stress occurred between them.

(7) The interface stress to behave monolithically derived from this study is too high. Therefore, it is recommended to retrofit the RC squat wall with the UHPFRC panel at the both web surfaces of the RC squat wall than the one – side UHPFRC web retrofitting of this study.

(8) This study applied the modified SMM to the web retrofitted single – layered squat wall with the single - layered panel, and compared it with the double – layered squat wall. Therefore, the validity of the modified SMM can be confirmed.

References

1. Fadis, M. N (2009) *Seismic Design, Assessment and Retrofitting of Concrete Buildings based on EN-Eurocode 8*, Springer Netherlands.

2. Marini, A. and Meda, A. (2009) “Retrofitting of R/C squat walls by means of high performance jackets”, Engineering Structures, Vol 31, Issue 12, pp 3059-3064.

3. Cervenka, V. and Gerstle, K. H. (1972) “Inelastic analysis of reinforced concrete panels : experimental verification and application”, IABSE publications, Vol 32, pp 25-37.

4. FEMA 306 (1998) *Evaluation of Earthquake Damaged Concrete and Masonry Wall Buildings*, Washington, D.C.

5. ACI 318 Committee (2011) *Building Code Requirements for Structural Concrete (ACI 318-11) and Commentary*, Farmington Hills.

6. Hwang, Fang, Lee, and Yu (2001) “Analytical model for predicting shear strength of squat walls”, Journal of Structural Engineering, Vol.127, No. 1, pp43-50.

7. Lang, K. (2002) *Seismic vulnerability of existing buildings*, No. 273. vdf Hochschulverlag AG.

8. Maidiawati, Sanada, Y., Konishi, D., and Tanjung, J. (2011) “Seismic performance of nonstructural brick walls used in Indonesian R/C buildings”, Journal of Asian Architecture and Building Engineering, Vol.10, No.1, pp 203-210

9. Gaynor, P. J. (1988) “The effect of opening on the cyclic behavior of reinforced concrete infilled squat walls”, In Partial Fulfillment of the Requirement for the Degree of Mater of Science in Engineering, The university of Texas at Austin.

10. Kang and Hong (2014), “Performance of fresh and hardened ultra high performance concrete without heat treatment”, Journal of the Korea Concrete Institute, Vol.26, No.1, pp 23-34.

11. Hawkins, N. M., and Ghosh, S. K. (2004), “Acceptance Criteria for Special Precast Concrete Structural Walls Based on Validation Testing,” PCI Journal, Vol. 49, No. 5, pp.78-92

12. KCI (2012) *Structural design standards for K-UHPC*, Seoul.

13. Nielsen, M. P. and Hoang, L. C. (1999) *Limit Analysis and Concrete Plasticity*, CRC press.

14. Mansour, M. Y. (2001) “Behavior of reinforced concrete membrane elements under cyclic shear : Experiments to theory”, In Partial Fulfillment of the Requirement for the Degree of Doctor of Philosophy in Civil Engineering, The university of Houston.

15. Hsu, T. T. C. and Mo, Y. L. (2010) *Unified theory of CONCRETE STRUCTURES*, WILEY and Sons, Ltd, Publication.

국 문 초 록

내진 상세를 지니지 않은 단근 배근된 전단벽체는 모든 면에서 취약한 내진성능을 지니고 있다. 따라서 부족한 내진성능을 향상시키기 위해 지금껏 다방면으로 연구가 돼 왔던 다양한 내진보강 기술들을 적용해 보강이 가능하다. 이들 중 단면 증타 공법은 경제적이면서도 익숙함으로 인해 현장에서도 보편적으로 사용되는 내진 보강 공법이다. 단면 증타 공법을 통해 낮은 단근 배근 벽체를 보강하는 경우, 부족한 휨 내력을 보강하는 방법으로는 벽체 양 단부에 기둥 상세를 지닌 기둥부재를 증타시켜 벽체에 경계요소를 부여해 부족한 휨 내력을 보강하는 것과, 부족한 전단내력을 보강하는 방법으로는 벽체 웨브 면을 철근과 함께 증타시키는 방법이 있다.

하지만 전자의 경우 증가하는 휨 내력뿐만 아니라 증타로 인한 전단내력에 대한 고려도 필요하다. 만약 증가한 휨 내력으로 인한 전단력이 보강 부재의 전단내력을 초과할 경우 예기치 못한 전단파괴로 이어질 수 있기 때문이다. 이에 본 연구에서는 증타 보강되는 기둥의 상세와 일체화 거동을 고려한 보강부재의 전단강도 모델을 제안했다. 이 모델은 증타된 기둥 부재의 전단변형이 집중되는 길이를 가정해, 이를 일체화된 벽체 내에 발생하는 스트럿 두께 산정에 이용하였다. 뿐만 아니라 이 길이 내에 집중 발생하는 전단 변형률을 유도, 이를 일체화 거동을 고려한 적합성 조건으로 기존 전단벽체의 해석 알고리즘에 도입함으로써 단부 증타 보강된 벽체의 해석 알고리즘을 새로이 제안했다. 또한 제안된 알고리즘을 통해 계산된 전단강도로 보강 부재의 횡력 저항 메커니즘을 단일 스트럿 화 시켜줌으로써 보강부재의 초기 강성을 제안하였다. 제안한 방법들은 본 연구의 실험 결과를 통해 그 타당성을 확인하였다. 그리고 채움 전단벽

으로 골조를 보강한 경우에도 본 연구에서 제안한 방법이 적용 가능하다는 것 역시 확인할 수 있었다.

그리고 후자의 경우, 기존 철근 콘크리트를 사용해 웨브 면을 증타할 시엔 보강 두께가 과도해져 건축적으로 공간 낭비가 발생하게 된다. 이에 본 연구에서는 기존 콘크리트에 비해 높은 강성, 인장응력, 그리고 압축응력이 특징인 UHPFRC를 사용해 보다 얇은 두께로 보강 하면서 동시에 유효한 보강 효과를 얻을 수 있을 것이라 보았다. 하지만 이에 대한 기존 연구가 미비해 본 연구에서는 실험과 이론적 접근을 통해 UHPFRC 웨브 증타된 단근 배근 전단벽체의 전단응력-전단 변형률 관계를 계산할 수 있는 알고리즘을 제안하였고, 이를 통해 UHPFRC 웨브 증타된 단근 배근 벽체의 파괴모드와 기존 벽체와 증타된 벽체의 보강 두께 비가 보강 부재의 거동에 미치는 영향을 확인했다. 그리고 정해진 파괴모드를 바탕으로 해 증타되는 UHPFRC와 기존 단근 전단벽체 사이 경계 면에서 발생하는 최대 응력을 유도해 이를 경계면 파괴 방지를 위한 조건으로써 제안하였다. 본 연구에서 제안한 알고리즘은 단근 배근된 철근 콘크리트 단면으로 증타 보강된 단근 배근된 철근 콘크리트 전단벽의 해석 결과와 이와 동일한 배근을 가지며 일체 타설된 복배근 철근 콘크리트 전단벽의 해석 결과를 비교함으로써 그 타당성을 확인할 수 있었다.

따라서 본 연구의 결과를 통해 기존의 취약한 단근 배근된 전단벽체에 단면 증타 공법을 적용 시, 보다 효율적인 보강이 가능하고, 나아가 단면 증타 공법의 가이드라인 제안에도 활용될 수 있다.

주요어 : 단근 배근 전단벽, 전단 보강, 단면 증타 공법, 스트럿 작용, UHPFRC

학 번 : 2013-20568

APENDIX

1. Cyclic behavior of WN (Non retrofitted single – layered squat wall)

Cycle to 0.05 % drift (4th cycle)

There occurred two vertical cracks prior to testing due to the tensile forces that caused by fastening both end boundary elements to provide fixed boundary condition. Therefore, when the load had applied to the specimen, cracks were occurred not only boundary between the wall panel and the boundary elements, also around this initial cracks until 4th cycle (0.0375 % drift ratio). At the 4th cycle, there occurred flexural-shear crack in the right wall panel around the middle boundary element. The crack pattern of the specimen at 0.05 % drift ratio is shown in **Fig. A-1**.

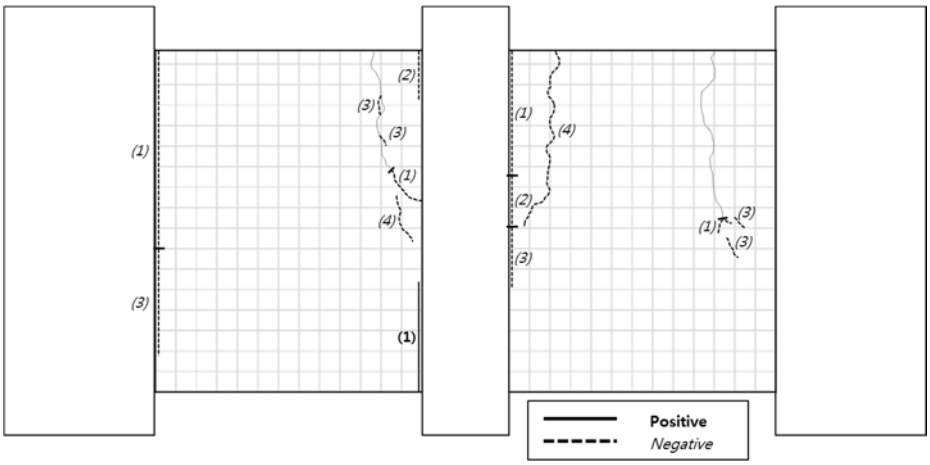

Fig. A-1 Crack pattern of WN (~ 0.05% drift ratio)

The specimen behaved elastically until that drift ratio as shown in **Fig. A-2**. The strain of the transverse and the vertical reinforcement measured from the attached steel strain gauges experienced very little change. The strain

variations of the transverse and the vertical reinforcements according to the positive directional drift ratio increment (~ 0.05 %) are shown in **Fig. A-3**. Since the strain gauges attached at the vertical reinforcements of the right wall panel were damaged, strain variation of it could not be measured.

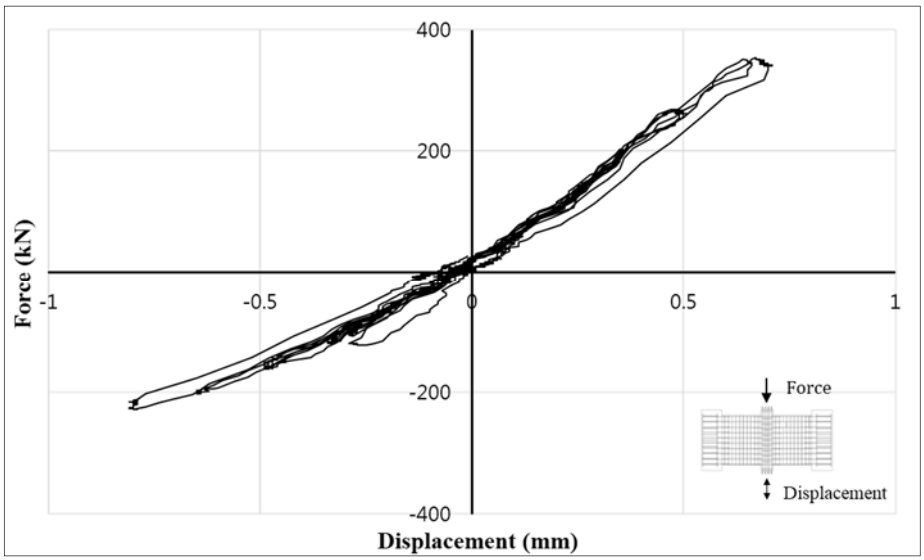

Fig. A-2 Load-deflection curve of WN (~ 0.05% drift ratio)

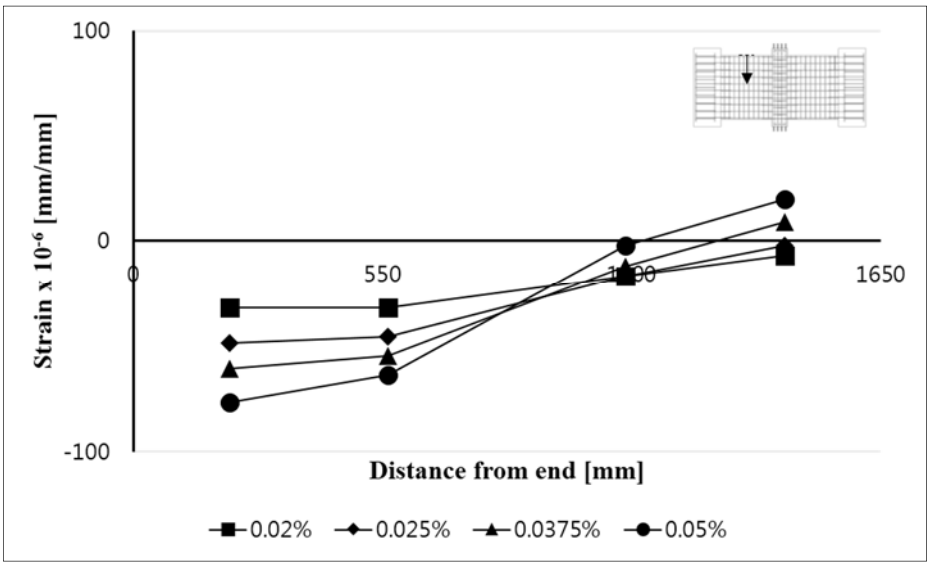

a) Strain variation of the vertical reinforcement in the left wall panel

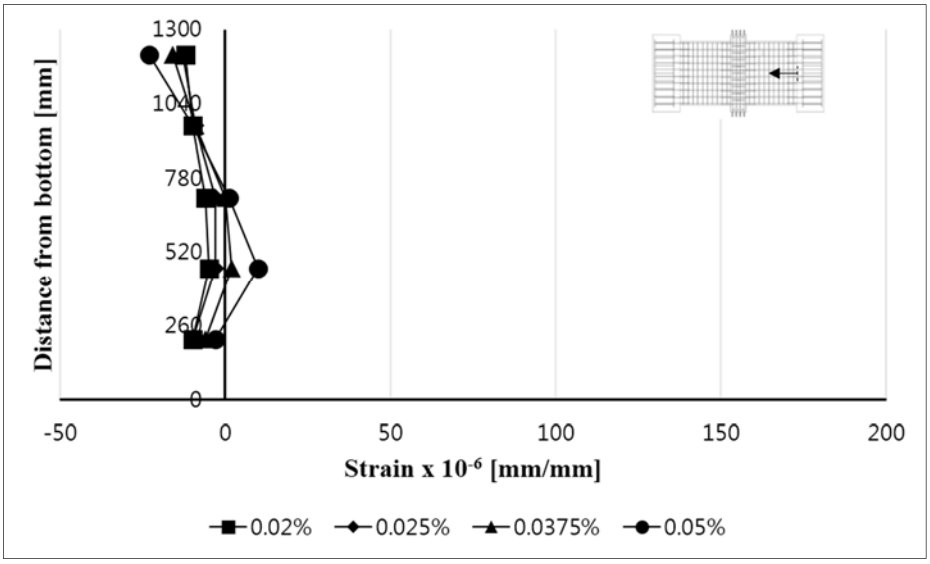

b) Strain variation of the transverse reinforcement in the right wall panel

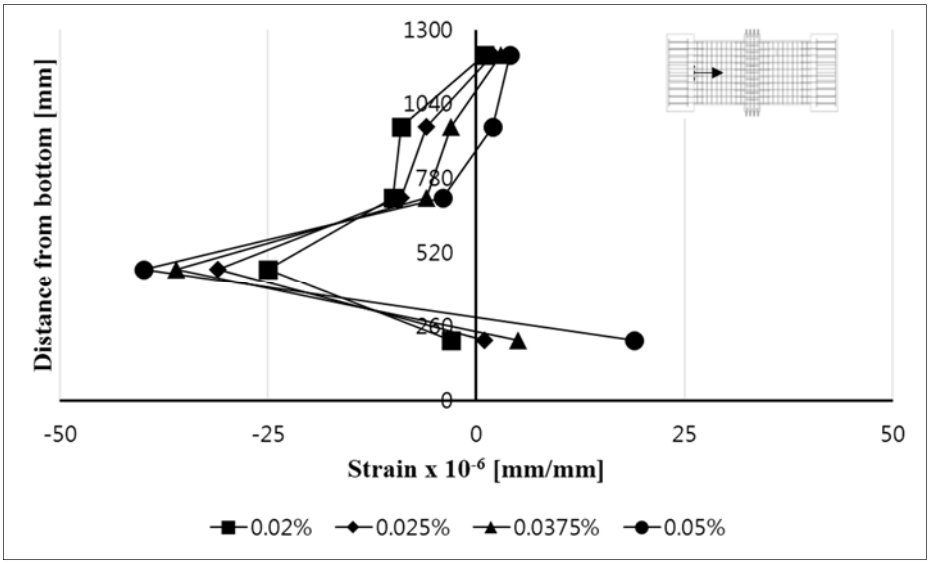

c) Strain variation of the transverse reinforcement in the left wall panel

Fig. A-3 Strain variation of the reinforcements (~ 0.05% drift ratio)

Cycle to 0.10 % drift (6th cycle)

After the 5th cycle (0.075 % drift ratio) of the load was applied to the specimen, diagonal cracks were occurred in the both wall panels. Positive directional diagonal crack was occurred in the both wall panels, and negative directional diagonal crack was occurred in the left wall panel at this cycle. Moreover, the cracks occurred before propagated a little. After the 6th cycle (0.10 % drift ratio) of the load was applied to the specimen, there occurred several positive directional diagonal cracks including major diagonal crack in the both wall panels contrary to no negative directional diagonal cracks occurred in that cycle. The crack pattern of the specimen at the 0.10 % drift ratio is shown in **Fig. A-4**.

The specimen started to behave in inelastic behavior. Therefore it is able to confirm that energy dissipation is occurred at the 6th cycle in earnest when the several positive directional diagonal cracks were occurred in both wall panels as shown in **Fig. A-5**. The strain of the transverse and the vertical reinforcement measured from the attached steel strain gauges are increased drastically at the 6th cycle. The strain variations of the transverse and the vertical reinforcements according to the positive directional drift ratio increment (0.05 % ~ 0.10 %) are shown in **Fig. A-6**.

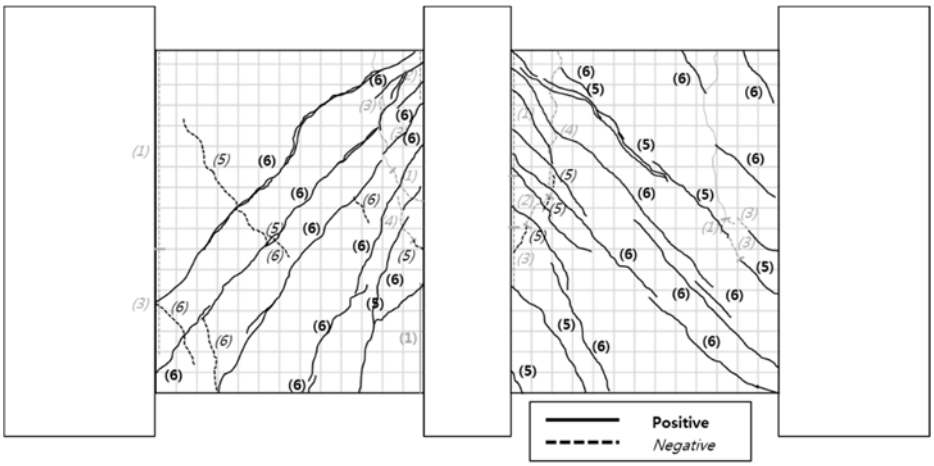

Fig. A-4 Crack pattern of WN (~ 0.10% drift ratio)

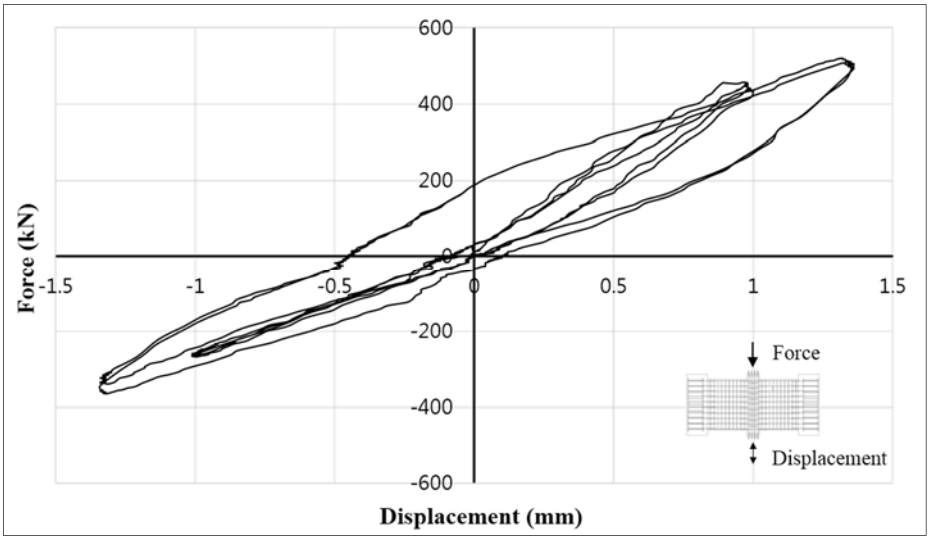

Fig. A-5 Load-deflection curve of WN (0.075% ~ 0.10% drift ratio)

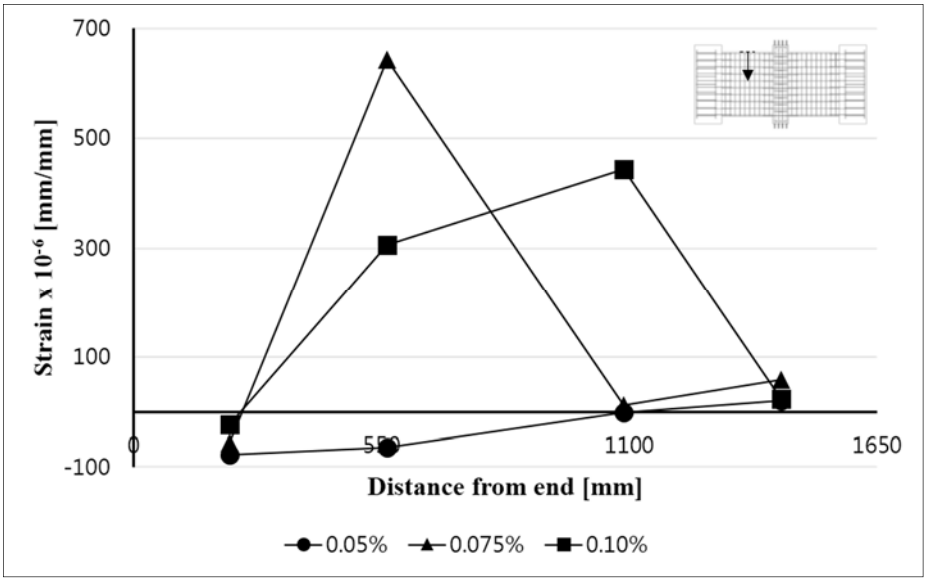

a) Strain variation of the vertical reinforcement in the left wall panel

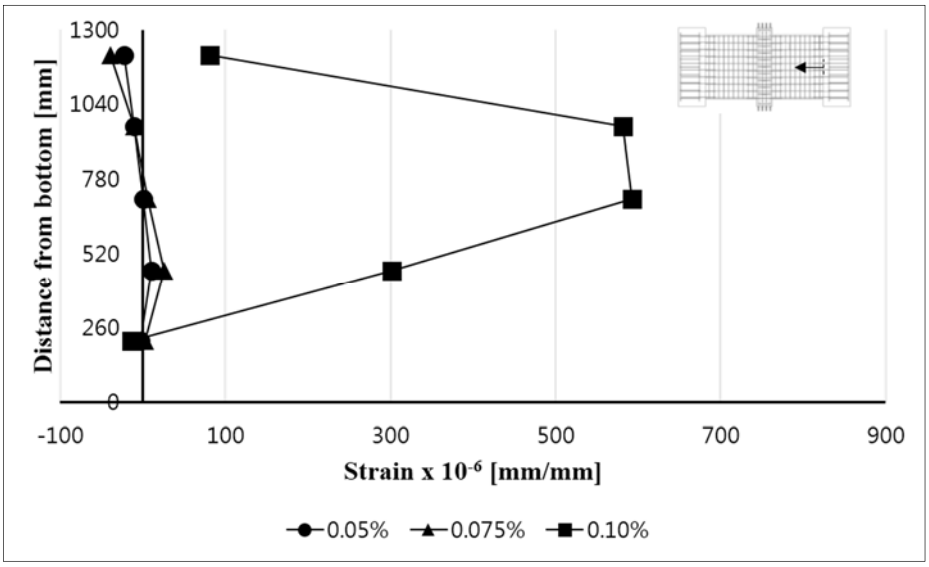

b) Strain variation of the transverse reinforcement in the right wall panel

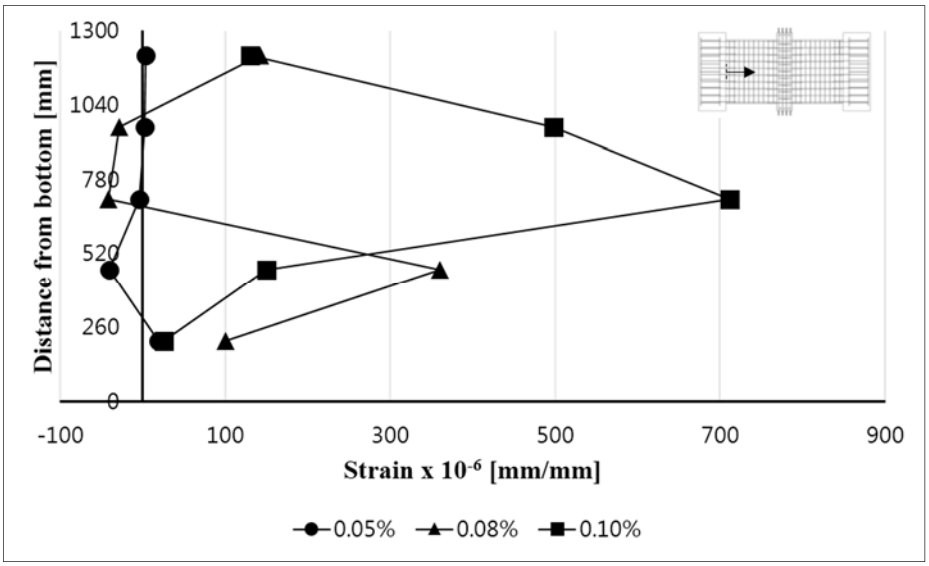

c) Strain variation of the transverse reinforcement in the left wall panel

Fig. A-6 Strain variation of the reinforcements (0.05% ~ 0.10% drift ratio)

Cycle to 0.35 % drift (9th cycle)

As the load cycle was increased, lots of negative and positive directional diagonal cracks were occurred in the both wall panels. Moreover, width of the positive directional major diagonal cracks occurred at the 6th cycle (0.10 % drift ratio) was widened gradually as the load cycle was increased. The crack pattern of the specimen at the 0.35 % drift ratio is shown in **Fig. A-7**.

The inelastic behavior of the specimen can be confirmed in these cycles. Moreover, a sudden increase of the area of the force-deformation graph shows that dissipated energy of the specimen is increased drastically in this interval as shown in **Fig. A-8**. The transverse reinforcements located at the center of the both wall panels were mainly increased until the 9th cycle. In addition, the vertical reinforcements were not yielded at that time, and the maximum strain was measured from the reinforcements located at the center of the wall panel similar tendency of the transverse reinforcement's strain variation. The strain variations of transverse and vertical reinforcements according to the positive directional drift ratio increment (0.10 % ~ 0.35 %) are shown in **Fig. A-9**.

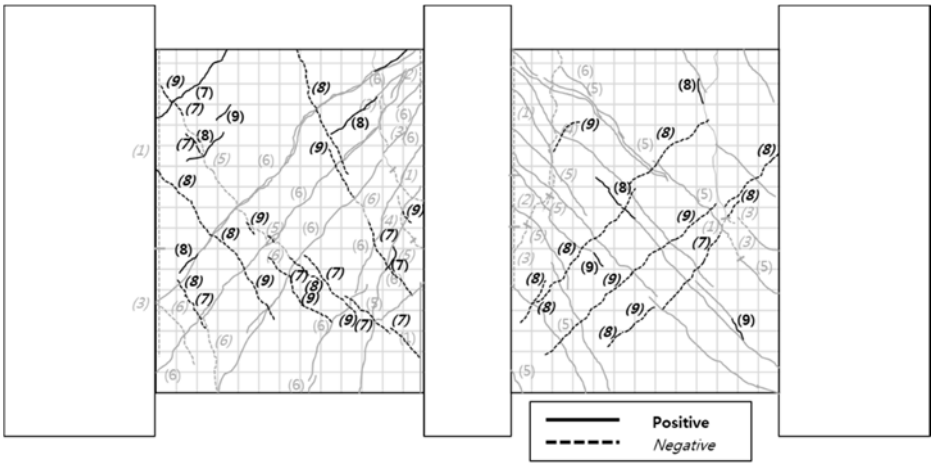

Fig. A-7 Crack pattern of WN (~ 0.35% drift ratio)

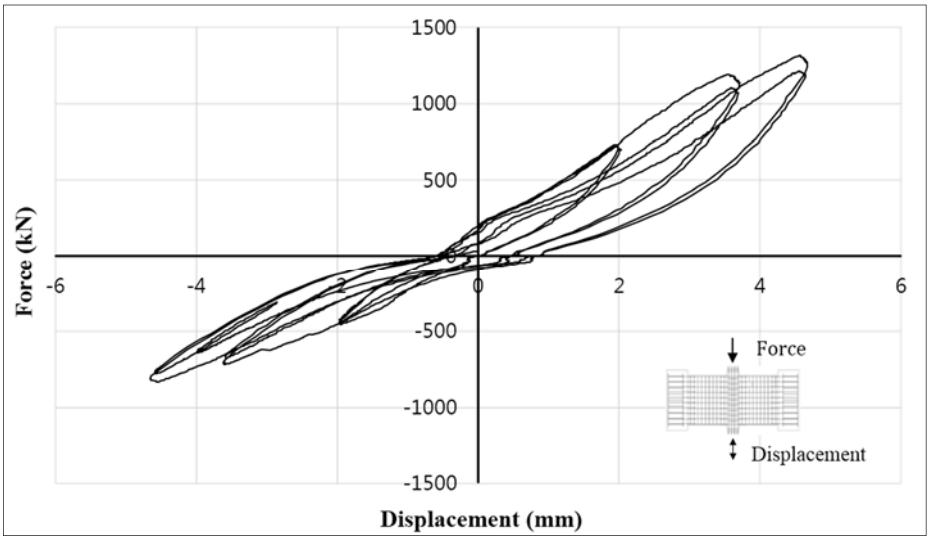

Fig. A-8 Load-deflection curve of WN (0.15% ~ 0.35% drift ratio)

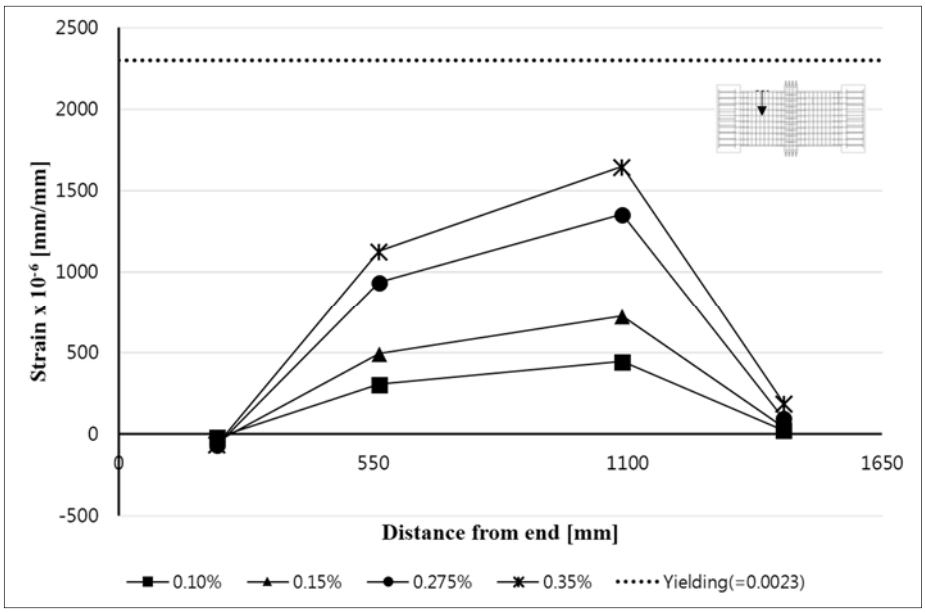

a) Strain variation of the vertical reinforcement in the left wall panel

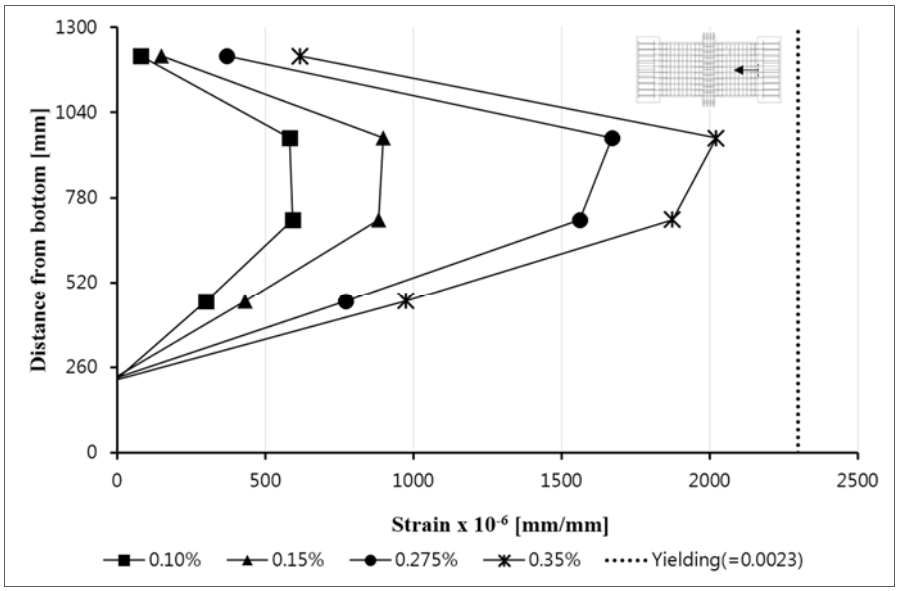

b) Strain variation of the transverse reinforcement in the right wall panel

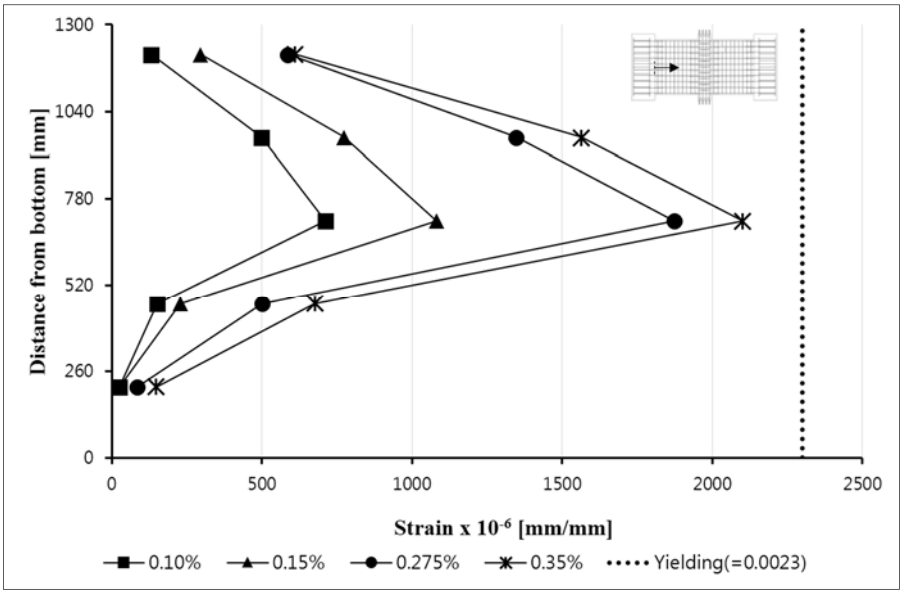

c) Strain variation of the transverse reinforcement in the left wall panel

Fig. A-9 Strain variation of the reinforcements (0.15% ~ 0.10% drift ratio)

Cycle to 0.60 % drift (11st cycle, Failure of WN)

Only micro cracks were occurred at the 10th cycle (0.45 % drift ratio), and widening positive directional major diagonal cracks were noticeable at that time. Finally, the right wall panel failed in diagonal tension failure during positive directional of the 11st cycle was imposed (0.56 % drift ratio). The crack pattern of the specimen at the ultimate state of the specimen is shown in **Fig. A-10**.

The ultimate strength of the specimen was occurred at that time. Since the specimen failed in brittle manner, there was no post peak behavior as shown in **Fig. A-11**. The transverse reinforcements located at the center of the both wall panels were yielded at the 9th cycle. The vertical reinforcements were not yielded at that time; however, the maximum strain was measured from the reinforcements located at the center of the wall panel. The strain variations of the transverse and the vertical reinforcements according to the positive directional drift ratio increment (0.35 % ~ 0.60 %) are shown in **Fig. A-12**.

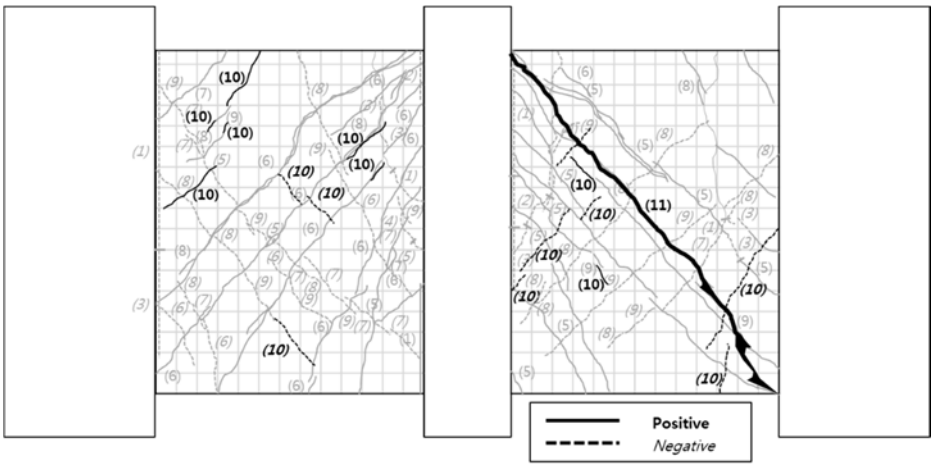

Fig. A-10 Crack pattern of WN (~ 0.60% drift ratio)

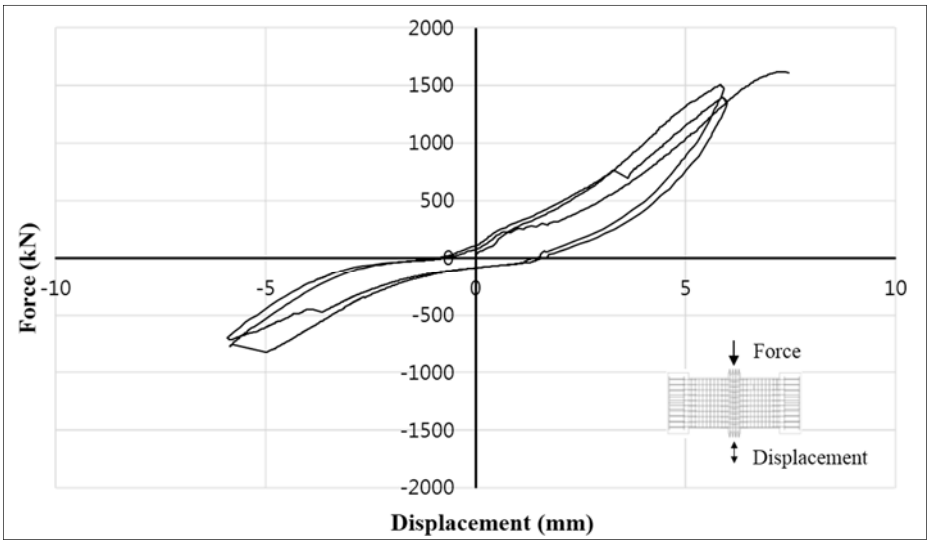

Fig. A-11 Load-deflection curve of WN (0.45% ~ 0.60% drift ratio)

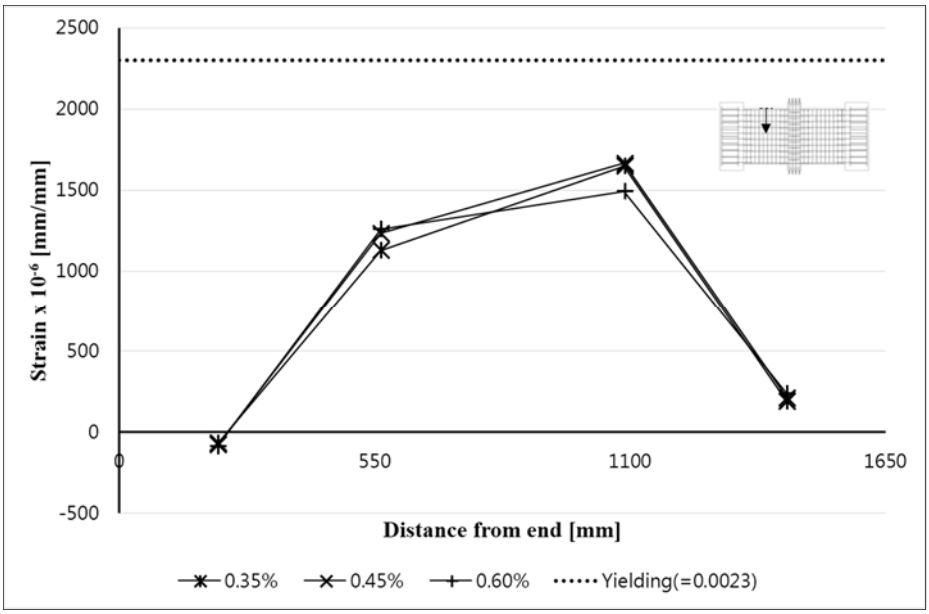

a) Strain variation of the vertical reinforcement in the left wall panel

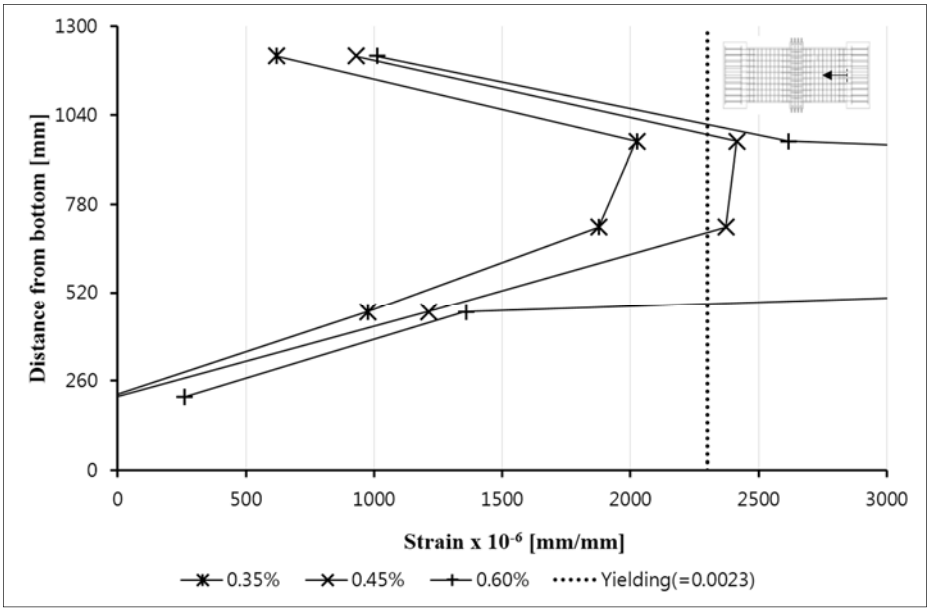

b) Strain variation of the transverse reinforcement in the right wall panel

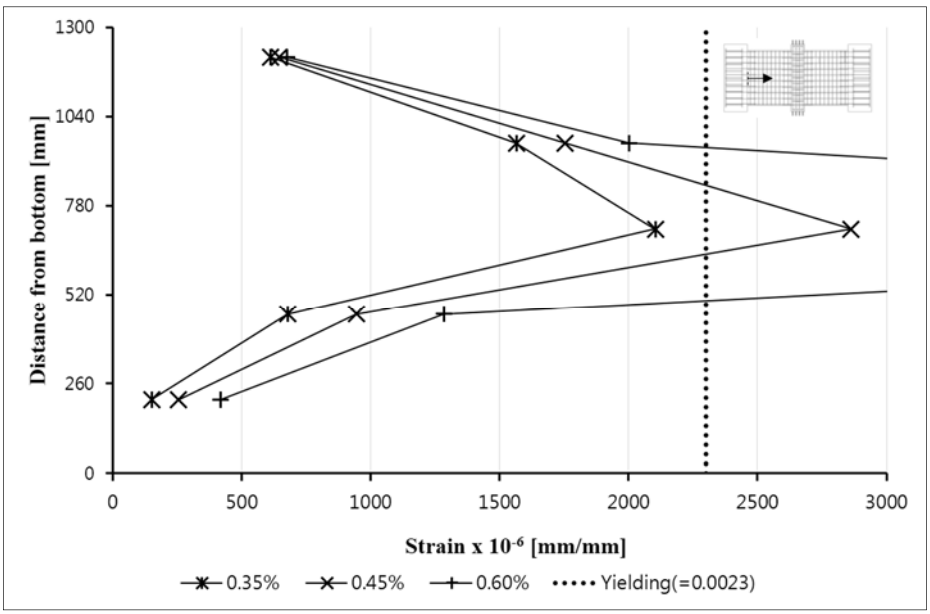

c) Strain variation of the transverse reinforcement in the left wall panel

Fig. A-12 Strain variation of the reinforcements (0.35% ~ 0.60% drift ratio)

2. Cyclic behavior of WR (UHPFRC web retrofitted squat wall)

Cycle to 0.075 % drift (5th cycle)

There occurred two flexural cracks in the left normal strength concrete wall panel prior to testing due to the tensile forces that caused by fastening both end boundary elements to provide fixed boundary condition similar to the case of WN. Until the 4th cycle (0.05 % drift ratio), sliding cracks were occurred in both normal strength concrete wall panels around the middle boundary element. There occurred some small diagonal cracks in the normal strength concrete wall panels at the 5th cycle (0.075 % drift ratio). However, there was no crack occurred in both UHPFRC panel until this cycle. The crack pattern of the specimen at the 0.075% drift ratio is shown in **Fig. A-13**.

The specimen behaved not perfectly elastic behavior, but energy dissipation was occurred from the 1st cycle (0.025 % drift ratio). However stiffness degradation did not occurred until the 0.075 % drift ratio (5th cycle) as shown in **Fig. A-14**. Almost all the strain variation of the transverse reinforcement until that cycle is almost zero, except for the reinforcement located at the middle of the right wall panel caused by diagonal crack occurred at the 5th cycle. Moreover, the strain distribution of the vertical reinforcement shows linear distribution. It can be confirmed from **Fig. A-15** that shows the strain variation of them according to the positive directional drift ratio increment (~ 0.075 %).

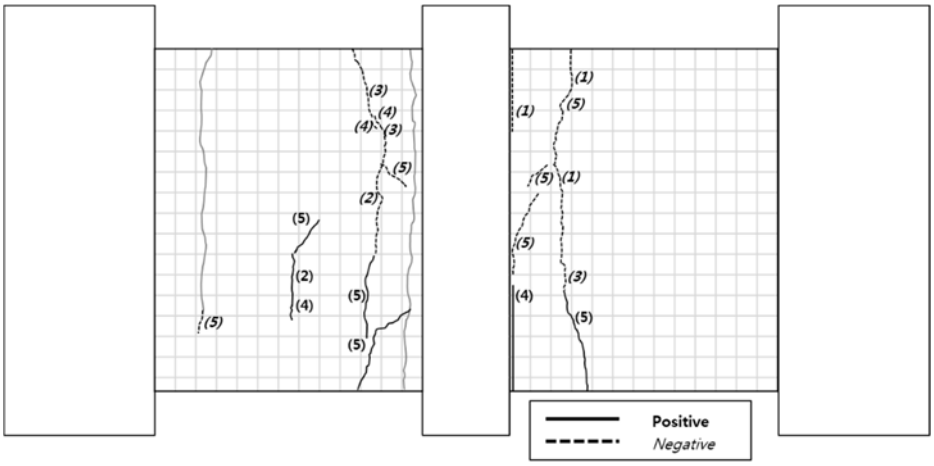

a) Crack pattern of normal compressive strength

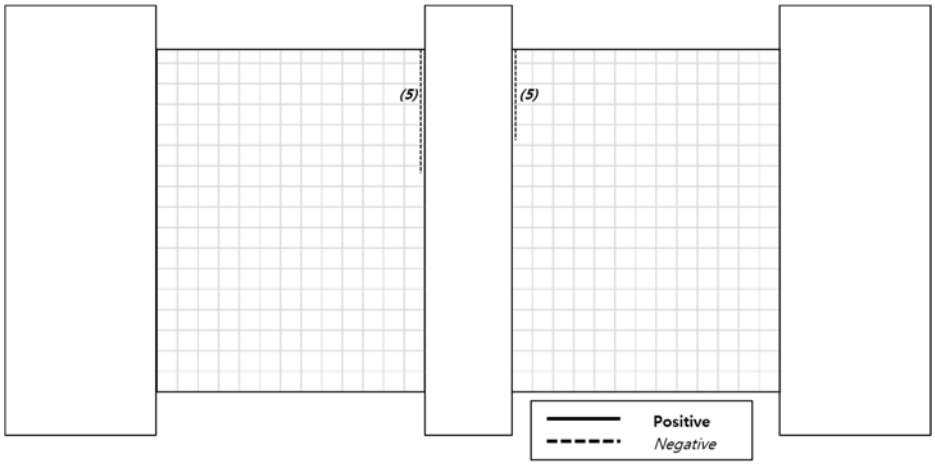

b) Crack pattern of UHPFRC panel

Fig. A-13 Crack pattern of WR (~ 0.075% drift ratio)

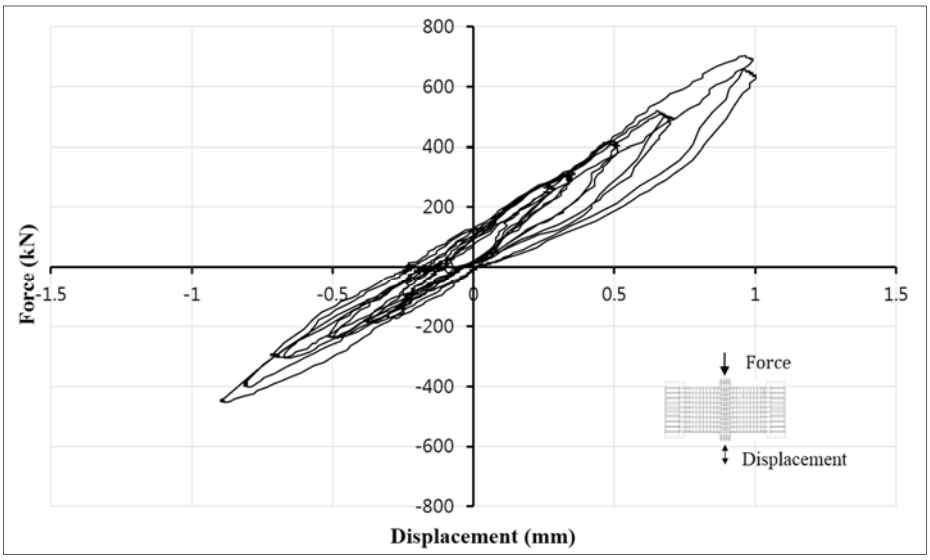

Fig. A-14 Load-deflection curve of WR (~ 0.075% drift ratio)

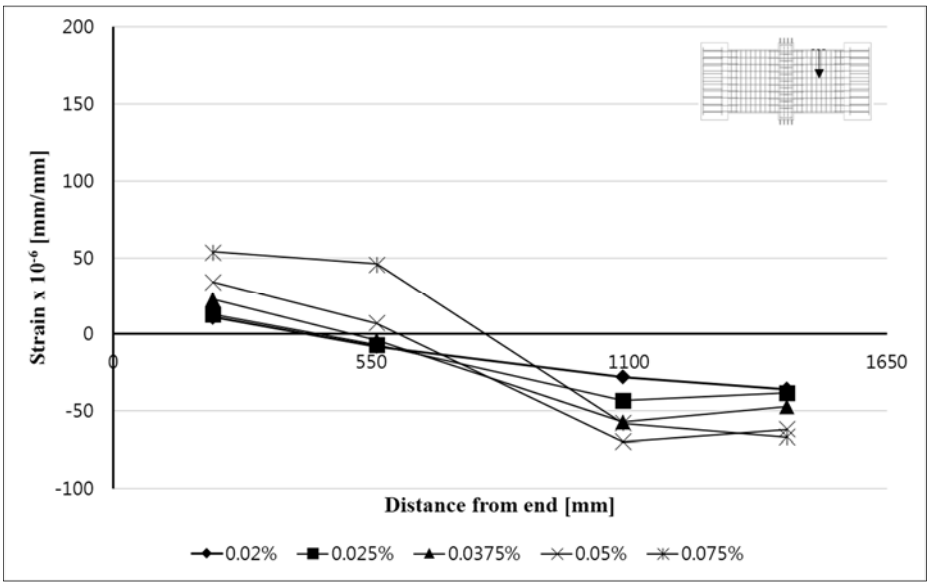

a) Strain variation of the vertical reinforcement in the right wall panel

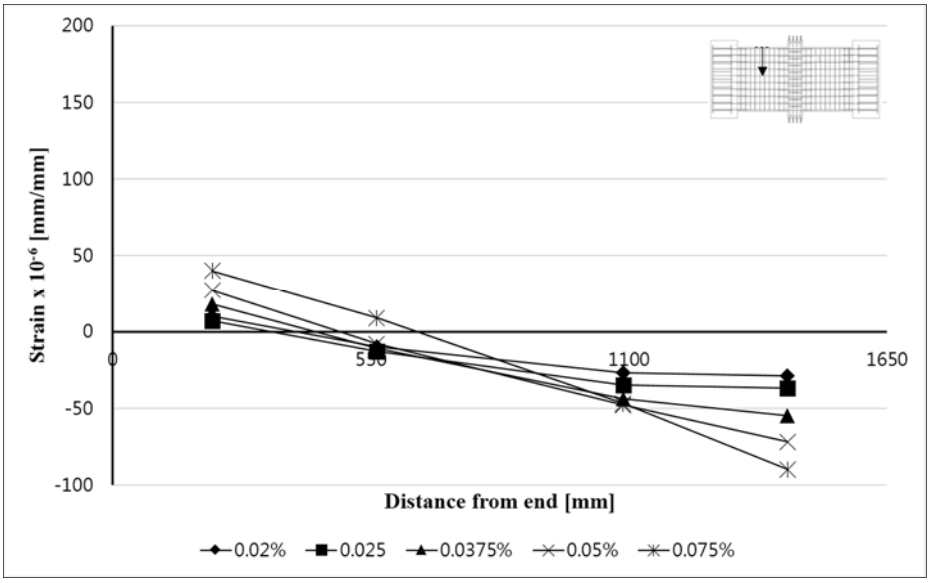

b) Strain variation of the vertical reinforcement in the left wall panel

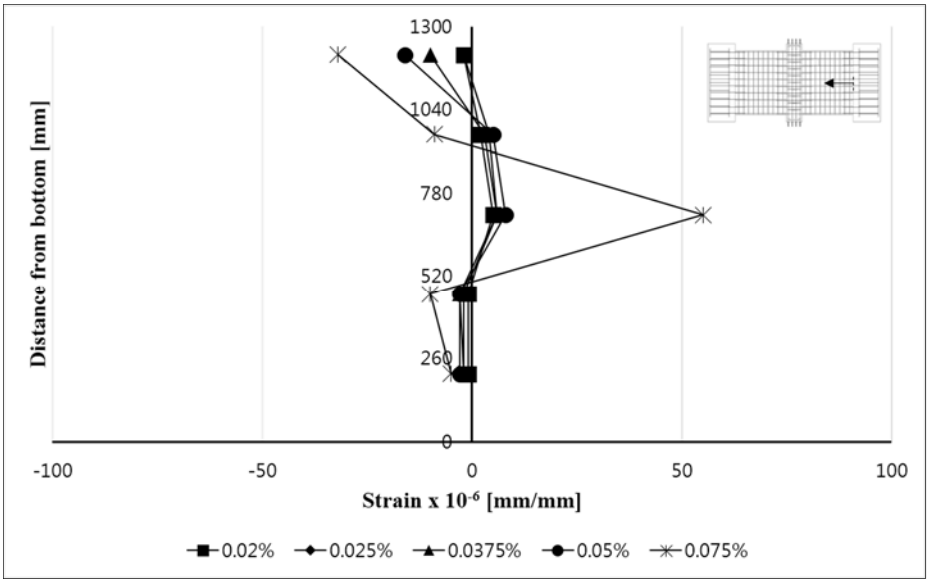

c) Strain variation of the transverse reinforcement in the right wall panel

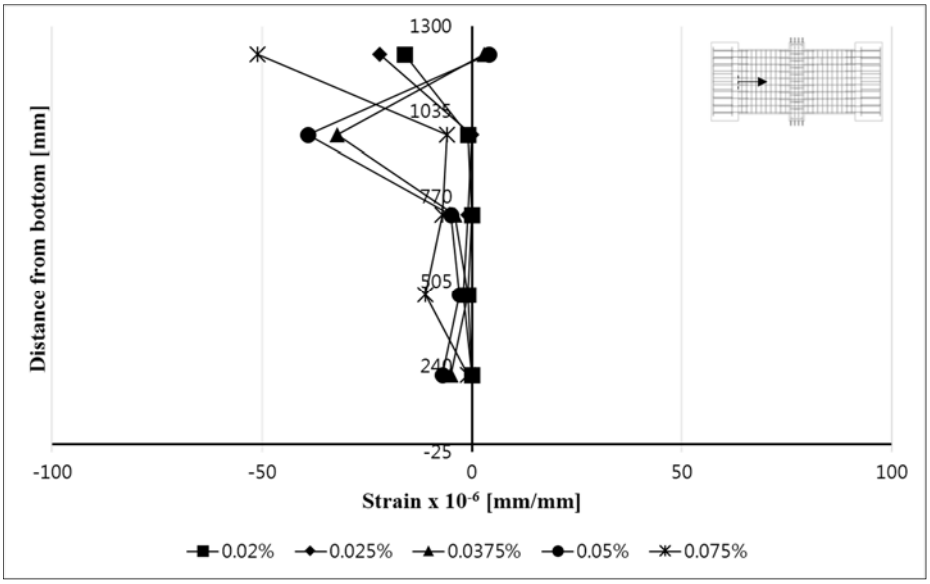

d) Strain variation of the transverse reinforcement in the left wall panel

Fig. A-15 Strain variation of the reinforcements (~ 0.075% drift ratio)

Cycle to 0.275 % drift (8th cycle)

There occurred major positive directional diagonal crack at the 6th cycle (0.10 % drift ratio) in the right normal strength concrete wall panel, and the 8th cycle (0.275 % drift ratio) in the left normal strength concrete wall panel, respectively. Moreover, small flexural cracks were found at the end of the UHPFRC panel at the 8th cycle. However, lots of flexural cracks were occurred at the middle boundary element of the specimen from negative directional cycles of the 7th to that of the 8th cycle. The crack pattern of the specimen at the 0.275 % drift ratio is shown in **Fig. A-16**.

The dissipated energy was enlarged at the 8th cycle when major diagonal cracks and flexural cracks were occurred in the normal strength concrete wall panel and the UHPFRC panel, respectively as shown in **Fig. A-17**. In addition, the strain of the vertical and the transverse reinforcements located at the middle of the left wall panel were increased at the 8th cycle due to diagonal cracks. The strain of the transverse reinforcement located at the middle of the right wall panel also increased drastically at the 8th cycle. It can be confirmed from **Fig. A-18** that shows the strain variation of them according to the positive directional drift ratio increment (0.075 % ~ 0.275 %).

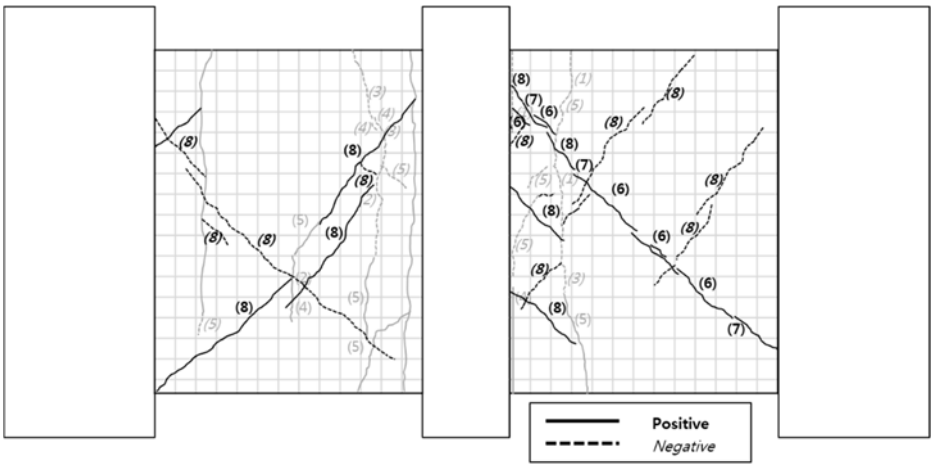

a) Crack pattern of normal compressive strength

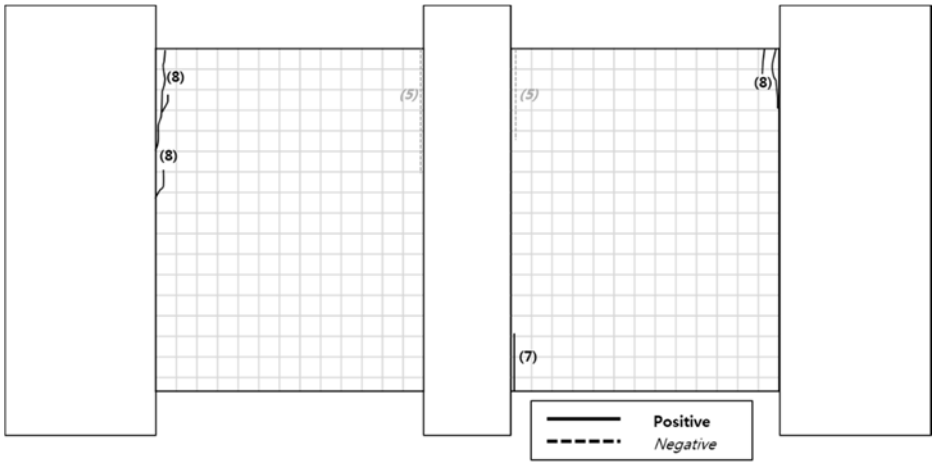

b) Crack pattern of UHPFRC panel

Fig. A-16 Crack pattern of WR (~ 0.275% drift ratio)

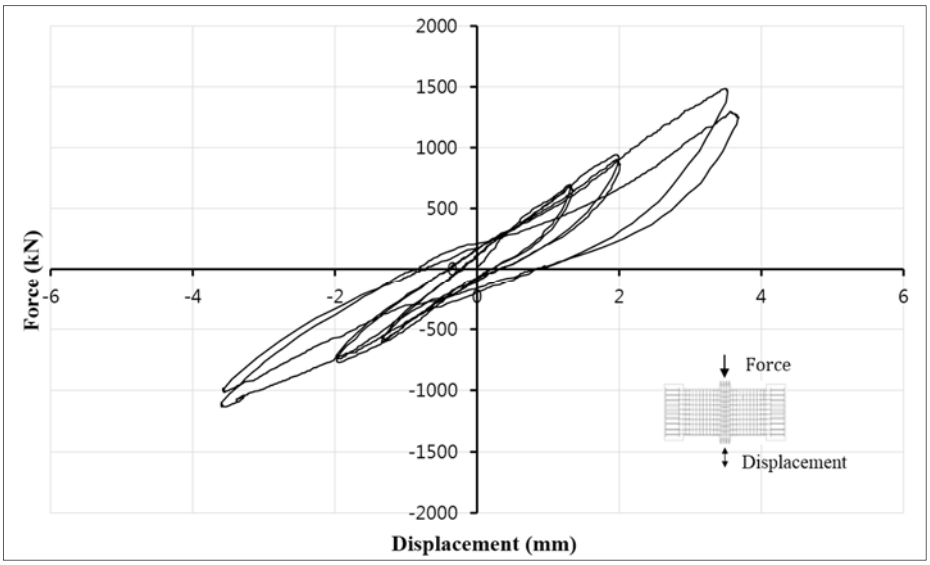

Fig. A-17 Load-deflection curve of WR (0.10 ~ 0.275% drift ratio)

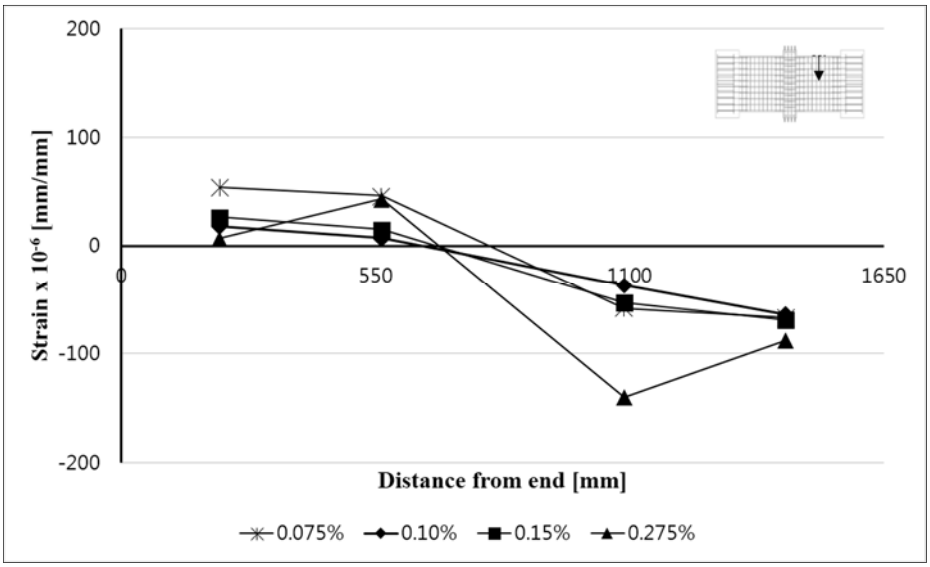

a) Strain variation of the vertical reinforcement in the right wall panel

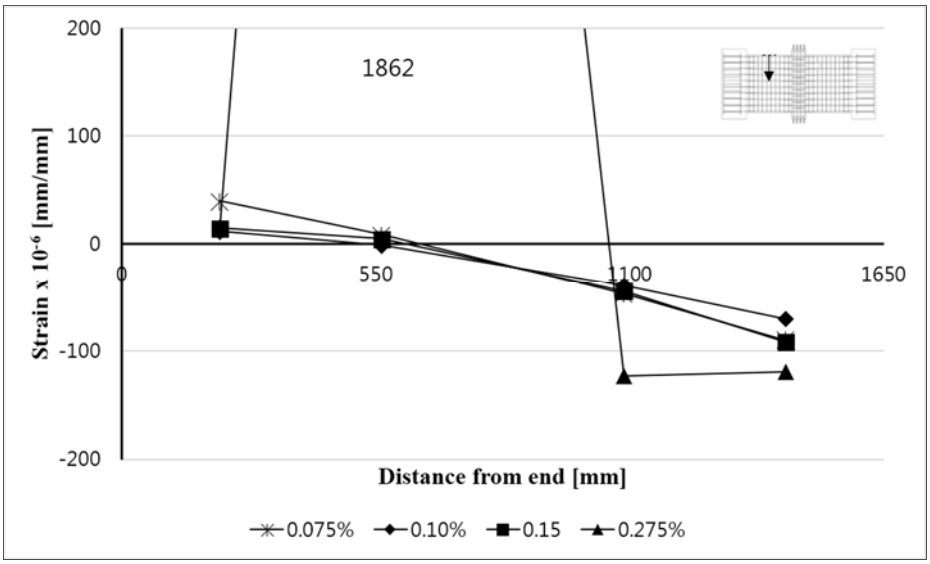

b) Strain variation of the vertical reinforcement in the left wall panel

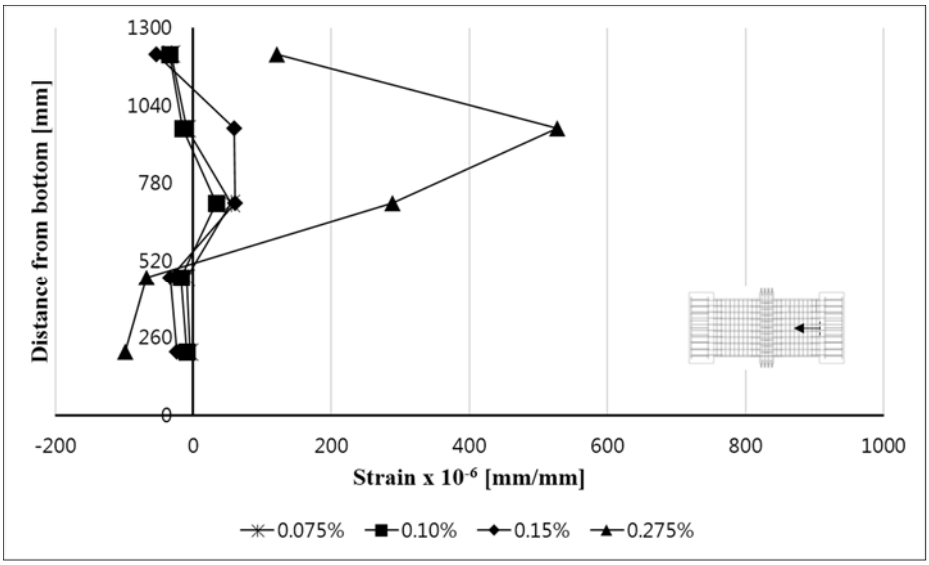

c) Strain variation of the transverse reinforcement in the right wall panel

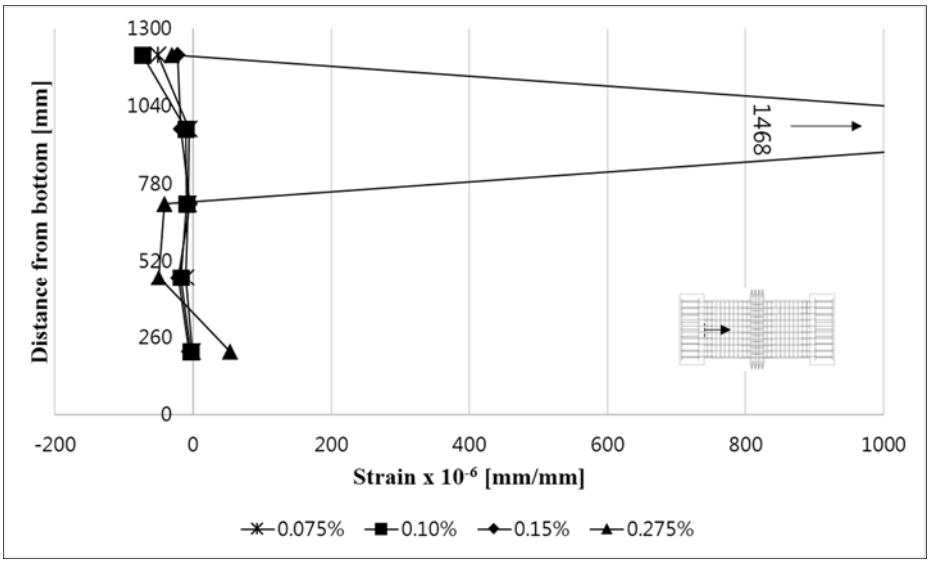

d) Strain variation of the transverse reinforcement in the left wall panel

Fig. A-18 Strain variation of the reinforcements (0.075% ~ 0.275% drift ratio)

Cycle to 0.75 % drift (12nd cycle)

There occurred unexpected problem during negative directional cycle of the 9th cycle (0.35 % drift ratio). Two of the through reinforcements functioned as applying tensile force to the specimen were fractured at the end of the screw as shown in **Fig. A-19**. Therefore, only the positive directional cycles were applied to the specimen form then.

Fig. A-19 Fracture of through reinforcement due to high tensile force

Several positive directional major diagonal cracks were occurred in the both normal strength concrete wall panels from the 10th cycle (0.45 % drift ratio) to the 11st cycle (0.60 % drift ratio), and width of the major diagonal cracks occurred at the previous cycle were widened from the 11st cycle. Moreover, some diagonal cracks were occurred in the both UHPFRC panel at that time. However, when first cycle of the 12nd cycle (0.75 % drift ratio) had applied to the specimen, distortion of the middle boundary element was occurred. The crack pattern of the specimen at that time is shown in **Fig. A-20**.

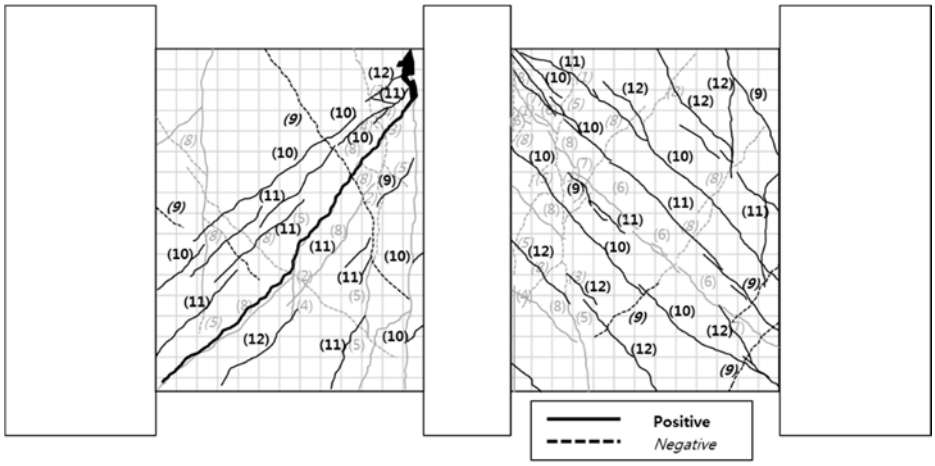

a) Crack pattern of normal compressive strength

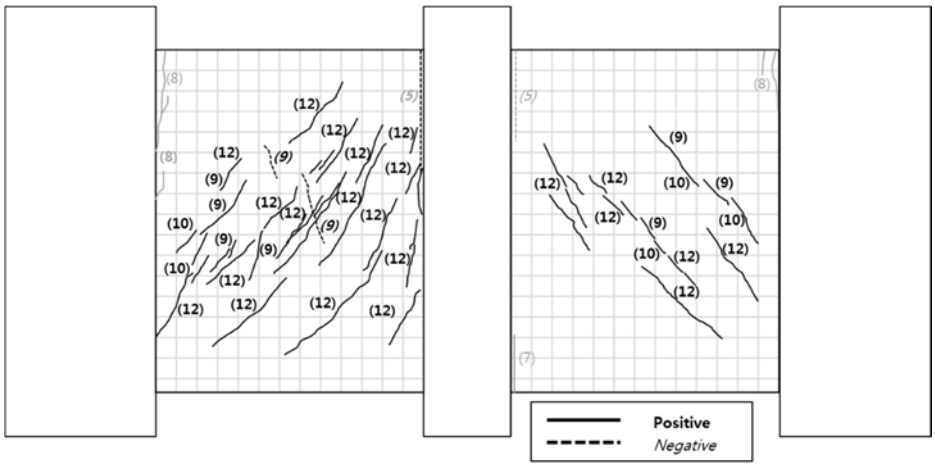

b) Crack pattern of UHPFRC panel

Fig. A-20 Crack pattern of WR (~ 0.75% drift ratio)

It is able to verify permanent deformation due to the cyclic loading from force-deformation graph of the specimen. Therefore, the specimen is subjected to relatively large tensile force when the specimen returns to 0mm deformation as shown in **Fig. A-21**. Almost all the strain of the transverse reinforcement located at the middle of the both wall panels increased gradually, and finally yielded at the 11st cycle and the 12nd cycle. Moreover, the strain of the vertical reinforcement located at the middle of the left wall panel also yielded at the 12nd cycle, while that of the right wall panel does not yielded. It can be confirmed from **Fig. A-22** that shows the strain variation of them according to the positive directional drift ratio increment (0.15 % ~ 0.75 %).

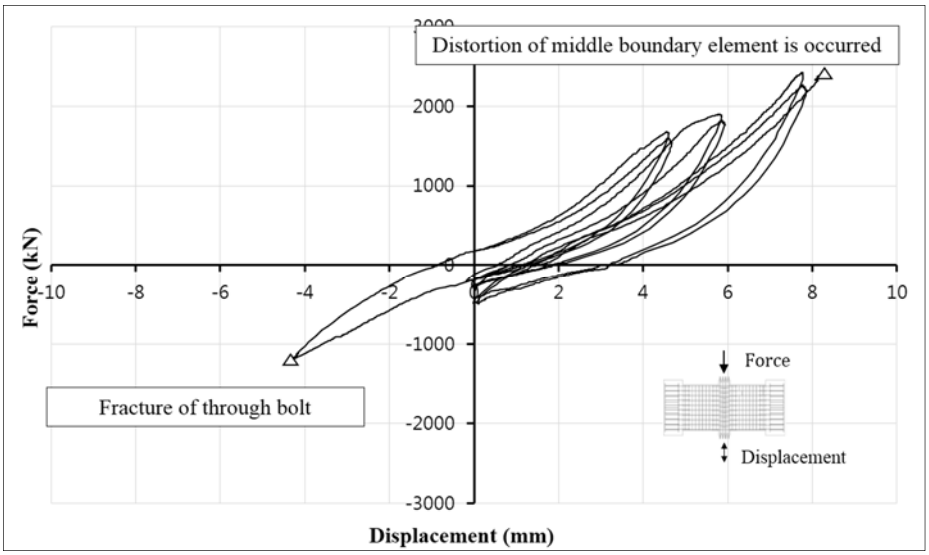

Fig. A-21 Load-deflection curve of WR (0.35% ~ 0.75% drift ratio)

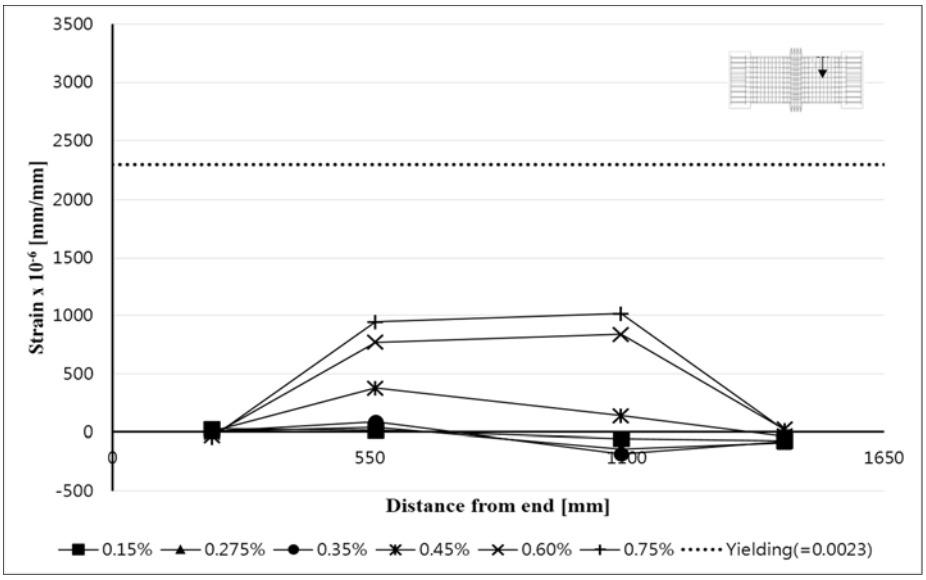

a) Strain variation of the vertical reinforcement in the right wall panel

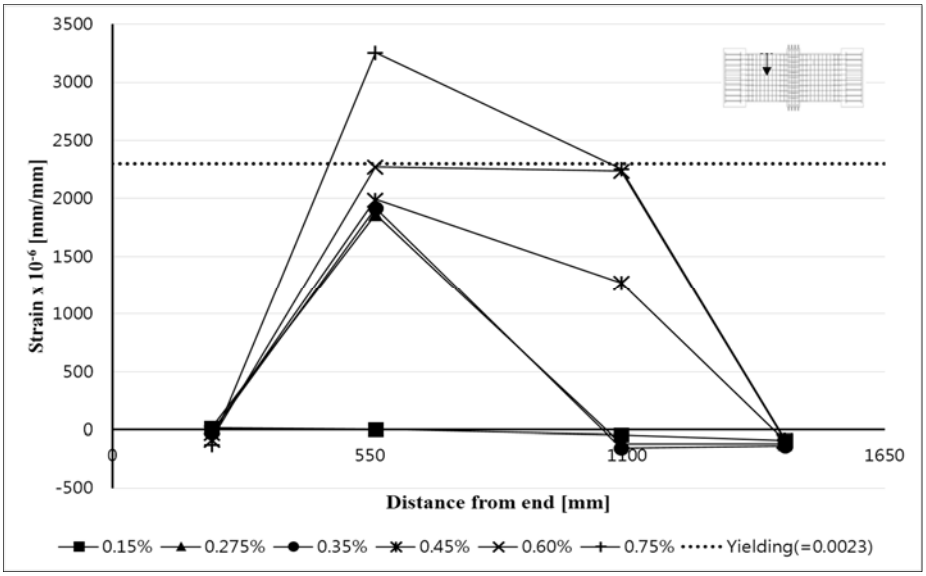

b) Strain variation of the vertical reinforcement in the left wall panel

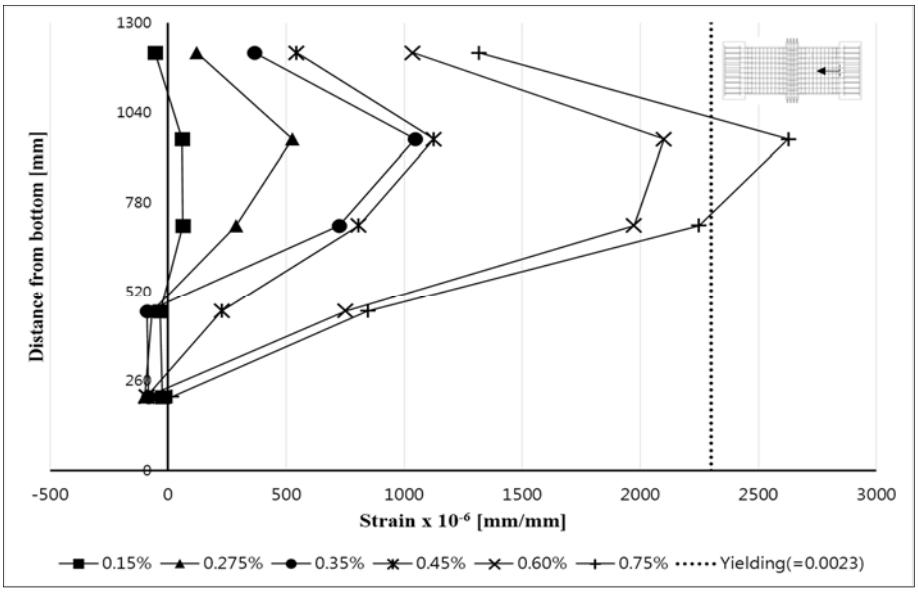

c) Strain variation of the transverse reinforcement in the right wall panel

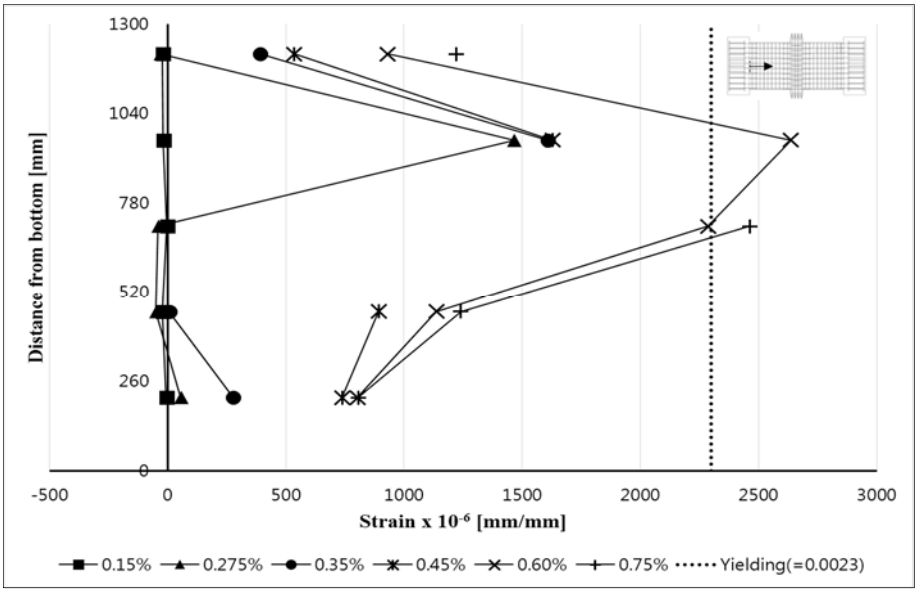

d) Strain variation of the transverse reinforcement in the left wall panel

Fig. A-22 Strain variation of the reinforcements (0.15% ~ 0.75% drift ratio)

Cycle to 1.25 % drift (14th cycle)

After readjusting the test set-up to remove the distortion occurred at the previous cycle, cyclic test was restarted from the 12nd cycle. However, there were no noticeable cracks were occurred at the specimen except for few diagonal cracks occurred in the UHPFRC panel at the 13rd cycle. Finally, part of the left normal strength concrete wall panel was slipped down by partial interface separation caused by widened crack width of the major positive directional diagonal crack. The crack pattern of the specimen at that time is shown in **Fig. A-23**.

Since 4.09mm permanent deformation caused by the distortion of the middle boundary element was confirmed by force-deformation graph of this interval, modified displacement-controlled cyclic load was applied to the specimen as shown in **Fig. A-24**. About 80% of the peak strength occurred at the 11st cycle was estimated at the modified 12nd cycle, and it was slowly reduced until the 14th cycle. Moreover, since almost all the measurable strains in these cycles experienced very little change, the test was finished at the 14th cycle. **Fig. A-25** shows the strain variation of them according to the positive directional drift ratio increment (modified 0.75% ~ Modified 1.25%).

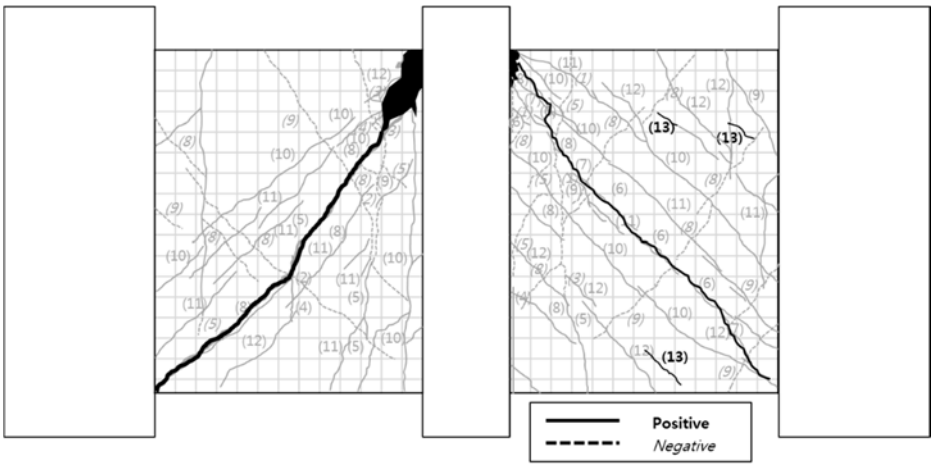

a) Crack pattern of normal compressive strength

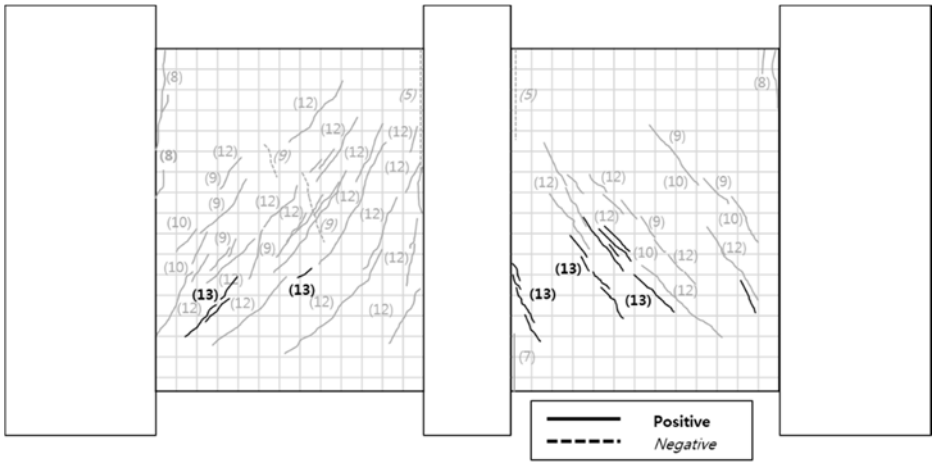

b) Crack pattern of UHPFRC panel

Fig. A-23 Crack pattern of WR (~ 1.25% drift ratio)

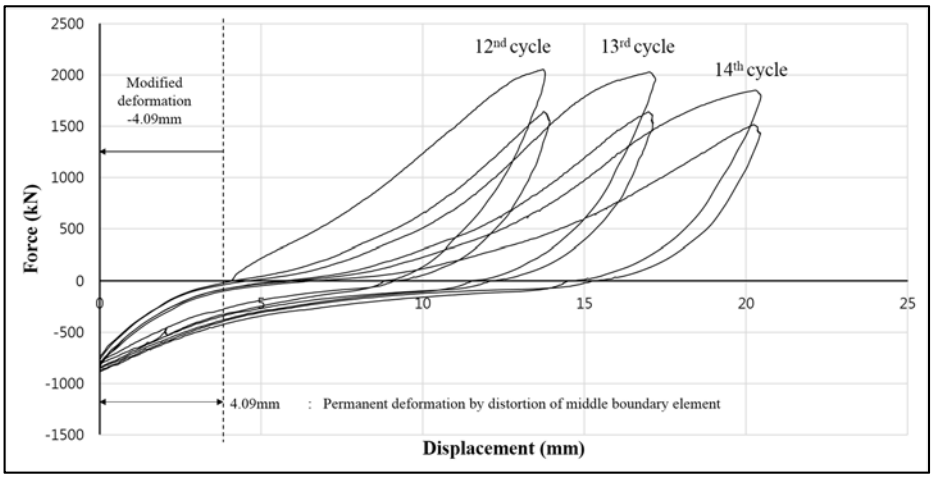

Fig. A-24 Load-deflection curve of WR (Modified 0.75% ~ 1.25% drift ratio)

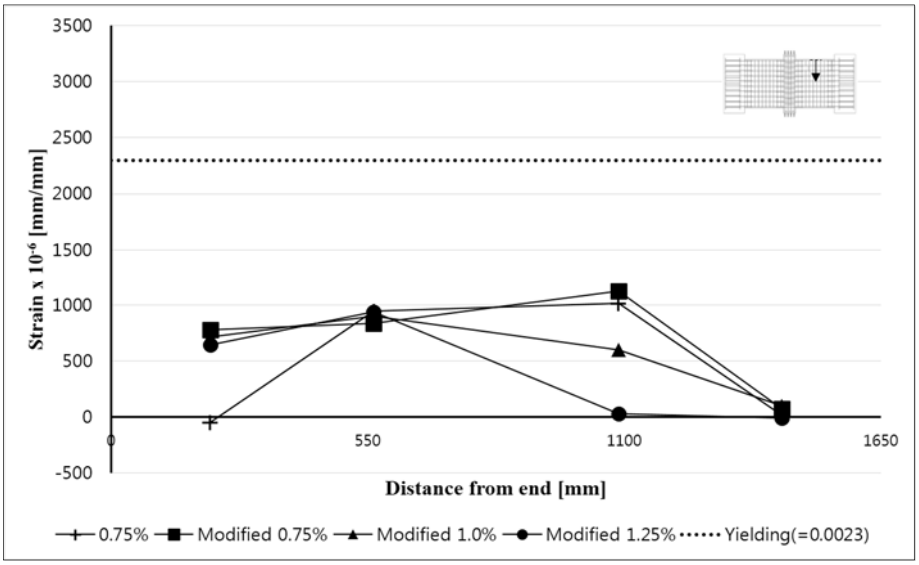

a) Strain variation of the vertical reinforcement in the right wall panel

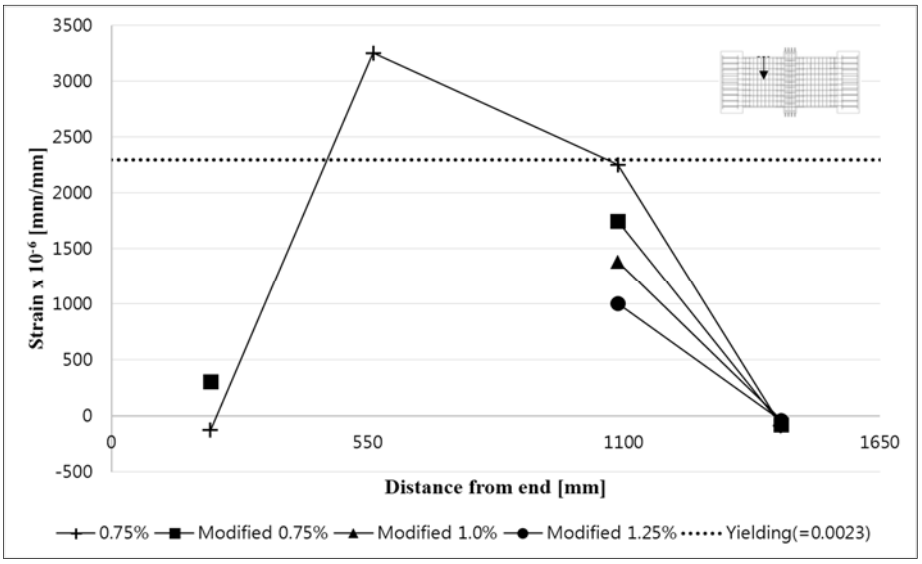

b) Strain variation of the vertical reinforcement in the left wall panel

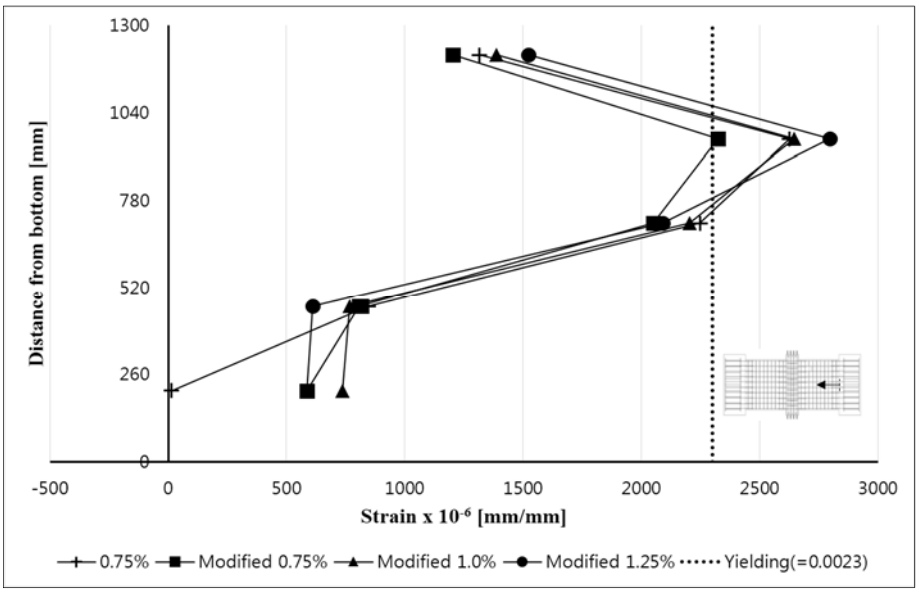

c) Strain variation of the transverse reinforcement in the right wall panel

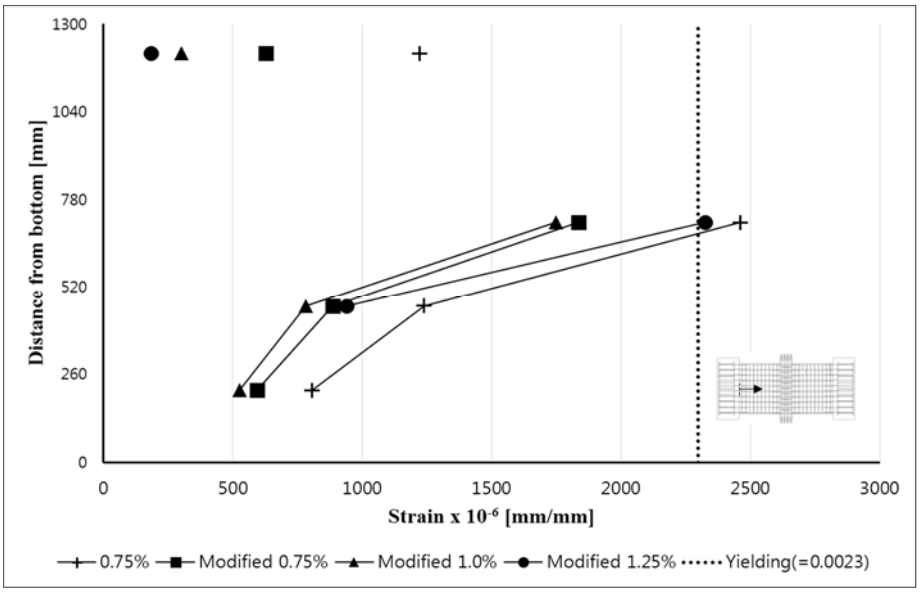

d) Strain variation of the transverse reinforcement in the left wall panel

Fig. A-25 Strain variation of the reinforcements (0.75% ~ Modified 1.25% drift ratio)